OPTIMAL OPERATION AND PLANNING OF SMART GRID WITH ELECTRIC VEHICLE PENETRATION

JIAN ZHAO

Ph.D

The Hong Kong Polytechnic University

2017

The Hong Kong Polytechnic University

Department of Electrical Engineering

OPTIMAL OPERATION AND PLANNING OF SMART GRID WITH ELECTRIC VEHICLE PENETRATION

JIAN ZHAO

A thesis submitted in partial fulfillment of the

requirements for the degree of Doctor of Philosophy

May 2017

CERTIFICATE OF ORIGINALITY

I hereby declare that this thesis is my own work and that, to the best of my knowledge and belief, it reproduces no material previously published or written, nor material that has been accepted for the award of any other degree or diploma, except where due acknowledgement has been made in the text.

_____(Signed)

____Jian ZHAO___(Name of student)

Abstract

Recent years have seen a fast development of electric vehicles (EVs) in the market, which can be attributed to the economic, environmental, and social benefits that can be potentially contributed by EVs. Specifically, these benefits include reduced national dependency on oils, reduced greenhouse gas emissions and reduced air pollution. As the transportation section accounts for large proportion in total energy consumption, the rapid shift to electrification of transportation will considerably increase the electricity usage. Thus, the current power infrastructure, especially the distribution network system, will suffer from some critical issues caused by large-scale EV charging demand. These issues include but are not limited to equipment overload, severe voltage fluctuation, power system reliability and so on. The investment in new generation capacity and upgrades of power infrastructures such as substation and transmission power line capacity may be urgently needed. Nevertheless, EV charging demand can be regarded as a flexible load and thus can be aggregated and managed so as to reduce the negative impact as well as to benefit to the power system. Besides, aggregated EVs also have the potential ability to provide ancillary service to power systems via vehicle to grid implementation in the future. In this regards, this thesis evaluates the challenges and opportunities introduced by large-scale EV charging in power system and developing new method to utilize EV charging flexibility to benefit power system economic and secure operation.

This thesis firstly focuses on power system distribution network operation planning, to hedge against negative impacts caused by large-scale random EV charging. The concept of an EV chargeable region is proposed to evaluate the distribution network EV hosting capacity, i.e., how much EV charging demand can be accommodated in a distribution network, within which the technical constraints of distribution network (e.g., voltage deviation) are guaranteed and EV owners' charging requests are maximally ensured. To further accommodate uncertain EV charging demand, a two-stage robust active distribution network planning model is then proposed. The distributed generator investment, location, and size are optimized in the first stage and the active distribution network

operation feasibility in the worst-case scenario is checked in the second stage to prevent any constraint violations. Finally, a modified column-and-constraint generation algorithm is adopted to solve the distribution system operation and planning problems. Simulations on modified IEEE 123-node distribution network demonstrate the effectiveness of the proposed two models.

Then this thesis proposes models for aggregated EV to provide ancillary service and bid in electricity market. To utilize the EV charging flexibility to benefit the grid, this thesis evaluates the potential ability of EVs in providing operating reserve, through optimizing day-ahead spinning reserve requirement with EV participation. Based on the probabilistic criteria, the cost of expected energy supplied by EV is formulated. The effects of EVs on system spinning reserve requirement quantification and unit commitment are comprehensively analyzed. At last, an information gap decision theory based EV scheduling method and bidding strategies are proposed. It aims at managing the revenue risk caused by the information gap between the forecasted and actual electricity prices. The proposed decision-making framework is used to offer effective strategies to either guarantee the predefined profit for risk-averse decision makers, or pursue the windfall return for risk-seeking decision makers considering the risks introduced by the electricity price uncertainty.

Publications Arisen from the Thesis

Refereed Journal Publications

1 **Jian Zhao**, Jianhui Wang, Zhao Xu, Cheng Wang, Can Wan, Chen Chen, "Distribution Network Electric Vehicle Hosting Capacity Maximization: A Chargeable Region Optimization Model", IEEE Trans. on Power System, 2017, Accepted.

2 **Jian Zhao**, Zhao Xu, "Ramp-Limited Optimal Dispatch Strategy for PV-Embedded Microgrid", IEEE Trans. on Power System, 2017, Accepted.

3 **Jian Zhao**, Can Wan, Zhao Xu, Kip Po Wong, "Spinning Reserve Requirement Optimization Considering Integration of Plug-in Electric Vehicles", IEEE Trans. on Smart Grid, 2016, Published.

4 **Jian Zhao**, Can Wan, Zhao Xu, Jianhui Wang, "Risk-Based Day-Ahead Scheduling of Electric Vehicle Aggregator using Information Gap Decision Theory", IEEE Trans. on Smart Grid, 2015, Published.

5 Can Wan, **Jian Zhao**, Yonghua Song, Zhao Xu, Zechun Hu, "Photovoltaic and Solar Forecasting Techniques for Smart Grid Energy Management", CSEE Journal of Power and Energy Systems, 2015, Published

6 Jiayong Li, Zhao Xu, **Jian Zhao**, Can Wan, "A Coordinated Dispatch Model for Distribution Network Considering PV Ramp" IEEE Power Engineering Letters, Accepted.

Refereed Conference Publications

7 **Jian Zhao**, Can Wan, Zhao Xu, Jiayong Li, "Impacts of Large-scale Photovoltaic Generation Penetration on Power System Spinning Reserve Allocation" 2016 Power & Energy Society General Meeting Conference, Accepted. (IEEE PES General Meeting Best Paper Award)

Submitted Journal papers for review

8 **Jian Zhao**, Zhao Xu, Jianhui Wang, Cheng Wang, Jiayong LI, "Active

Distribution Network Planning with Integration of Distributed Generation and Large-scale Electric Vehicle Charging Demand", IEEE Trans. on Power System, Under review.

9 Xue Lyu, Zhao Xu, **Jian Zhao**, Kit Po Wong, "Advanced Frequency Support Strategy of Photovoltaic System Considering Changing Working Conditions", IET Generation, Transmission & Distribution, Under review.

Acknowledgements

This work is accomplished during my Ph.D. candidature in The Hong Kong Polytechnic University and my visit in Argonne National Laboratory, with the immense support and guidance of various personalities. Firstly, I would like to express my heartfelt gratitude to my chief supervisor, Prof. Zhao Xu, for his continuous guidance, encouragement, support and patience throughout my entire graduate study. Without him, I may end up in a completely different path. All this will store up in my heart during my lifetime. I would like to express my sincere thanks to my co-supervisor Dr. Jianhui Wang at Argonne National Laboratory for his invaluable supervision that indeed guides me to step forward for my research. I also would like to express my deep gratitude to my co-supervisor Prof. Siu-lau Ho, for his continuous help and constructive advices during my Ph.D. study. In addition, I am equally indebted to Prof. Kit Po Wong for his insightful lectures and instructive comments on my published papers and PhD thesis.

Special thanks should go to my parents, my grandparents and my relatives for their continuous support and encouragement. I would like to express my special thanks to my fiancée, who has always been there for me. It is her understanding, encouragement and loving support that keep me focused and motivated. My thanks also go to my research colleagues who make progress together with me, inspire each other and become better than ever before during the precious lifetime in Hong Kong. Especially, I would thank Dr. Can Wan for his help and his encouragement on my academic path. I would also thank my friends at Argonne National Laboratory and Zhejiang University and wish you a wonderful life. Finally and most importantly, I would like to acknowledge the support from Ph.D studentship awarded by The Hong Kong Polytechnic University.

Table of Contents

List of Abbreviations

EV	Electric vehicle
DN	Distribution network
ARC	Atlanta regional commission
PLA	Piecewise linearization approximation
CDF	Cumulative distribution function
PDF	Probability distribution function
SOC	State of charge
AVR	Automatic voltage regulator
C&CG	Column & constraint generation
OA	Outer approximation
MILP	Mix integer linear programming
MP	Master problem
SP	Subproblem
DG	Distributed generator
DDG	Dispatchable distributed generator
NDG	Non-dispatchable distributed generator
RP-I/II	Robust optimization based program – I/II
WP	Wind power
PV	Photovoltaic generation
V2G	Vehicle to grid
EENS	Expected energy not supplied
EESEV	Expected energy supplied by electric vehicle
SRR	Spinning reserve requirement
UC	Unit commitment
IGDT	Information gap decision theory
CVaR	Conditional value at risk

List of Figures

List of Tables

1. Introduction

1.1 Backgrounds

The ratio of automobiles to people has been climbing around the world for the past century. Taking USA for example, transportation uses nearly a third of the energy consumed annually (27.5 quads in 2014), 92% of which is provided by petroleum [1]. Oils can be easily transported and thus traded among countries as bulk cargo. The fuel price has a considerable impact on personal consumption and economy of the countries. Historically, economic downturns always coincided with a decrease of gasoline supply and increase of international oil price [2]. Thus having such an important sector of the economy so dependent on one type of fuel is an economic risk and regarded as a threat to national security. Besides, consumers appear to have little elasticity to gasoline prices, which further aggravate the economic risk. Actually, the cost of crude oil has fluctuated significantly, which has triggered several economic crisis in the last century. On the other hand, burning petroleum in conventional vehicles significantly contributes to total pollutant emissions [3]. Especially, vehicle usage usually occurs in urban areas making the population close to where people live, localizing the negative environmental effects in cities and residential areas. The transportation also accounts for a significant proportion of CO2 emissions, taking almost one third in USA as seen in Fig. 1.1. To control global warming caused by greenhouse effect, countries have achieved some agreement to reduce CO2 emissions. The transportation sector should take responsibility in it.

Electric vehicles have the potential to mitigate these issues. The usage of EVs can diversify the energy supply and reduce the importance of fuel in economies, so that the economic entities can better accommodate the fluctuation of the international oil price. Those fossil driven power generators are usually far from

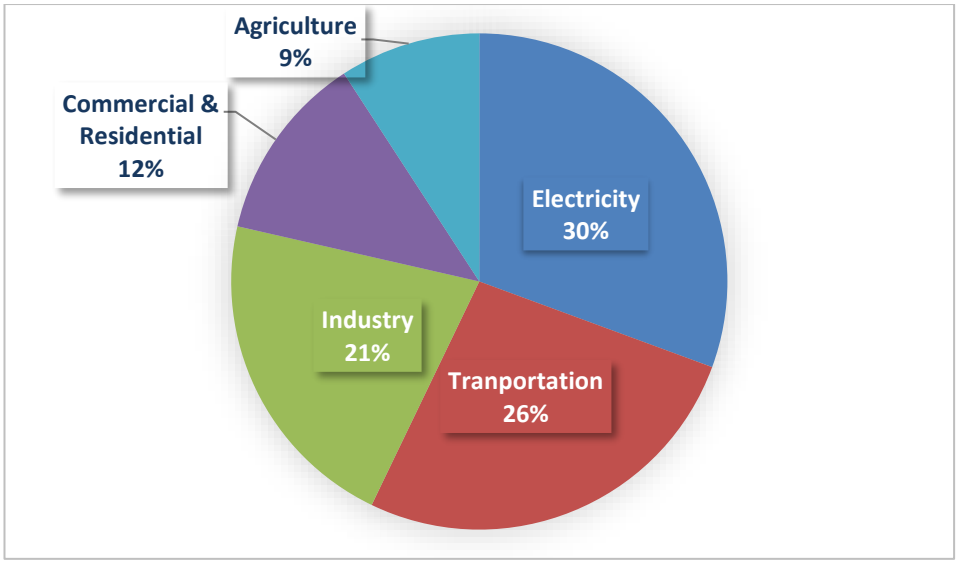

Figure 1.1 Total U.S. Greenhouse Gas Emissions by Economic Sector in 2014 [4]

where people live and thus bring less pollution to people. Besides, with fast development of renewable energies, power generation becomes much more environmentally friendly, which provides an opportunity to widely adopt EVs from the point of environment protection. Electric vehicles are not a new idea. Electric vehicles experienced golden ages during late 19th century and early 20th century [5]. Later, EVs lose its position in automobile market during the past century due to technical and economic factors. Until late 20th century, things begin to change. Especially the global economic recession in the late 2000s led to increased calls for automakers to abandon fuel-inefficient vehicles, which were seen as a symbol of the excess that caused the recession, in favor of small vehicles, hybrid vehicles and electric vehicles. Then recent decades have witnessed a globally increasing interest in EVs. The reappearance of EVs in the market seems to be very substantively persistent, given the large numbers of companies developing EVs and their ambitions reflected from the huge investment on EVs. In the foreseeable future, EVs have large potential to dominate the automobile market [6]. A range of potential EVs' market penetration rates have been projected for a number of regions and countries including North America, Australia, New Zealand, Denmark, Belgium, Sweden, Ireland and Netherlands, with the established EV development targets given in Table 1.1.

Table 1.1 Global EV Penetration Target

Country	EV uptake target	Country	EV uptake target
North America	52% by 2035;62% by 2050 [7]	Australia	65% by 2050 [8]
New Zealand	2040 60% market share [8]	Denmark	200,000 by 2020
Belgium	30% by 2030 [9]	Sweden	600,000 by 2020 [10]
Ireland	40% market share by 2030 [10]	Netherlands	200,000 by 2040

With the widespread of EV adoption, power system utilities are facing lots of challenges due to large-scale EV charging demand in the grid operation in terms of power stability, power quality and top of that, power reliability. As EVs are connected to the low voltage distribution system, quantifying the potential impact of EV charging on electricity distribution network and developing new methods for accommodating large EV popularity should be regarded as major challenges. The distribution networks are usually radial, typically starting with the distribution substation including substation transformers. The electricity transmits along distribution lines to the sub-connection nodes. To avoid huge voltage drops caused by large load demands, voltage regulators (usually the shunt capacitors, step voltage transformers and the line drop compensators) are installed. The customers are connected to these utility feeders with the sub-distribution system through distribution transformers which transfer voltage down from distribution voltage to lower voltage. In the absence of any coordinating strategy, uncontrolled charging of EVs will result in some detrimental effects to distribution networks. A review of [9, 11, 12] indicates that the large-scale random EV charging demand will introduce significant impacts on the secure and economical operation of distribution networks. These negative influences mainly include,

- Distribution network loss increase
- Distribution network lines and substations overload
- Voltage deviations

- Peak demand necessitating additional investment

The distribution network loss on electric power lines and substations depends on both resistance/reactance values of distribution lines, and active/reactive power of electricity demands. The resistance and reactance of distribution networks are relatively large compared with that in transmission system and the EV charging demand arising as additional load will lead to huge economic loss in distribution system operation. It will either make some distribution network equipment overload or necessitate additional investment. Voltage deviation is one of the major issues caused by large-scale EV charging demand. Case study in [9] demonstrates that the voltage of residential distribution grid will drop very likely below 0.95 p.u. when the uncontrolled EV charging demand increase.

Coordinated and smart charging control of EVs is the widely-accepted method to address these negative impacts. Charging behavior can be defined as a combination of the characteristics including travel starting and end time, charging duration, and charging decision [13]. The fact that an average vehicle is most of the time parking and connected to the grid makes an electric vehicle flexible regarding the charging time schedule, known as EV charging flexibility [14]. By rescheduling the EV charging demand, some benefits to power distribution networks can be achieved, which should include loss reduction, congestion avoidance, voltage profile improvement. These EV charging behavior can be defined as coordinated charging or smart charging [15-18]. Many researches in open literatures demonstrate that significant voltage drop in DN can be prevented via using optimal EV flexible charging strategy by properly rescheduling the EV charging demand [14, 19-21]. With distributed generators increasingly installed in distributed networks, coordination of EVs and DGs is receiving increased concerns in recent years. The integration of DGs introduces new challenges for distribution network operation and planning, largely because the design of distribution network relying on the assumption that power flow is unidirectional. Historically, the penetration of DGs was relatively small and therefore can be regarded as negative loads in system operation and planning. But the situation is changing with the increase of DG penetration. With more renewable energies penetrating into power systems, they will inevitably bring many uncertainties to distribution network

operation and planning. As such, the potentials of EVs to provide alternatives for accommodating more DGs and improving overall social warfare become attractive.

Although EV charging flexibility can be well utilized to serve the grid, challenges to optimally dispatch these resources arise. EVs cannot be scheduled directly by the power system operators as EVs spread over a geographic span and EV drivers have their own travel patterns. In this regard, the concept of EV aggregator has been proposed by many researches for the sake of management of large number of EVs. It acts as an intermedia between EV owners and power systems by representing EV owners to interact with power system operators to participate in electricity market. Especially aggregated EVs can be used to provide operating reserve for power system through quickly interrupting EV charging and feeding energy back to the grid, known as V2G. However, the implementation of charging interruption and V2G will considerably affect user experience and travel behavior and lead to battery degradation, which prevent frequent action of such functions. Thus, they are more likely used for providing contingency reserve with less activations, i.e., to provide energy when high-capacity generation break down. For the sake of cost saving, power system spinning reserve requirement, traditionally provided by thermal generators, can be somewhat reduced.

1.2 Purpose of the Thesis

This thesis aims at analyzing the challenges and opportunities introduced by large-scale EV charging in power system and developing new method to utilize EV charging flexibility to benefit power system economic and secure operation. Thus, the purpose of the thesis involves two aspects: to evaluate the negative impact as well as the benefits to the grid and EV owners by introducing large scale EV penetration. Specifically, this thesis innovatively proposes the concept of EV chargeable region to evaluate distribution system electric vehicle hosting capacity and proposes the framework for distributed generator investment to further improve distribution network hosting capacity. Then this thesis analyzes the potential ability of aggregated EV charging in providing ancillary service and proposes risk based bidding strategy for EV aggregators in electricity market.

Firstly, this thesis evaluates distribution network EV hosting capacity. It aims at addressing the negative impacts, such as voltage drop and equipment overload,

caused by large-scale EV charging demand, based on which the concept of EV chargeable region is proposed to estimate how much EV charging demand can be accommodated in a distribution network. The EV chargeable region dynamically varies according to distribution system operation conditions, such as constantly changing load and controllable resources. Generally, several goals should be achieved to find an optimal EV chargeable region, which should include maintaining distribution system security, satisfying EVs' charging requirement, simplifying information exchange between EV owners and distribution system and managing EV charging uncertainties.

Secondly, this thesis proposes a novel distributed generator investment framework considering EV and DG coordination. DG investment in distribution system is another alternative to address the aforementioned negative impact through locally supplying energy to owners. Especially the renewable distributed generators can be well coordinated with EV charging demand by utilizing the flexibility of EV charging demand, which can better reduce the total operation costs. This thesis proposes a robust optimization based DG investment framework to accommodate EV charging demand, which should hedge against various uncertainties including EV penetration level, conventional load increase, coordinated charging participation rate and daily output of renewable energies and EV charging demand.

Thirdly, this thesis evaluates the potential ability of aggregated EV charging and discharging to provide operating reserve for power systems. Especially EVs are assumed to provide contingency reserve, i.e., to supply energy through charging interruption and vehicle to grid service when generator outage induced energy deficit happen. This thesis aims at executing comprehensive cost/benefit analysis to compare the reserve provision cost of thermal generators and EVs. Similar to expected energy not supplied, expected energy supplied by EV is formulated to quantify EVs' provision of operating reserve. This thesis also systematically investigates the impacts of the EV penetration level and the compensation to EV owners on spinning reserve provision.

Fourthly, this thesis proposes risk-based bidding strategies for EV aggregators to participate in electricity market. In the context of electricity market and smart

grid, the uncertainty of electricity prices due to the high complexities involved in market operation would significantly affect the profit and behavior of EV aggregators. To address electricity market price uncertainties, the thesis proposes an information gap decision theory based approach to optimize day-ahead scheduling of EV aggregators and bidding decisions. It focuses on the gap between predicted and actual variables. The IGDT-based risk management decision model is formulated according to the decision makers' attitudes towards risk. Risk-averse decision makers tend to make robust decisions against high costs, while risk-taking decision makers tend to seek more benefits when the cost is low.

1.3 Primary contributions

To achieve the objectives of the research, the scientific contributions achieved in this thesis are summarized as follows:

1. The thesis models EV charging demand and the uncertainties using data mining method. Previous works usually use Monte Carlo simulation method to generate user travel behaviour data from either the travel statistical results in travel survey reports or a self-defined distribution function of travel parameters [13, 15-19]. In comparison, this thesis obtains EV charging profile by directly sampling with the replication from raw vehicle travel data, which can better resemble the reality.
2. The concept of "EV chargeable region" is innovatively proposed to evaluate the largest amount of EV charging demand under a DN node that will not lead to network constraint violations. The EV chargeable region optimization problem is formulated as a two-stage model, where the EV chargeable region and DN decision variables are optimized in the first stage and the feasibility of the DN worst-case scenario is checked in the second stage. This model not only guarantees the secure operation of DN, but also maximizes the EV hosting capacity for DN. Compared with the previous EV aggregator-oriented coordinated charging strategy method, the proposed model is user-friendly and enforceable for practical application.
3. The framework of robust active distribution network planning against

uncertain EV charging demand and distributed generators is proposed. Security constraints of active distribution network, such as upper and lower bound of voltage and branch capacity, are imposed to enforce the feasibility of the planning strategy. A two-stage robust optimization formulation is established, where the first stage problem optimizes the sizing and sitting of distributed generation, and the second stage problem checks the feasibility of planning strategy in the worst realization of uncertainties of both uncertain EV charging demand and renewable distributed generators is proposed.

4. EVs are innovatively considered in the determination of power system spinning reserve requirement. The costs of reserves from thermal generators and EVs as well as expected energy not supplied (EENS) are taken into account together to determine optimal spinning reserve requirement. The concept of expected energy supplied by EV (EESEV) is innovatively proposed in the study to quantify the expected energy supplied by EVs. The EVs' capacity of interruptible charging demand and V2G service under both smart charging and immediate charging strategy is formulated.
5. An information gap decision theory based day-ahead EV scheduling and bidding framework is proposed to take into consideration the electricity price. It enables EV aggregators to manage potential risks while pursuing the desired profit. Through ensuring a predetermined level of total profit, both robust and opportunistic scheduling strategies are made for negative and positive decision makers respectively. Compared with other risk management tool such as conditional value at risk, the proposed approach can effectively enable decision makers to secure the desired profit irrespective of the potential risks and reduces computation burdens.

1.4 Organization of the Thesis

The remainder of this thesis is organized as follows,

Chapter 2 proposes the concept of an EV chargeable region to evaluate the distribution network EV hosting capacity, i.e., how much EV charging demand

can be accommodated in a distribution network, within which the technical constraints of distribution network (e.g., voltage deviation) are guaranteed and EV owners' charging requests are maximally ensured. The optimization of the EV chargeable region is formulated as a two-stage robust optimization model with adjustable uncertainty set. The EV chargeable region and distribution network decision variables are optimized in the first stage and the feasibility in the real-time worst-case scenario is checked in the second stage, considering the uncertainty of EV charging demand and distribution network active and reactive power. A modified column & constraint generation and outer approximation method is adopted to address the proposed problem. Simulations on an IEEE 123-node DN demonstrate the effectiveness of the proposed model.

Chapter 3 proposes a two-stage robust active distribution network planning model capable of accommodating uncertain large-scale EV charging demand. The distributed generator investment location and size are optimized in the first stage and the active distribution network operation feasibility in the worst-case scenario is checked in the second stage to avoid various constraint violations. The EV charging demand uncertainty is modeled using a data mining method based on raw data of vehicle travel behavior. Finally, a modified column-and-constraint generation algorithm is adopted to solve the proposed problem. Simulations on modified IEEE 123-node distribution network demonstrate the effectiveness of the proposed model.

Chapter 4 proposes a novel model to optimize day-ahead spinning reserve requirement considering EVs' contribution in providing operating reserve. Based on the probabilistic criteria, the cost of expected energy supplied by EV (EESEV) is formulated. The capacities of EV interruptible charging demand and vehicle to grid service are calculated respectively under the conditions of both immediate charging and smart charging strategies. The effects of EVs on system spinning reserve requirement quantification, unit commitment are comprehensively analyzed using IEEE reliability test system (RTS-96). Numerical results systematically demonstrate the effectiveness of EVs' participation on the reduction of operation costs and the improvement of power system reliability.

Chapter 5 proposes an information gap decision theory based approach to manage the revenue risk of the EV aggregator caused by the information gap between the forecasted and actual electricity prices. The proposed decision-making framework is used to offer effective strategies to either guarantee the predefined profit for risk-averse decision makers, or pursue the windfall return for risk-seeking decision makers. Day-ahead charging and discharging scheduling strategies of the EV aggregators are arranged using the proposed model considering the risks introduced by the electricity price uncertainty. The results of case studies validate the effectiveness of the proposed framework under various price uncertainties.

Chapter 6 gives the conclusions and the discussion of the thesis.

2. Distribution Network Electric Vehicle Hosting Capacity Maximization: A Chargeable Region Optimization Model

2.1 Introduction

Smart/coordinated charging strategy of EVs is the commonly accepted method to improve voltage quality in distribution system [4-11]. Many researches in literatures show that significant voltage drop in distribution network can be avoided utilizing the flexibility of EV charging strategy by optimally rescheduling the EV charging demand [4-6]. Lots of implementation algorithms and models of smart/coordinated charging strategies are proposed to handle the voltage issues. [7] proposes a market mechanism for aptimal allocation of available charging capacity ensuring EV owners' preferences on charging rates and distribution network voltage security. [8] develops a market based multi-agent control mechanism using remaining capacity of EV chargers for reactive voltage control, in which the iterative exchange of messages is not considered. A real-time smart load management strategy is developed in [9] for the coordination of EV charging based on real-time such as every 5 min, minimization of total operation cost at the same time complying with network operation requirement. A rolling multi-period optimization based EV charging optimization method is developed in reference [10], to avoid severe voltage deviations and equipment overload with the input data updated at each time step. A local control method for EV smart charging strategy in distribution network is developed. The advantage and disadvantage of centralized and local EV charging strategy are compared and discussed.

Moreover, considering the fact that the large number of EVs cannot be managed directly by the power system, the EV aggregator is thus proposed to manage a large number of EVs, which acts as an intermediary to communicate with power system operators so that the distribution network operation security can be ensured [12-14]. [13] presents hierarchical decomposition model to minimize the total cost of dispatched generators and EV aggregators in the upper-level model and to present specific charging strategies in the lower-level model. However, using these methods, the basic assumption is that the EV aggregator obtains the privilege from EV owners to determine the schedule of EVs as long as the customers' travel demand is satisfies. This implies that EV owners should report their required energy and daily departure time to the EV aggregator, which will create inconvenience for end users. Another problem is that demands for unexpected and urgent usage of EVs may not be satisfied, because EV aggregator can not obtain this information in advance by. Besides, it is uncertain whether complex communication facilities will be generated among the distribution network operators, EV aggregators, and EV owners in the distribution networks.

To address these problems, EVs are firstly assumed charged randomly according to users' requests. Then EV hosting capacity is maximized by finding out the largest admissible charging demand at each distribution network node that can be accommodated. Within the hosting capacity, the line capacity and DN voltage will not vary beyond the requirement. Outside of the hosting capacity, the EV charging demand may be postponed. The EV chargeable region problem is formulated as a two-stage optimization model, in which the EV chargeable region and distribution network decision variables are optimized in the first stage and the feasibility of the distribution network worst-case scenario is checked in the second stage. Using this model, not only the secure operation of distribution network is guaranteed, but also the EV hosting capacity for distribution network is maximized.

The nomenclature of symbols used in this chapter are given as follows,

Indices and Sets

t/T	Index and set of time slots.
k/K	Index and set of the trips whose destination is home
$N_{c,t}^{'}$	Set of EV charging demand in all scenarios

γ/Γ	Index and set of piecewise linearization approximation method, in which Γ^{DE}, Γ^{AP}, Γ^{RP} represent set for PLA method of EV delayed charging demand, quadratic term of active and reactive power respectively
j/J	Index and set of distribution network nodes.
c/C	Index and set of EV charging equipment.
r/R	Index and set of reactive power support equipment, such as shunt capacitors and automatic voltage regulators.
$\delta(j)$	Set of child nodes of distribution network node j.
$\Psi_{EV}/\Psi_{RP}(J)$	Set of EV charging equipment and reactive power support facilities under distribution network node j.

Parameters

P^{ch}	EV charging rate.
t_k^{arr},t_k^{dep}	EV arrival and departure time at k.
DT_k	Travel distance during the day at k.
E_{CS}	Per-mile energy consumption.
η_{ch}	Efficiency of EV charging demand.
$P_{c,t,s}^{CH,S}$	Aggregated charging demand at c,t in scenario s
$P_{c,t}^{CH,AV}$	Average aggregated EV charging demand at c,t.
$P_{c,t}^{EV,max}$	Maximum EV charging demand at c,t.
$K_{\gamma,c,t}^{PDF}/B_{\gamma,c,t}^{PDF}$	Linearization approximation auxiliary coefficients for EV charging demand PDF function
$K_{\gamma,c,t}^{DE}/B_{\gamma,c,t}^{DE}$	Linearization approximation auxiliary coefficients for delayed EV charging demand
$p_{j,t}/q_{j,t}$	Active and reactive power load at j,t.
r_{ij}/x_{ij}	Resistance and reactance of DN line ij.
V_0	Voltage reference value.
V_{ST}	Voltage at distribution network substation.
ζ_r	Step value of shunt capacitor r.
$Q_{r,t}^{AVR,AV}$	Automatic voltage regulator average output at r,t.
LC_{ij}	Distirbution network line capacity at ij.
ε	Limitaiton of voltage fluctuation.
λ_t	Electricity price at t.
$P_{c,t}^{CH,LB}$	Lower bound of EV charging demand at c,t.

$\Lambda_t^{CH}/\Lambda_c^{CH}$	Uncertainty budget of EV charging demand at t and at c.
$p_{j,t}^{LB}/p_{j,t}^{UB}$	Lower and upper bound of active power at *j*,*t*.
$\Lambda_t^{AP}/\Lambda_c^{AP}$	Uncertainty budget of active power at t and at c.
$q_{j,t}^{LB}/q_{j,t}^{UB}$	Lower and upper bound of reactive power at *j*,*t*.
$\Lambda_t^{RP}/\Lambda_c^{RP}$	Uncertainty budget of reactive power at t and at *c*.
$Q_r^{AVR,LB}/Q_r^{AVR,UB}$	Lower and upper bound of automatic voltage regulator output of *r*.

Variables

$P_{k,t}^{ch}$	Per EV charging rate at *k*,*t*
$DE_{c,t}$	Delayed EV charging demand at *c*,*t*.
$CC_{c,t}$	Compensation cost for EV charging demand delay at *c*,*t*.
$P_{c,t}^{CH}$	Average EV charging demand *c*,*t*.
$P_{c,t}^{Bound}$	EV chargeable bound at *c*,*t*.
$\chi_{c,t}$	Actual EV charging demand at *c*,*t*.
$P_{j,t}/Q_{j,t}$	Active and reactive power flow at *j*,*t*.
$P_{j,t}^{QU}/Q_{j,t}^{QU}$	Quadratic term of active and reactive power flow at *j*,*t*.
$V_{j,t}$	Voltage at *j*,*t*.
$d_{r,t}^{SC}$	Integral variables for shunt capacitors at *r*,*t*.
$VP_{c,t}^{CH}$	Real-time EV charging demand at *c*,*t*.
$Vp_{j,t}/Vq_{j,t}$	Real-time active and reactive power at *j*,*t*.
$Q_{r,t}^{AVR}$	AVR output at *r*,*t*.
$P_{j,t}^{W}/Q_{j,t}^{W}$	Real-time worst-case active and reactive power flow at *j*,*t*.
$P_{j,t}^{QU,W}/Q_{j,t}^{QU,W}$	Quadratic term of real-time worst-case active and reactive power flow at *j*,*t*.
$V_{j,t}^{W}$	Worst-case real-time voltage at *j*,*t*.
$S_{j,t}^{V}/S_{j,t}^{PQ}$	Slack variables of real-time voltage deviation requirement and distirbtion network line capacity limitation at *j*,*t*.

2.2 EV Charging Demand Uncertainty

2.2.1 EV Travel Behavior

It is commonly known that location-varying and time-varying EV charging demand can be modeled based on EV owners' travel behavior. Monte Carlo simulation method is mostly used to acquire EV owners' travel behavior data on

the basis of travel survey reports, where the the charging demand of each vehicle and the parking duration can be estimated [22-24]. To model spatial-temporal dynamics of EVs' charging demand, some other works use self-defined hypothetical distribution functions to randomly generat daily trip chains [25-27].

In contrast, the uncertainty of charging behavior in the proposed framework is modeled by sampling directly from the 2011 Raw Data of Travel Behavior, which is released by the Atlanta Regional Commission. It can be found in the ARC Metropolitan Travel Survey Archive[28]. This survey dataset includes totally 119,480 trips, which is collected within 3 months. For each trip, the information given by the data includes: arrival time, arrival location, departure time, departure location, trip distance, transit access mode, and so on. The large number of trips and the comprehensive record of each trip provide valuable assistance to model the uncertainty of EV charging demand. In this thesis, it is firstly assumed that EVs are charged once arriving home, and the each EV charging demnad can be formulated as

$$P_{k,t}^{\mathrm{ch}} = P^{ch},\ if\ \ t \geq t_k^{\mathrm{arr}}\ \&\, t \leq \frac{DT_k E_{CS}}{\eta_{\mathrm{ch}} P^{ch}} + t_k^{\mathrm{arr}}\ \&\, t \leq t_k^{dep}, \forall k \in K, \forall t \in T \qquad (2.1)$$

where κ and K are the index and set of the trips whose destination is home. It will trigger the charging reaction. P^{ch} denotes the fixed charging rate, randomly selected from the predefined charging power dataset with corresponding probability. DT_K represents the total travel distance in the day, E_{CS} represents the per-mile energy consumption, η_{ch} is the efficiency of EV charging, and t_k^{arr} and t_k^{dep} denote the *EV* arrival and departure time.

Sampling with the replication method is proposed to model the aggregated charging demand under a distribution network node with N_k total EVs as well as to randomly select N_k samples from the EV charging demand database *K*. By summarizing them, one scenario of charging demand at each distribution network node is obtained. By repeating this procedure, various scenarios can be found, given as

$$P_{c,t,s}^{CH,S} = \sum_{k \in N_{c,s}} P_{k,t}^{\mathrm{ch}}, c \in C, t \in T, s \in S \qquad (2.2)$$

$$P_{c,t}^{CH,AV} = \frac{1}{\left|N_{c,t}^{'}\right|} \sum_{s \in N_{c,t}^{'}} P_{c,t,s}^{CH,S}, c \in C, t \in T \tag{2.3}$$

where $P_{c,t,s}^{CH,S}$ represents the total charging demand under a distribution network node c in scenario s and $P_{c,t}^{CH,AV}$ represens its average value, in which $|\cdot|$ denotes the Cardinality of the set. When the sample size S becomes large enough, the uncertainty of charging demand can be optimally modeled and the estimated cumulative distribution function can be thus obtained from the statistical results.

2.2.2 Delayed EV Charging Demand

In this subsection, the relationship between the EV chargeable region and the compensation cost of delayed charging energy is illustrated based on the statistical results of EV charging demand uncertainties. As discussed before, when the charging demand is larger than the chargeable region upper boundary, the excessive portion of the energy should be delayed, as follows:

$$DE_{c,t} = \int_{P_{c,t}^{Bound} - DE_{c,t-1}}^{P_{c,t}^{EV,\max}} (\chi_{c,t} - P_{c,t}^{Bound} + DE_{c,t-1}) g(\chi_{c,t}) d\chi_{c,t}, \forall c \in C, \forall t \in T \tag{2.4}$$

$$g(\chi_{c,t}) \geq K_{\gamma,c,t}^{PDF} \chi_{c,t} + B_{\gamma,c,t}^{PDF}, \forall \gamma \in \Gamma^{DE}, \forall c \in C, \forall t \in T \tag{2.5}$$

where (2.4) describes the relationship between electric vehicle chargeable bound $P_{c,t}^{Bound}$ and delayed charging energy $DE_{c,t}$. $\chi_{c,t}$ represents the actual EV charging demand, and $g(\chi_{c,t})$ represents the probability distribution function of $\chi_{c,t}$. The PDF function is found from formulation in (2.5) using the PLA, rather than the exact distribution function, in which $K_{\gamma,c,t}^{PDF}$ and $B_{\gamma,c,t}^{PDF}$ are the auxiliary coefficients of linearization approximation. The PDF is actually the linearly estimated gradient of its CDF, obtained from the sampling results found in subsection IIA. It should be noted that the delayed energy is influenced not only by the chargeable bound but also by the charging demand increase due to the delayed energy of the last time interval, as shown in (2.4). Then, the delayed EV charging energy is acquired as the cumulative energy between the boundary and the maximum EV charging demand $P_{c,t}^{EV,max}$. However, (2.4) and (2.5) are still difficult to solve due to the nonlinearity and the integral term of $\chi_{c,t}$. To address this problem, the PLA method is used to find out the approximate linear term of (2.4) and (2.5). Finally, the EV charging demand can be given as:

$$CC_{c,t} \geq K_{\gamma,c,t}^{DE}(P_{c,t}^{Bound} - DE_{c,t-1}) + B_{\gamma,c,t}^{DE}, \forall \gamma \in \Gamma^{DE}, \forall c \in C, \forall t \in T \quad (2.6)$$

$$P_{c,t}^{CH} = P_{c,t}^{CH,AV} + DE_{c,t-1} - DE_{c,t}, \ \forall c \in C, \forall t \in T \quad (2.7)$$

$$DE_{c,t} \in R^{+}, CC_{c,t} \in R^{+}, P_{c,t}^{CH} \in R^{+}, P_{c,t}^{Bound} \in R^{+}, \forall c \in C, \forall t \in T \quad (2.8)$$

where (2.6) are the linearization approximate versions of constraint (2.4) and (2.5). They are auxiliary constraints generated by the PLA, in which $K_{\gamma,c,t}^{DE}$ and $B_{\gamma,c,t}^{DE}$ are the linearization approximation constant coefficients. Besides, (2.7) describes the actual charging demand considering the delayed charging energy, with the boundaries of the variables stated in (2.8).

Some remarks on the EV chargeable region is given as follows:

1) An EV controller should be invested at the distribution network node to interrupt the excessive charging demand outside of the chargeable region.
2) The EV charging delay priority can be dependent on the EV charging urgent level, such as the remained EV charging demand. The EVs with larger SOC of the battery is suggested to be interrupted with higher priority, so that the urgent usage of EVs can be guaranteed to the maximum extend.
3) EV onwers can reschedule their charging profiles according to their intentions. Electricity price based EV charging mode is considered and discussed in the case study.

2.3 Mathematical Model

2.3.1 Distribution Network Operation Constraints

The complex distribution network power flow at each node j can be modeled using DistFlow equations from [29]:

$$P_{j,t} = \sum_{i \in \delta(j)} P_{i,t} + \sum_{i \in \delta(j)} r_{ij} \frac{P_{i,t}^2 + Q_{i,t}^2}{V_{i,t}^2} + p_{j,t}, \forall j \in J, \forall t \in T \quad (2.9)$$

$$Q_{j,t} = \sum_{i\in\delta(j)} Q_{i,t} + \sum_{i\in\delta(j)} x_{ij} \frac{P_{i,t}^2 + Q_{i,t}^2}{V_{i,t}^2} + q_{j,t}, \forall j \in J, \forall t \in T \quad (2.10)$$

$$V_{j,t}^2 = V_{i,t}^2 + 2(r_{ij}P_{i,t} + x_{ij}Q_{i,t}) - (r_{ij}^2 + x_{ij}^2)\frac{P_{i,t}^2 + Q_{i,t}^2}{V_{i,t}^2}, \forall j \in J, i \in \delta(j), \forall t \in T \quad (2.11)$$

where (2.9) describes the active power flow, (2.10) describes the reactive power flow, and (2.11) describes the voltage transmit along the branch. To handle the nonlinearity issues, the linear version of the DistFlow equations is presented and justified from [29, 30] by Baran and Wu, which is later adopted by lots of researchers [31-33]. The approximation method is proposed based on two assumptions. First, the nonlinear terms denoting the loss is much smaller than the branch power P_j, Q_j and voltage terms V_j^2, so that they can be neglected in the calculation of power flow. Second, the approximation of $(V_j - V_0)^2 = 0$ is adopted. It is valid as long as the voltage deviation is always within the requirement and the quadratic terms of voltage can be replaced.

Compared with the previous work involving a linear version of Distflow, the *piecewise linearized Distflow* is presented in this thesis, which is achieved by linearizing the quadratic terms of active power and reactive power so that the loss terms can be maintained. The set of power flow, taking into consideration linearization, EV charging demand, and reactive power facilities, can be characterized by the following constraints:

$$P_{j,t} = \sum_{i\in\delta(j)} P_{i,t} + \sum_{i\in\delta(j)} r_{ij} \frac{P_{i,t}^{QU} + Q_{i,t}^{QU}}{V_0^2} + p_{j,t} + \sum_{c\in\Psi_{EV}(j)} P_{c,t}^{CH}, \forall j \in J, \forall t \in T \quad (2.12)$$

$$Q_{j,t} = \sum_{i\in\delta(j)} Q_{i,t} + \sum_{i\in\delta(j)} x_{ij} \frac{P_{i,t}^{QU} + Q_{i,t}^{QU}}{V_0^2} + q_{j,t} + \sum_{r\in\Psi_{RP}(j)} (d_{r,t}^{SC}\zeta_r V_{j,t} + Q_{r,t}^{AVR,AV}), \forall j \in J, \forall t \in T \quad (2.13)$$

$$V_{j,t} = V_{i,t} + \frac{r_{ij}P_{i,t} + x_{ij}Q_{i,t}}{V_0} - (r_{ij}^2 + x_{ij}^2)\frac{P_{i,t}^{QU} + Q_{i,t}^{QU}}{2V_0^3}, \forall j \in J, \forall i \in \delta(j), \forall t \in T \quad (2.14)$$

$$V_{j,t} = V_{ST}, j = 1, \forall t \in T \quad (2.15)$$

where constraints (2.12)–(2.14) are modified from constraints (2.9)–(2.11), where $P_{j,t}^{QU}$ $Q_{j,t}^{QU}$ are used to estimate the quadratic terms of $P_{j,t}$ $Q_{j,t}$ and the EV charging demand and the reactive power output of shunt capacitors and AVRs are taken into

consideration in calculating the power flow. The disposition of the quadratic terms of transmitting voltage is similar to that in the previous work, while the voltage in the $V_{j,t} = V_{ST}, j = 1, \forall t \in T$ denominator of the voltage drop terms is replaced by its reference value. It is acceptable as long as the loss term is much small. Anyway it is more accurate than neglecting the whole terms. The substation voltage is set as V_{ST}, defined by (2.15). The quadratic terms $P_{j,t}^{QU} Q_{j,t}^{QU}$ can be obtained using the PLA method according to the following auxiliary constraints:

$$P_{j,t}^{QU} \geq K_{\gamma,j,t}^{AP} P_{j,t} + B_{\gamma,j,t}^{AP}, \forall j \in J, \forall \gamma \in \Gamma^{AP}, \forall t \in T \tag{2.16}$$

$$Q_{j,t}^{QU} \geq K_{\gamma,j,t}^{RP} Q_{j,t} + B_{\gamma,j,t}^{RP}, \forall j \in J, \forall \gamma \in \Gamma^{RP}, \forall t \in T \tag{2.17}$$

where $K_{\gamma,c,t}^{AP}$ $K_{\gamma,c,t}^{RP}$ and $B_{\gamma,c,t}^{AP}$ $B_{\gamma,c,t}^{RP}$ are the linearization approximation constant coefficients. The operation limitation constraints are given as

$$P_{j,t}^{QU} + Q_{j,t}^{QU} \leq LC_{ij}^{2}, \forall j \in J, \forall i \in \delta(j), \forall t \in T \tag{2.18}$$

$$1 - \varepsilon \leq V_{j,t} \leq 1 + \varepsilon, \forall j \in J, \forall t \in T \tag{2.19}$$

where (2.18) describes the distribution network branch active and reactive power limitation and (2.19) describes the voltage fluctuation limitation.

2.3.2 EV Chargeable Region Optimization Model

This subsection presentes a two-stage EV chargeable region optimization framework is. To maintain the distribution network voltage deviation within the requirement and to minimize the distribution network line loss, the coordination of shunt capacitors and automatic voltage regulators is commonly used. In practice, shunt capacitors cannot react continually and immediately based on the rapid fluctuation of demand and voltage in the distribution network, so that the automatic voltage regulators can respond immediately to the real-time distribution network status. Besides, the EV chargeable region is assumed to be optimized on a day-ahead basis before the uncertainty is revealed. In this way, the real-time interaction and complex communication between the EV owners and the EV aggregators are avoided.

In this regard, a two-stage robust optimization framework is proposed to find out the optimal EV chargeable region and distribution network decision variables,

hedging against any possible realization of uncertainty. The distribution network uncertainty contains EV charging demand and other active/reactive power loads. Therein, shunt capacitors, the chargeable region, and expected DN operation variables is regarded as the first-stage decision variables, served as "here-and-now," which cannot be modified after the uncertainty is revealed, while the automatic voltage regulators and real-time power flow is regarded as the second-stage decision variables, served as "wait-and-see," which will respond according to the uncertainties. It should be mentioned that both distributed generators and other schedulable loads in distribution system can be modeled as second-stage "wait-and-see" variables and thus infuence EV chargeable region. But they are not taken into account, as this thesis focuses on the EV charging demand itself. Thus, the average operation cost is factored into the first-stage decision-making and the feasibility in the real-time worst-case scenario is checked during the second-stage decision-making, with the following formulation:

$$min \sum_{t\in T}(\lambda_t \sum_{ij\in L} r_{ij} \frac{P_{j,t}^{QU}+Q_{j,t}^{QU}}{V_0^2} + \sum_{c\in C} CC_{c,t}) \tag{2.20}$$

s.t. (2.6)–(2.8),(2.12)–(2.15),(2.16)–(2.17),(2.18)–(2.19)

$$(\max_{M_1\in\Omega_{US}(P_{c,t}^{Bound})} \min_{M_2\in\Omega_{WS}(d_{r,t}^{SC})} \sum_{t\in T}\sum_{j\in J} S_{j,t}^{V} + S_{j,t}^{PQ}) = 0 \tag{2.21}$$

The objective function (2.20) aim at minimizing total distribution network operation cost, where the first term denotes the total distribution network line loss and the second term denotes the compensation cost given to the EV owners due to the charging delay. Power flow constraints, active/reactive power quadratic term linearization, and the operation limitation are given in (2.6)–(2.8) and (2.12)–(2.17), respectively in subsection IIIA. The relationship among EV charging demand delay, EV chargeable boundary, and the compensation cost is illustrated in (2.18)–(2.19). Constraints (2.21) are used to check the feasibility of the real-time worst-case scenario, given the EV chargeable region and the operation status of shunt capacitors, where $S_{j,t}^{V}$ and $S_{j,t}^{PQ}$ represent the slack variables of voltage deviation constraints and distribution network line capacity deviation constraints. The distribution network operation is secure on the condition that all the slack variables are zero in all the scenarios. The uncertainty set $\Omega_{US}(\cdot)$ in constraint (2.21) is defined as follows:

$$\Omega_{US}(P_{c,t}^{Bound}) = \{ \quad M_1 : \; M_1 = [VP_{c,t}^{CH}, Vp_{j,t}, Vq_{j,t}] \sum_{c \in C} VP_{c,t}^{CH} \le \Lambda_t^{CH}, \forall t \in T$$

$$VP_{c,t}^{CH} \le P_{c,t}^{Bound}, \forall c \in C, \forall t \in T \tag{2.22}$$

$$VP_{c,t}^{CH} \ge P_{c,t}^{CH,LB}, \forall c \in C, \forall t \in T \tag{2.23}$$

$$\sum_{c \in C} VP_{c,t}^{CH} \le \Lambda_t^{CH}, \forall t \in T \tag{2.24}$$

$$\sum_{t \in T} VP_{c,t}^{CH} \le \Lambda_c^{CH}, \forall c \in C \tag{2.25}$$

$$Vp_{j,t} \ge p_{j,t}^{LB}, j \in J, \forall t \in T \tag{2.26}$$

$$Vp_{j,t} \le p_{j,t}^{UB}, j \in J, \forall t \in T \tag{2.27}$$

$$\sum_{j \in J} Vp_{j,t} \ge \Lambda_t^{AP}, \forall t \in T \tag{2.28}$$

$$\sum_{\forall t \in T} Vp_{j,t} \ge \Lambda_j^{AP}, j \in J \tag{2.29}$$

$$Vq_{j,t} \ge q_{j,t}^{LB}, j \in J, \forall t \in T \tag{2.30}$$

$$Vq_{j,t} \le q_{j,t}^{UB}, j \in J, \forall t \in T \tag{2.31}$$

$$\sum_{j \in J} Vq_{j,t} \ge \Lambda_t^{RP}, \forall t \in T \tag{2.32}$$

$$\sum_{\forall t \in T} Vq_{j,t} \ge \Lambda_j^{RP}, j \in J \quad , \tag{2.33)}\}$$

where the uncertainty set $\Omega_{US}(\cdot)$ containes three kinds of variables, i.e., EV charging demand, active power, and reactive power. As the EV charging demand and the active power and reactive power at each distribution node can not be precisely forecasted on a day-ahead basis, they are regarded as variables in the second-stage optimization in order to find the real-time worst-case scenario. Constraints (2.22)–(2.25) represent the uncertainty set of EV charging demand, (2.26)–(2.29) represent the uncertainty set of active power and constraints, and (2.30)–(2.33) represnet the uncertainty set of reactive power. In each set, the bound of the variables and the uncertainty budget at each time interval or at each distribution network node are defined respectively. It should be noticed that the uncertainty set $\Omega_{US}(\cdot)$ is influenced by the first-stage variable EV chargeable

bound. The worst-case feasibility set $\Omega_{WS}(\cdot)$ of constraint (2.21) is listed as follows:

$$\Omega_{WS}(d_{r,t}^{SC}) = \{ M_2 :$$

$$M_2 = [P_{j,t}^{W}, Q_{j,t}^{W}, P_{j,t}^{QU,W}, Q_{j,t}^{QU,W}, V_{j,t}^{W}, Q_{r,t}^{AVR}, VP_{c,t}^{CH}, Vp_{j,t}, Vq_{j,t}, S_{j,t}^{V}, S_{j,t}^{PQ}]$$

$$P_{j,t}^{W} = \sum_{i\in\delta(j)} P_{i,t}^{W} + \sum_{i\in\delta(j)} r_{ij} \frac{P_{i,t}^{QU,W} + Q_{i,t}^{QU,W}}{V_0^2} + Vp_{j,t} + \sum_{c\in\Psi_{EV}(j)} VP_{c,t}^{CH}, \forall j \in J, \forall t \in T \tag{2.34}$$

$$Q_{j,t}^{W} = \sum_{i\in\delta(j)} Q_{i,t}^{W} + \sum_{i\in\delta(j)} x_{ij} \frac{P_{i,t}^{QU,W} + Q_{i,t}^{QU,W}}{V_0^2} + Vq_{j,t} + \sum_{r\in\Psi_{RP}(j)} (d_{r,t}^{SC}\zeta_r V_{j,t}^{W} + Q_{r,t}^{AVR}), \forall j \in J, \forall t \in T \tag{2.35}$$

$$V_{j,t}^{W} = V_{i,t}^{W} + \frac{r_{ij}P_{i,t}^{W} + x_{ij}Q_{i,t}^{W}}{V_0} - (r_{ij}^2 + x_{ij}^2)\frac{P_{i,t}^{QU,W} + Q_{i,t}^{QU,W}}{2V_0^3}, \quad \forall j \in J, \forall i \in \delta(j), \forall t \in T \tag{2.36}$$

$$V_{j,t}^{W} = V_{ST},\ j = 1, \forall t \in T \tag{2.37}$$

$$P_{j,t}^{QU,W} \geq K_{\gamma,j,t}^{AP} P_{j,t}^{W} + B_{\gamma,j,t}^{AP}, \forall j \in J, \forall \gamma \in \Gamma^{AP}, \forall t \in T \tag{2.38}$$

$$Q_{j,t}^{QU,W} \geq K_{\gamma,j,t}^{RP} Q_{j,t}^{W} + B_{\gamma,j,t}^{RP}, \forall j \in J, \forall \gamma \in \Gamma^{RP}, \forall t \in T \tag{2.39}$$

$$P_{j,t}^{QU,W} + Q_{j,t}^{QU,W} - S_{j,t}^{PQ} \leq LC_{ij}, \forall j \in J, \forall i \in \delta(j), \forall t \in T \tag{2.40}$$

$$1 - \varepsilon \leq V_{j,t}^{W} + S_{j,t}^{V}, \forall j \in J, \forall t \in T \tag{2.41}$$

$$Q_{r}^{AVR,LB} \leq Q_{r,t}^{AVR} \leq Q_{r}^{AVR,UB}, \forall r \in R, \forall t \in T \tag{2.42}$$

$$P_{j,t}^{QU,W}, Q_{j,t}^{QU,W}, S_{j,t}^{V}, S_{j,t}^{PQ} \in R^{+}, \forall j \in J, \forall t \in T \ \ , \tag{2.43)\}}$$

where power flow in the real-time worst-case scenario is demonstrated by (2.34)–(2.37). Different from the first-stage power flow in (2.12)–(2.15), EV charging demand, active power, and reactive power become variables which are quantified in uncertainty set (2.22)–(2.33) and the automatic voltage regulator is the real-time controllable variables with the bound defined in(2.42). The first-stage variable $d_{r,t}^{SC}$ is fixed in the real-time worst-case feasibility check. Quadratic terms of active and reactive power flow in the real-time worst-case scenario are linearized in (2.38)–

(2.39). The constraints of voltage deviation requirement and distribution network power flow capacity limitation in the worst-case scenario are relaxed with variables $S_{j,t}^{V}$ and $S_{j,t}^{PQ}$, as shown by (2.40)–(2.41). The boundaries of these variables are quantified by (2.43). It should be mentioned that the feasible region given by constraints (2.20)–(2.33) guarantees the secure and reliable distribution network operation.

2.4 Solution Methodology

2.4.1 Compact Formulation and Duality

For simplicity, the compact formulation is written in this section as follows:

$$\min_{\mathbf{x_1},\mathbf{x_2},\mathbf{x_3}} \mathbf{a}^{\mathrm{T}}\mathbf{x_1} + \mathbf{b}^{\mathrm{T}}\mathbf{x_3} \tag{2.44}$$

$$\text{s.t.} \quad \mathbf{A}\mathbf{x_1} + \mathbf{B}\mathbf{x}_2 + \mathbf{C}\mathbf{x_3} \le \mathbf{c} \tag{2.45}$$

$$\left(\max_{\mathbf{z_1},\mathbf{z}_2 \in \Omega_{US}(\mathbf{x}_2)} \min_{\mathbf{y},\mathbf{z_1},\mathbf{z}_2,\mathbf{s} \in \Omega_{WS}(\mathbf{x_1})} \mathbf{d}^{\mathrm{T}}\mathbf{s}\right) = 0 \tag{2.46}$$

$$\Omega_{US}(\mathbf{x}_2) = \{\ \mathbf{z_1},\mathbf{z}_2 : \mathbf{D}\mathbf{z_1} + \mathbf{E}\mathbf{x}_2 \le \mathbf{e}, \mathbf{F}\mathbf{z}_2 \le \mathbf{f}\ \} \tag{2.47}$$

$$\Omega_{WS}(\mathbf{x_1}) = \{\ \mathbf{y},\mathbf{z_1},\mathbf{z}_2,\mathbf{s} : \mathbf{G}\mathbf{x_1} + \mathbf{H}\mathbf{y} + \mathbf{I}\mathbf{z_1} + \mathbf{J}\mathbf{z}_2 + \mathbf{K}\mathbf{s} \le \mathbf{g}\ \} \tag{2.48}$$

By the characteristics, the first-stage variables consist of three groups; namely, $\mathbf{x_1} = [d_{r,t}^{SC}]$ denotes the first-stage distribution network decision variable which influences second-stage DN operation status, $\mathbf{x}_2 = [P_{c,t}^{Bound}]$ denotes the one that influences the uncertainty set, and $\mathbf{x_3} = [P_{j,t}, Q_{j,t}, P_{j,t}^{QU}, Q_{j,t}^{QU}, V_{j,t}, DE_{c,t}, CC_{c,t}, P_{c,t}^{CH}]$ represents other first-stage variables. Based on whether or not they are influenced by first-stage variables, the variables in the uncertainty set includes $\mathbf{z_1} = [VP_{c,t}^{CH}]$ and $\mathbf{z}_2 = [Vp_{j,t}, Vq_{j,t}]$, in which the bound of $\mathbf{z_1}$ is quantified by $\mathbf{x}_2$. The second-stage slack variables are denoted as $\mathbf{s} = [S_{j,t}^{V}, S_{j,t}^{PQ}]$ and the second-stage operation variables are given as $\mathbf{y} = [P_{j,t}^{W}, Q_{j,t}^{W}, P_{j,t}^{QU,W}, Q_{j,t}^{QU,W}, V_{j,t}^{W}, Q_{r,t}^{AVR}]$.

The optimization problem (2.44)–(2.48) is a two-stage optimization model, in which the first-stage master problem is described as (2.44)–(2.45) and the second-stage subproblem is given as follows:

$$\max_{\mathbf{z}_1,\mathbf{z}_2\in\Omega_{US}(\mathbf{x}_2)} \min_{\mathbf{y},\mathbf{z}_1,\mathbf{z}_2,\mathbf{s}\in\Omega_{WS}(\mathbf{x}_1)} \mathbf{d}^{\mathrm{T}}\mathbf{s} \tag{2.49}$$

$$\text{s.t. (2.47)-(2.48)} \tag{2.50}$$

Hence, (2.49)-(2.50) is formulated as a bi-level linear optimization program. Due to the strong duality of the linear program, the inner optimization problem is replaced by its dual problem so that (2.49) can be reformulated as a single-level bilinear program, given as follows:

$$\max_{\mathbf{z}_1,\mathbf{z}_2,\boldsymbol{\psi}} \boldsymbol{\psi}^{\mathrm{T}}(\mathbf{g}-\mathbf{G}\mathbf{x}_1)+\boldsymbol{\psi}^{\mathrm{T}}(-\mathbf{I}\mathbf{z}_1-\mathbf{J}\mathbf{z}_2) \tag{2.51}$$

$$\boldsymbol{\Omega}_{\mathbf{DL}}=\{\boldsymbol{\psi}:\mathbf{H}^{\mathrm{T}}\boldsymbol{\psi}\le\mathbf{0},\mathbf{K}^{\mathrm{T}}\boldsymbol{\psi}\le\mathbf{d},\boldsymbol{\psi}\in\mathbf{R}^{+}\},\mathbf{z}_1,\mathbf{z}_2\in\Omega_{US}(\mathbf{x}_2) \tag{2.52}$$

where $\boldsymbol{\Psi}$ is the dual variable vector of the inner problem of (2.49)-(2.50). It should be mentioned that the second term of (2.51) is the bilinear term, due to the fact aht both $\boldsymbol{\Psi}$ and $\mathbf{z}_1$ $\mathbf{z}_2$ are variables.

The single-level bilinear program (2.51)-(2.52) can be solved by either the big-M linearization method or the OA method [34]. Although the exact optimal value can be found by the big-M method, the computational burden is largely dependent on the number of bilinear terms. As the uncertainty set in the proposed mathematical model is huge, the big-M method is low-efficient in computation, or even intractable to address these cases. Hence, the OA method is adopted in this thesis to cope with the bilinear problem.

2.4.2 Solution Algorithm

To handle the two-stage optimization problem with an adjustable uncertainty set, a two-level algorithm is presented. The outer level uses the C&CG method [35] to obtain $\mathbf{x}_1$, $\mathbf{x}_2$, $\mathbf{x}_3$ from the results of inner-level optimization, and the inner level adopts the OA algorithm [34] to address the bilinear problem.

The outer-level C&CG algorithm is given as,

Step 0: Initialization. Set outer-level iteration index $k=1$, lower bound

$LB_{OUT} = -\infty$, upper bound $UB_{OUT} = +\infty$. Then, find a feasible solution $(\mathbf{z}^*_{1,k-1}, \mathbf{z}^*_{2,k-1}, \mathbf{x}^*_{2,k-1})$.

Step 1: Solve master problem defined as (12a)–(12b), taking into account the following constraints, where $\mathbf{w_k}$ is the newly created variable vector at each iteration:

$$\Omega_{CCG}(\mathbf{z}^*_{1,m}, \mathbf{z}^*_{2,m}, \mathbf{x}^*_{2,m}) = \{\ \mathbf{w_m}, \mathbf{x_1}, \mathbf{x_2}:$$

$$\mathbf{Gx_1} + \mathbf{Hw}_m + (\mathbf{Iz}^*_{1,m} / \mathbf{x}^*_{2,m})\mathbf{x_2} + \mathbf{Jz}^*_{2,m} \le \mathbf{g}\}, \forall m = 1, ..., k \qquad (2.53)$$

Let $(\mathbf{x}^*_{1,k}, \mathbf{x}^*_{2,k}, \mathbf{x}^*_{3,k})$ be the optimal solution. Set $LB_{OUT} = \mathbf{a}^{\mathrm{T}}\mathbf{x}^*_{1,k} + \mathbf{b}^{\mathrm{T}}\mathbf{x}^*_{3,k}$ $UB_{OUT} = \mathbf{a}^{\mathrm{T}}\mathbf{x}^*_{1,k-1} + \mathbf{b}^{\mathrm{T}}\mathbf{x}^*_{3,k-1}$.

Step 2: Solve the subproblem (2.51)-(2.52). Let $(\mathbf{z}^*_{1,k}, \mathbf{z}^*_{2,k})$ be the optimal solution. Check outer-level convergence. If $UB_{OUT} - LB_{OUT} < \varepsilon_{CCG}$, stop. Otherwise, let $k = k+1$, go to step 1.

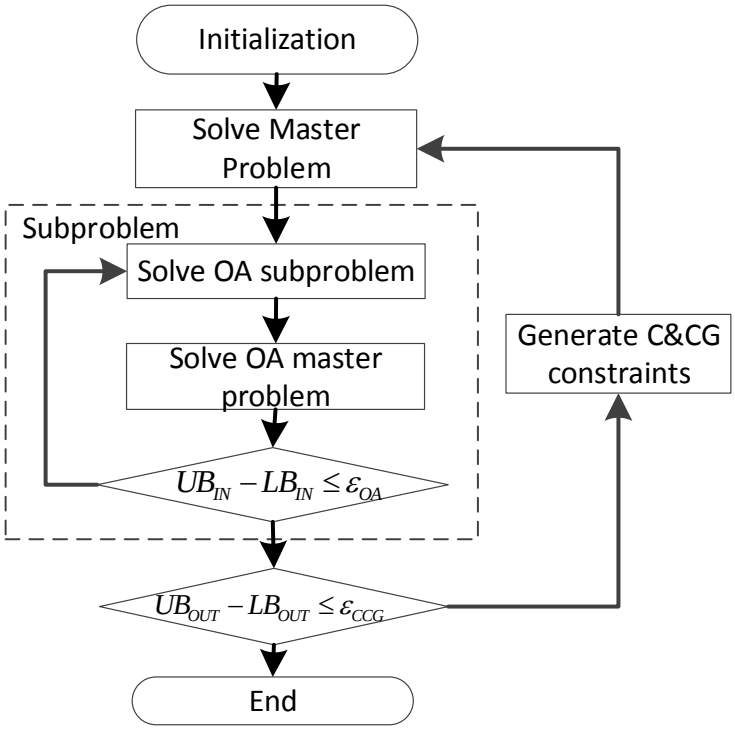

Figure 2.1 The framework of the EV chargeable region optimization algorithm.

The inner-level OA is given as,

Step 0: Initialization. Fix the first-stage decision variables $\mathbf{x}_1^*$ $\mathbf{x}_2^*$. Set the inner-level iteration index $j=1$, lower bound $LB_{IN}=-\infty$, upper bound $UB_{IN}=+\infty$. Find an initial $\mathbf{z}_{1,j}^*, \mathbf{z}_{2,j}^*$.

Step 1: Solve the OA subproblem,

$$S(\mathbf{x}_1^*, \mathbf{z}_{1,j}^*, \mathbf{z}_{2,j}^*) = \max_{\boldsymbol{\psi}} \boldsymbol{\psi}^{\mathbf{T}}(\mathbf{g} - \mathbf{G}\mathbf{x}_1^* - \mathbf{I}\mathbf{z}_{1,j}^* - \mathbf{J}\mathbf{z}_{2,j}^*) \tag{2.54}$$

$$\text{s.t.} \quad \boldsymbol{\psi} \in \boldsymbol{\Omega}_{\mathbf{DL}} \tag{2.55}$$

Let $\boldsymbol{\psi}^*$ be the optimal solution. Set $LB_{IN} = S(\mathbf{x}_1^*, \mathbf{z}_{1,j}^*, \mathbf{z}_{2,j}^*)$.

Step 2: Linearize the bilinear term $\boldsymbol{\psi}^{\mathrm{T}}(-\mathbf{I}\mathbf{z}_1 - \mathbf{J}\mathbf{z}_2)$ at $(\mathbf{z}_{1,j}^*, \mathbf{z}_{2,j}^*, \boldsymbol{\psi}_j^*)$, as follows:

$$\mathbf{L}_j(\mathbf{z_1}, \mathbf{z_2}, \boldsymbol{\psi}) = \boldsymbol{\psi}^{*\mathbf{T}}(-\mathbf{I}\mathbf{z}_1^* - \mathbf{J}\mathbf{z}_2^*) + (\boldsymbol{\psi} - \boldsymbol{\psi}^*)^{\mathrm{T}}(-\mathbf{I}\mathbf{z}_1^* - \mathbf{J}\mathbf{z}_2^*)$$

$$+\boldsymbol{\psi}^{*\mathbf{T}}(-\mathbf{I}(\mathbf{z}_1 - \mathbf{z}_1^*) - \mathbf{J}(\mathbf{z}_2 - \mathbf{z}_2^*)) \tag{2.56}$$

Step 3: Solve the OA master problem. Solve the linearized version of the second-stage problem, given as follows:

$$\mathbf{U}(\mathbf{z}_{1,j}^*, \mathbf{z}_{2,j}^*, \boldsymbol{\psi}_j^*) = \max_{\mathbf{z_1}, \mathbf{z_2}, \boldsymbol{\psi}, \boldsymbol{\beta}} \boldsymbol{\psi}^{\mathbf{T}}(\mathbf{g} - \mathbf{G}\mathbf{x_1}) + \boldsymbol{\beta} \tag{2.57}$$

$$\text{s.t.} \quad \boldsymbol{\beta} \le \mathbf{L_i}(\mathbf{z_1}, \mathbf{z_2}, \boldsymbol{\psi}), \forall i = 1, \ldots, j \tag{2.58}$$

$$\mathbf{z_1}, \mathbf{z_2} \in \Omega_{US}(\mathbf{x}_2^*), \quad \boldsymbol{\psi} \in \boldsymbol{\Omega}_{\mathbf{DL}} \tag{2.59}$$

Let $(\mathbf{z}_{1,j+1}^*, \mathbf{z}_{2,j+1}^*, \boldsymbol{\psi}_{j+1}^*, \boldsymbol{\beta}_{j+1})$ be the optimal solution. Set UB_{IN} = $\mathbf{U}(\mathbf{z}_{1,j+1}^*, \mathbf{z}_{2,j+1}^*, \boldsymbol{\psi}_{j+1}^*)$.

Step 4: Check inner-level convergence. If $UB_{IN} - LB_{IN} \le \varepsilon_{OA}$, give the current solution. Otherwise, set j = j+1, go to Step 1.

It should be noticed that the C&CG constraints are additionally added at each iteration, originally formulated as

$$\mathbf{G}\mathbf{x}_1 + \mathbf{H}\mathbf{w}_m + \mathbf{I}\mathbf{z}^*_{1,m} + \mathbf{J}\mathbf{z}^*_{2,m} \le \mathbf{g}\,, \forall m = 1,\ldots,k \qquad (2.60)$$

However, the first-stage variable $\mathbf{x_1}$ is not contained in the constraints (2.60) and cannot be modified at each iteration. This is because $\mathbf{x_1}$, denoting the EV chargeable bound, influences the bound of the uncertainty set rather than the worst-case scenario decision variables, which is different from the typical robust optimization. To address the problem, the auxiliary term $\mathbf{x}_2 / \mathbf{x}^*_{2,m}$ is multiplied with the third term, and finally reformulated as (2.53). The general framework of the algorithm is illustrated as Fig. 2.1.

2.5 Case Study

In this section, the case studies are presented to demonstrate the proposed model based on the modified IEEE 123 node DN in this section. All the algorithms are implemented on MATLAB, taking Cplex as the MILP solver. The optimality gap is set as 10^{-3}.

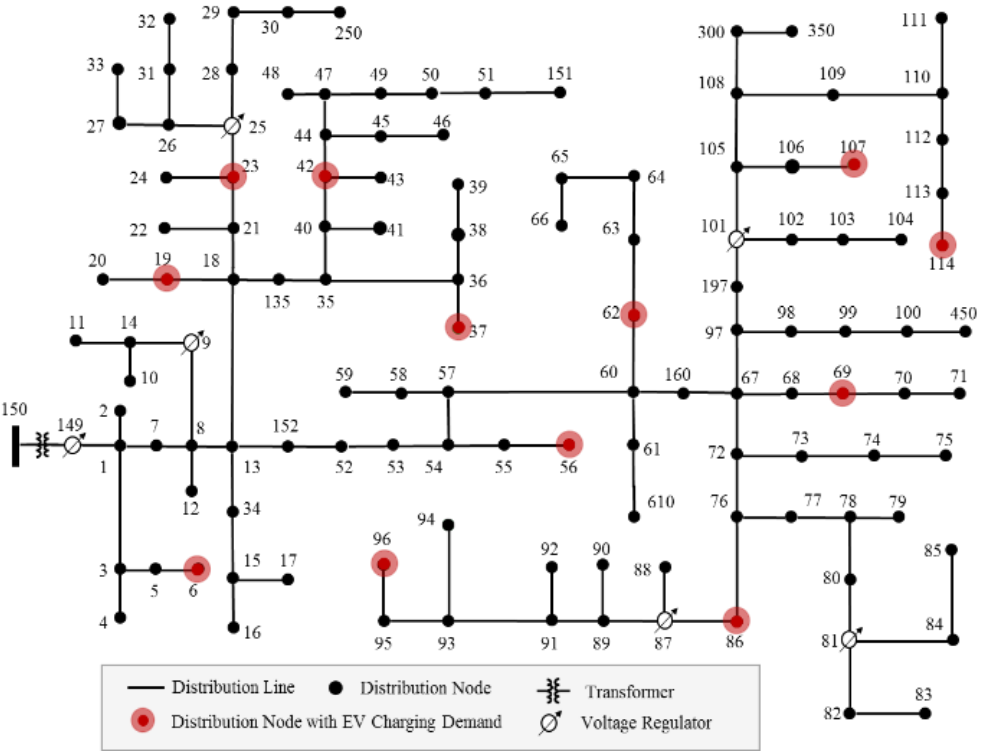

Figure 2.2 Modified IEEE 123-node distribution network for DN operation.

2.5.1 Test System and EV Charging Uncertainty

In the modified 123-node distribution network system, 12 distribution network nodes are connected with EV charging facilities and 6 distribution network nodes are connected with voltage regulator facilities, as shown in Fig. 2.2. The average distribution network peak load without consideration of the EV charging demand is set as 2.84 MW/1.53 MVAR. The average distribution network load at each of the 24 one-hour time intervals, compared with the peak load, is given as 0.64 0.645 0.635 0.64 0.705 0.81 0.86 0.83 0.85 0.87 0.905 0.83 0.81 0.85 0.89 0.96 1 0.99 0.94 0.91 0.87 0.8 0.72 0.66. The upper and lower boundaries of each distribution network active and reactive power are set as 1.2 and 0.8 of the average value, respectively. Without loss of generalities, the uncertainty budgets Λ_t^{AP} Λ_j^{AP} Λ_t^{RP} Λ_j^{RP} are set as 1.05 of the average value. The voltage violation requirement is given as [0.95 1.05]. The voltage at the substation node is given as 1.0125. The DN line loss fee is given as 0.1$/kWh.

At each distribution network EV node, 50 EVs are assumed to arrive in one day. The EV charging power rate is given as 4 kW, 6 kW and 8 kW with the probability of 25%, 50% and 25%, respectively. The compensation cost of the EV charging delay is set as 0.1$/(kWh*h). The EV penetration level is defined as the ratio of total EV charging demand to distribution network demand during the day, with the formulation

$$EVP = \frac{\sum_{t\in T}\sum_{c\in C} P_{c,t}^{CH,AV}}{\sum_{t\in T}\sum_{j\in J} p_{j,t} + \sum_{t\in T}\sum_{c\in C} P_{c,t}^{CH,AV}} \tag{2.61}$$

To effectively explain the proposed model, three cases with different charging modes and different EV penetration levels are proposed as follows:

Case 1: Immediate charge; EV penetration: 16.82%.

Case 2: Charging response to price; EV penetration:16.82%.

Case 3: Charging response to price; EV penetration: 20.18%.

The sample size of nodal EV charging demand is set as 4000 to effectively model the uncertainty of the total EV charging demand under each distribution network node at each time interval. Then the estimated CDF of aggregated EV charging demand is obtained accordingly. Fig. 2.3 depicts the CDFs at two typical time intervals. Simulation results demonstrate that EV charging demand at t = 20 is larger than the one at t = 17. Then the PDF is estimated from the gradient of CDF data, as depicted in Fig. 2.4. It should be noticed that the PDF and the CDF are estimated with discrete data rather than the exact distribution function, such that a piecewise linearized function can be used to model the EV charging demand uncertainty.

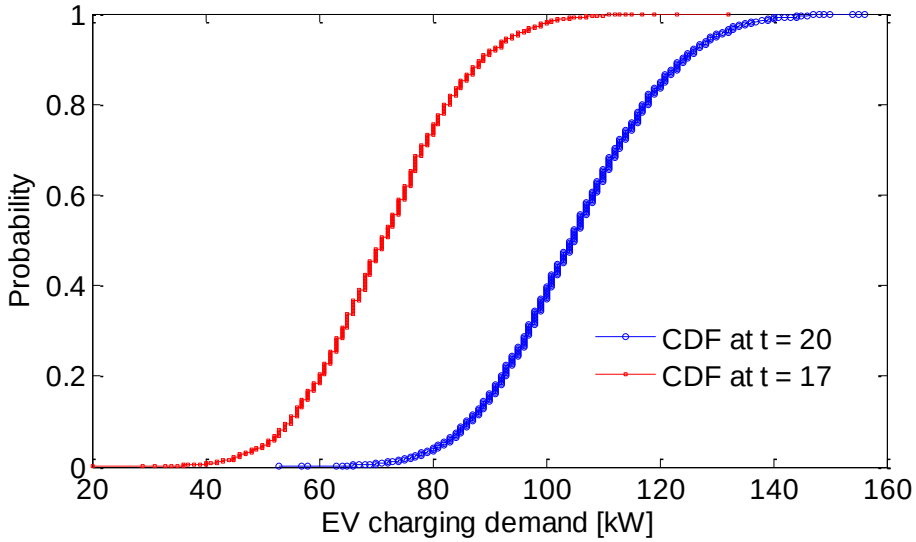

Figure 2.3. Estimated CDF of EV charging demand during two typical periods.

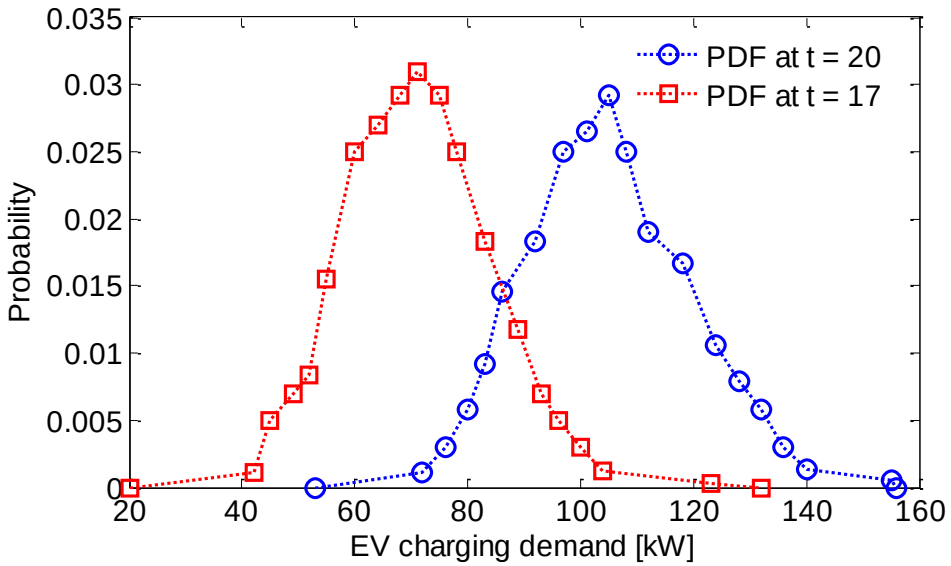

Figure 2.4. Estimated PDF of EV charging demand during two typical periods.

2.5.2 Optimal EV Chargeable Region

This subsection shows the results of case 1. Two typical charging bounds are depicted with the various uncertainty intervals of EV charging demand in Fig. 2.5. The EV chargeable region is defined as the area that is lower than the chargeable bound. It can be observed that the EV charging demand can be completely met during most times of the day, when both the distribution network load and the EV demand are low. However, EV charging may be delayed in the period from hours 16 to 22, when the distribution network voltage at some nodes will drop down out of the requirement if the EV charging demand is larger than the chargeable bound. By comparing the difference value between the chargeable bounds of node 6 and node 114, it can be found that the location of EV charging demand in the distribution network area has a considerable impact on hosting capapcity of EVs. Generally, more serious issues of voltage drop happen near the end of the distribution network, where the EV chargeable region is influenced and narrowed.

It is well noticed that EV owners will respond to electricity price by rescheduling their charging profile. To demonstrate the effectiveness of the EV chargeable region in this demand response scenario, two assumptions are firstly presented: 1) half of the EV owners respond to the electricity price and make their EVs charge at the lowest electricity price; 2) the electricity price has a positive correlation with total distribution network demand. In this regard, EV charging

demand is modeled by sampling from the travel dataset with half of the charging demand shifting to the distribution network demand valley period.

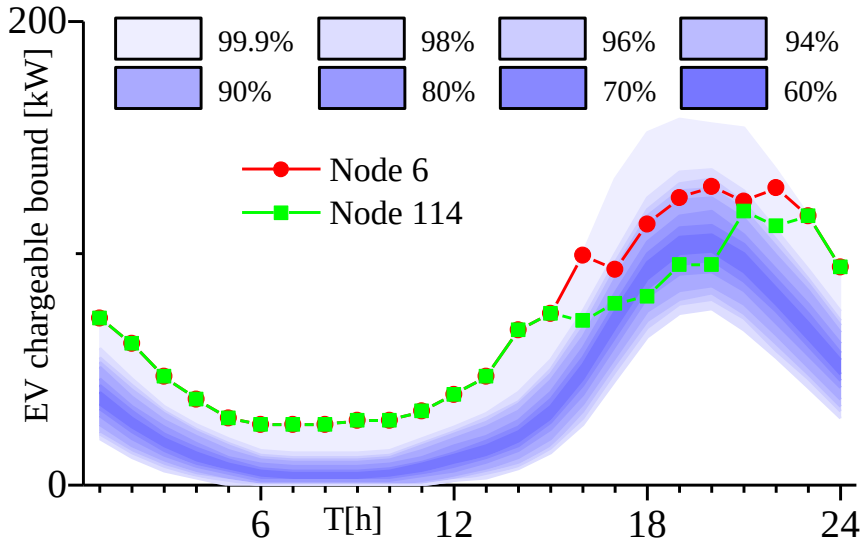

Figure 2.5. Optimal EV chargeable region in case 1.

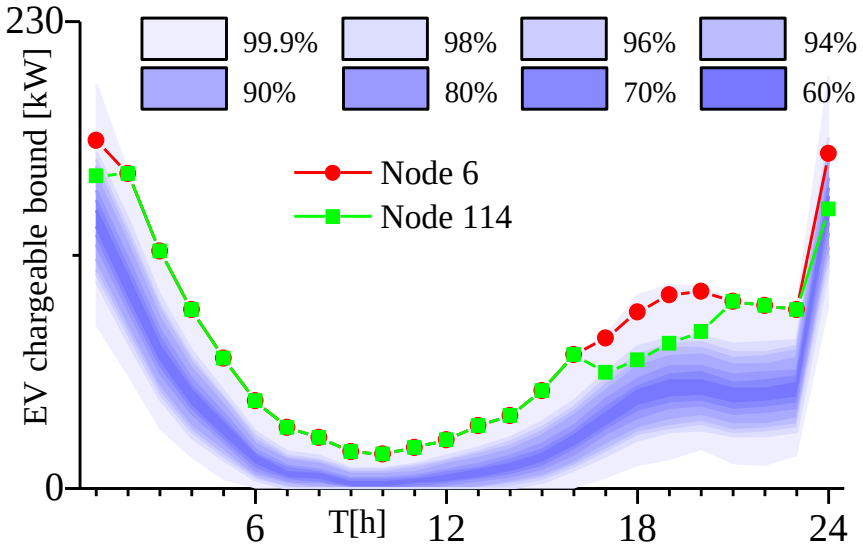

Figure 2.6. Optimal EV chargeable region in case 2.

Fig. 2.6 depicts the EV charging demand uncertainty and the EV chargeable region of case 2 at two typical time intervals. The simulation results show that

more EV charging demand can be accommodated by the EV chargeable region compared with case 1 in Fig. 2.5. It is known that the demand response of EV charging demand helps to shift part of the distribution network load to the valley period, which will contribute to maintain the voltage profile in peak period. Nevertheless, Fig. 2.6 demonstrates that the network constraint deviation requirement can not necessarily be met, as EV charging demand is still random and uncontrolled. Especially if the EV penetration level in DN is increased, the distribution network will become more heavily loaded and the EV chargeable region will take on a more significant role in maintaining the voltage profile of the DN. To illustrate this point, Table 2.1 gives the simulation results for the three cases. The concept of EV chargeability in the distribution network is proposed to evaluate the general level of the EV chargeable region in different distribution network nodes, with its definition listed as,

$$CB = \min_{c,t}(P_{c,t}^{Bound} / P_{c,t}^{CH,AV}) \tag{2.62}$$

By comparing the results of cases 2 and 3, it can be found that EV owners' response to electricity price can not prevent the distribution network violation, especially when the EV charging demand is large. The proposed EV chargeable region method becomes more advantageous with the increase of EV penetration level in the distribution network.

Table 2.1 Simulation Results of EV chargeable region optimization model

Case	Total cost ($)	EV compensation cost ($)	Chargeability
1	515.51	30.28	0.884
2	448.35	0.573	0.982
3	492.60	4.568	0.707

2.5.3 Optimization Procedure and Computation Efficiency

In this subsection, the optimization procedure and computational burden are discussed to verify the proposed solution method. The simulation results at each iteration of case 1 are listed in Table 2.2, in which the final solution is shown with fold type. It is found that the objective value of subproblem is considerably

reduced in each iteration and the algorithm terminates in the third iteration when the objective value of subproblem meets the convergence criterion. The computation efficiency is given in Table 2.3. It can be found that the subproblem contributes more to the total computation time. It is that it takes several iterations to achieve the convergence of OA method for the bilinear subproblem.

Table 2.2 Simulation Results of EV chargeable region optimization model at Each Iteration of Case 1

Iteration	Total cost ($)	Loss cost ($)	compensation cost ($)	Objective of SP ($)
1	458.93	458.93	0	$3.81*10^5$
2	513.31	482.57	30.74	$5.99*10^3$
3	**515.51**	**485.23**	**30.28**	**0.556**

Table 2.3 Computation Efficiency of Case 1

Total (s)	MP (s)	SP (s)	Iteration
141	40	101	3

2.5.4 Sensitivity Analysis

In this subsection, sensitivity analysis of piecewise linearization approximation method is carried out to check the accuracy of the linearization approximation. The results under different segment numbers of piecewise linearized delayed EV charging demand are given in Table 2.4, where the simulation results of case 1 are shown with fold type. It can be concluded that the EV compensation cost and EV chargeability are affected by the number of segment of PLA model. It can be also noticed that the difference values between simulation results of k=13 and k=10 are small and the difference values among results of k=10, k=7 and k=4 are relatively

larger, which shows that the parameters in the PLA method is proper for this case. Similarly, the simulation results under different segment numbers of piecewise linearized Distflow are given in Table 2.5. It can be concluded that the difference values among different costs is smaller when the number of segment *n* increases. Hence, the PLA accuracy in modelling Distflow is within the acceptable range.

Table 2.4 Simulation Results under Different Segment Number of Piecewise Linearized Delayed EV Charging Demand

n^*	k^*	Total cost ($)	Loss cost ($)	compensation cost ($)	Chargeability
	13	515.88	486.48	29.40	0.8841
10	**10**	**515.51**	**485.23**	**30.28**	**0.8848**
	7	526.71	487.14	39.57	0.8863
	4	533.98	487.85	46.13	0.8894

* n denotes segment number of the piecewise linearized delayed EV charging demand.

* k denotes segment number of the piecewise linearized Distflow

Table 2.5 Simulation Results under Different Segment Number of Piecewise Linearized Distflow

k	n	Total cost ($)	Loss cost ($)	compensation cost ($)	Chargeability
	16	495.31	467.54	27.77	0.8848
	13	503.68	474.99	28.69	0.8848
10	**10**	**515.51**	**485.23**	**30.28**	**0.8848**
	7	552.58	519.65	32.93	0.8848

4	--*	--	--	--

* -- denotes infeasibility of optimization model.

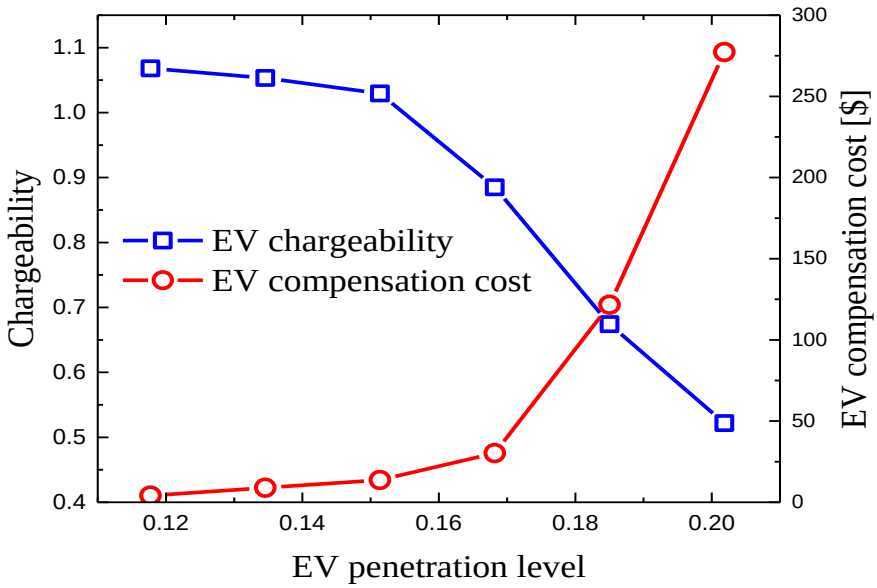

Figure 2.7. Impact of EV penetration level on EV chargeability and compensation cost.

In order to address the uncertainty of the EV population in the distribution network, a sensitivity analysis of the EV penetration level with EV immediate charging mode is carried out. Fig. 2.7 shows the impact of EV penetration level on the EV compensation cost and the chargeability. The simulation results show that with increased EV penetration level, the EV chargeability has a slow decrease at first and then a rapid decline when more EVs interact with the distribution network. This is because larger EV charging demand may lead to distribution network line overload. Under such conditions, EV charging demand delay is the only solution to avoid distribution network congestion. distribution network line capacity expansion planning will be suggested if the chargeability is too small to be accepted by EV owners.

2.6 Conclusions

This chapter innovatively presentes the concept of “EV chargeable region” to evaluate the maximum amount of distribution network EV hosting capacity for each node. The uncertainty of EV charging demand is modeled by sampling from raw vehicle travel data. The EV chargeable region optimization problem is formulated as a two-stage optimization model, in which the EV chargeable region and distribution network decision variables are optimized in the first stage and the feasibility of the distribution network worst-case scenario is checked in the second stage. Mathematically, the framework is formulated as a two-stage robust optimization problem with an adjustable uncertainty set. A modified C&CG/OA method is used to solve the two-level problem. Case studies demonstrate the effectiveness of the proposed model in both immediate charging mode and charging demand response mode, considering different EV penetration levels.

Using the proposed model, not only operating constraint deviation of distribution network is prevented, but also EV owners’ charging requests, including immediate charging and price-response charging, are guaranteed to the largest extent. EV owners’ daily report of charging demand to the EV aggregator may be waived, as the EV charging profile can be well rescheduled directly by the EV owners themselves. The urgent usage of EVs can be maximally met. Besides, communication of the proposed framework is simple and the only communication is to pass message of EV chargeable region from distribution network operator to each controller at distribution network node, which is unidirectional and occurs once a day. Overall, the proposed framework shows a high potential for practical applications.

3. Robust Distributed Generator Planning Accommodating Electric Vehicle Charging Demand

3.1. Introduction

Basically, distributed generator (DG) can be categorized into dispatchable distributed generator (DDG), e.g., gas turbines, micro-turbines, and non-dispatchable distributed generator (NDG), e.g., wind and photovoltaic generations. The investment issue of DDG and NDG have been well discussed in [36-38] and [39-41], respectively. Compared with DDGs, NDGs are more cost-effective and environment-friendly, which seem to be a more prior choice for active distribution network. However, NDGs will introduce additional operation uncertainties to active distribution network as their generation capability highly depend on weather conditions. For a active distribution network with large number of EV users, the flexibility of EV charging demand can be utilized to coordinate with NDGs and offset their uncertainty. Some pioneer works have been done on coordinated dispatch and operation of EVs and NDGs [27, 42, 43]. To the best of the authors' knowledge, the coordinated planning of NDGs and EVs, especially in active distribution network level, has not been systematically explored. Although the DG investment problem in active distribution network has been well studied in the literature [44, 45], high-level penetration of EVs would pose new challenges to this topic, such as new types of uncertainties. Different from uncertainties of NDGs, the uncertainties of EV mainly include the following three aspects: 1) EV penetration level, which is almost intractable due to the factors such as battery technology; 2) EV charging demand, which varies from day to day and is influenced by the EV owners' travel behaviors; 3) Involvement of EV owners, which equals how many EV owners would like to reschedule their charging

demand according to electricity price, known as price-responsive charging mode.

To hedge against the aforementioned uncertainties, various methodologies have been developed and applied to power system planning problems, where stochastic optimization and robust optimization are among the most efficient mathematical tools. Stochastic optimization models have been applied to power system planning problems for decades, such as power system expansion planning [46] and wind power allocation planning [47]. The distributions of uncertainties, which serve as the key input of stochastic optimization models, may not be able to be accurately depicted in the time scale of planning. Robust optimization method, however, is almost distribution-free and has received much attention especially in planning problems, whose recent applications can be found in transmission network expansion [48], optimal storage [49] and DG placement in Microgrid [50].

The framework of robust active distribution network planning against uncertain EV charging demand and NDGs is proposed in this chapter. Security constraints of active distribution network, such as upper and lower bound of voltage and branch capacity, are imposed to enforce the feasibility of the planning strategy. A two-stage robust optimization formulation is established, where the first stage problem optimizes the sizing and sitting of DGs, including DDGs and NDGs, and the second stage problem checks the feasibility of planning strategy in the worst realization of uncertainties. Particularly, the uncertainty realization of NDGs in the second stage depends on the corresponding planning strategy of NDGs, rendering a decision-dependent optimization formulation. Column-and-constraint generation (C&CG) methodology and big-M method are modified accordingly to solve proposed problem.

The nomenclature of symbols used in this chapter are given as follows,

Indices and Sets

t/T	Index/set of time slots.
j/J	Index/set of distribution network nodes.
κ/K	Index and set of the trips whose destination is home, which will trigger the EV charging action.
v/V	Index/set of EV charging stations.

w/W Index/set of wind power generators.

c/C Index/set of photovoltaic generators.

g/G Index/set of dispatchable distributed generators.

r/R Index/set of reactive power support facilities, i.e., shunt capacitors and automatic voltage regulators.

$N_{v,t}$ Set of EV charging demand in all sampled scenario in EV charging station v at t.

$\delta(j)$ Set of child nodes of distribution network node j.

s Index of feasibility checking scenarios

Parameters

$t_{\kappa}^{arr}, t_{\kappa}^{dep}$ EV arrival time and departure time.

D_{κ} Total EV travel distance during the day.

$\xi_t^{PV,MO}$ Ratio of hourly maximum output of PV generator to the investment capacity. $\xi_t^{PV,MO} \in [0\ 1]$

$\underline{P}_{v,t}^{CH}$ / $\overline{P}_{v,t}^{CH}$ Lower/upper bound of EV charging demand at v,t.

$\underline{\Lambda}_t^{CH,C}$ / $\overline{\Lambda}_t^{CH,C}$ Lower/upper bound of the location-aggregated EV charging demand at time t.

$\underline{\Lambda}_v^{CH,T}$ / $\overline{\Lambda}_v^{CH,T}$ Lower/upper bound of time-aggregated EV charging demand at EV charging station v.

$c_w^{WP}/c_c^{PV}/c_g^{DD}$ Installation cost of wind power generator, PV generator and dispatchable generator.

$\beta^{WP}/\beta^{PV}/\beta^{DD}$ Capital recovery factors of wind power generator, PV generator and dispatchable generator.

$\delta^{WP}/\delta^{PV}/\delta^{DD}$ Minimum investment capacity of wind power generator, PV generator and dispatchable generator.

ξ_t^{WP}/ξ_t^{PV} Average output of wind power generator, and PV generator. $\xi_t^{WP}/\xi_t^{PV} \in [0\ 1]$

ζ Yearly interest rate.

n^{WP}/ n^{PV}/ n^{DD}/ Lifetime of wind power generator, PV generator and dispatchable generator.

λ_t^{EP} Electricity price.

λ^{DD} Generation cost of dispatchable generators.

Φ^D Number of days in a year.

r_{ij}/x_{ij} Resistance/reactance of distribution network branch ij.

$\hat{P}_{j,t}^{LD}$ Current Distribution network load at j,t.

V_0 Voltage reference value.

U^{WP}/U^{PV}/U^{DD} Maximum investment number of wind power generator, PV generator and dispatchable generator.

V^{SB} Voltage at distribution network substation.

LC_{ij} Capacity of distribution network branch ij.

Variables

X^{EV} EV penetration rate during the planning horizon.

X^{LD} Conventional load increase rate during the planning horizon.

X^{DS} The rate of EV charging respond to electricity price.

u_w^{WP}/u_c^{PV}/ u_g^{DD} Binary variable, with 1 to install wind power generator, PV generator, dispatchable generator.

I_w^{WP}/I_c^{PV}/ I_g^{DD} Integer variable for installation capacity of wind power generator, PV generator, dispatchable generator.

$P_{w,t}^{WP}$ / $P_{c,t}^{PV}$ /$P_{g,t}^{DD}$ Output of wind power generator, PV generator and dispatchable generator.

$P_{j,t}$/$Q_{j,t}$ Active/reactive power flow at j,t.

$P_{j,t}^{QU}$/$Q_{j,t}^{QU}$ Quadratic term of active/reactive power flow at j,t.

$P_{j,t}^{LD}$/$Q_{j,t}^{LD}$ Active/reactive power load at j,t.

$V_{j,t}$ Voltage at j,t.

$Q_{r,t}^{SVC}$ Output of static voltage compensator at r,t.

$P_{v,t}^{CH}$ EV charging demand at *c,t.*

$S_{j,t}^{V,LB}/S_{j,t}^{V,UB}$ Slack variables for lower/upper bound of real-time worst-case voltage violation requirement at *j,t*.

$S_{j,t}^{LC}$ Slack variables for line capacity of real-time worst-case power flow at *j,t*.

3.2. Uncertainties in Planning Problem

3.2.1 Planning Uncertainty

The uncertainties in this paper can be divided into two levels, namely the upper-level planning uncertainty and the lower-level operation uncertainty. The upper-level planning uncertainty is defined as the one caused by demand variation during the whole planning horizon, such as EV penetration level, distribution network load increase and EV owners' price-responsive behavior, while the lower-level operation uncertainty is defined as the one caused by daily operation, such as the daily operation uncertainty of EV charging demand and the NDG output. The upper-level planning uncertainty is unpredictable and non-repetitive, especially considering the EVs are emerging participant in distribution network. It also remains uncertain how many EVs would respond to electricity price to determine their charging decisions. In this paper, we assume the planning uncertainties can be quantified with the upper and lower bounds according to practical experience, given as follows,

$$\mathrm{X}^{EV} \in [\underline{\mathrm{X}}^{EV}, \overline{\mathrm{X}}^{EV}], \mathrm{X}^{LD} \in [\underline{\mathrm{X}}^{LD}, \overline{\mathrm{X}}^{LD}], \mathrm{X}^{DS} \in [\underline{\mathrm{X}}^{DS}, \overline{\mathrm{X}}^{DS}] \tag{3.1}$$

where X^{EV}, X^{LD}, X^{CC} represent EV penetration level, distribution network load increase rate and EV owns' price responsive rate, respectively. The overline and underline are used to represent the lower bound and upper bound respectively.

For the lower-level operation uncertainty, lots of previous works use uncertainty budget constraints to model the uncertainty of renewable energy outputs for the input of robust optimization model. In this method, the worst-case scenario is usually obtained when the NDGs output keeps switching from the upper bound, lower bound or expected values in a day. However, it would be not suitable for

planning problems. As seen from the historical data, it is quite frequent that NDGs output at maximum or minimum output during the whole day. As the power system reliability is the major concern for a planning problem, the worst-case scenario is better to be selected as the maximum or minimum output, which is considerably depends on the investment capacities,

$$P_{w,t}^{WP} \in [0, \delta^{WP} I_w^{WP}], P_{c,t}^{PV} \in [0, \xi_t^{PV,CA} \delta^{PV} I_c^{PV}] \tag{3.2}$$

where the lower bounds of the NDGs are set as zero and the upper bounds are set as the installation capacity. $\xi_t^{PV,MO}$ denotes the ratio of hourly maximum output of PV generations with respect to its investment capacity.

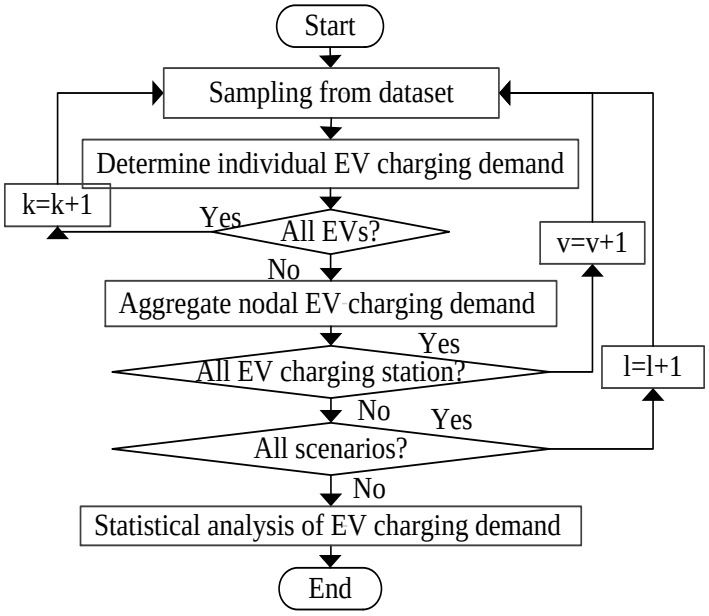

Figure 3.1 Flowchart for modeling EV charging demand

3.2.2 Modelling individual EV charging demand

As EVs are emerging products, the future EV quantity increase and EV owners' charging behavior remain considerably uncertain. Modelling the uncertainty of EV charging demand is quite different from the NDGs. This paper adopts data mining method to find out user travel behavior and then obtain the statistical information of EV charging demand, which can be further used to formulate polyhedral uncertainty set for robust optimization. Note that this kind of distribution-free uncertainty modelling method is suitable for the non-predictive EV charging

demand and the data mining method improves the accuracy in modelling uncertainty. The EV charging demand uncertainty is processed with the following three steps: 1) modelling EV owners' travel behavior; 2) modelling individual EV charging behavior; 3) statistical analysis of EV charging demand.

1) **Modelling individual EV charging demand**. In this mode, EVs are assumed to be plugged into grid and charged as soon as the last trip in a day ends and to be plugged out when the batteries are full. The charging duration is dependent on the accumulated mileage in a day. The charging load for each EV can be formulated as

$$P_{k,t}^{\mathrm{ch}} = P_{\upsilon}^{ch},\ if\ \ t \geq t_k^{\mathrm{arr}}\ \&\, t \leq \frac{DT_k E_{CS}}{\eta_{\mathrm{ch}} P_{\upsilon}^{ch}} + t_k^{\mathrm{arr}}\ \&\, t \leq t_k^{dep}, \forall k \in K, \forall t \in T \qquad (3.3)$$

where κ and K are the index and set of the trips whose destination is home, which will trigger the charging action. P_{υ}^{ch} denotes the fixed charging rate, which can be randomly selected from the predefined charging power dataset with corresponding probability, and υ is the index of variously rated charging power. DT_K is the total travel distance during the day, E_{CS} is the per-mile energy consumption, η_{ch} is the charging efficiency, and t_{κ}^{arr} and t_{κ}^{dep} are the *EV* arrival and departure time.

2) **Price-responsive charging mode**. In this mode, EV owners are assumed to respond to electricity price by rearranging their charging profiles. To obtain proper EV charging profile, two assumptions are proposed: 1) EV owners respond to the electricity price by charging their EVs at the lowest electricity price and the batteries are fully charged before next trip begins; 2) the electricity price has a negative correlation with total active distribution network demand. In this regard, EV charging demand is reformulated by shifting the EV charging demand to the active distribution network demand valley period. The individual EV charging demand should be optimized as follows,

$$\min\ f_{\kappa} = \sum_{t \in [t_{\kappa}^{\mathrm{arr}}, t_{\kappa}^{dep}]} \lambda_t P_{\kappa,t}^{\mathrm{ch}}, \forall \kappa \in \mathrm{K} \qquad (3.4)$$

$$\lambda_t = a P_t^L + b \qquad (3.5)$$

$$\text{Subject to} \sum_{t \in [t_{\kappa}^{\mathrm{arr}}, t_{\kappa}^{dep}]} P_{\kappa,t}^{\mathrm{ch}} \geq \frac{D_{\kappa} E^C}{\eta_{\mathrm{ch}} P_{\upsilon}^{ch}}, \forall \kappa \in \mathrm{K} \qquad (3.6)$$

$$0 \le P_{\kappa,t}^{\mathrm{ch}} \le P_{\upsilon}^{ch}, \forall \kappa \in \mathrm{K}, \forall t \in T \tag{3.7}$$

where the objective function (3.4) is to minimize total charging cost for each EV, λ_t denotes electricity price at t and is assumed to have an inverse linear correlation with total active distribution network load. In (3.6), the EV charging demand, which is the total energy consumption during the day, should be guaranteed before departure. (3.7) describes the charging rate limitation.

3.2.3 Statistical Analysis of EV Charging Demand

The survey dataset [51] contains 119,480 trips in total, collected within 3 months. For each trip, the information provided by the data includes: departure time, departure location, arrival time, arrival location, trip distance, transit access mode, etc. The large number of trips and the detailed record of each trip provide valuable assistance in modeling the uncertainty of EV charging demand. The flowchart for modelling EV charging demand profile is given in Fig. 3.1. By randomly sampling from travel database, a bunch of parameters [t^{arr},t^{dep},D] can be obtained. Then the EV charging profile can be acquired either by immediate charging strategy or price-responsive charging strategy, with the ratio related to X^{DS}. Then the charging demand of all EVs under an active distribution network node is summarized and regarded as one scenario. By repeating this procedure, various scenarios can be obtained, given as

$$P_{v,t,l}^{CH} = \sum_{\kappa \in N_{v,l}^{IC}} P_{\kappa,t}^{\mathrm{ch}} + \sum_{\kappa \in N_{v,l}^{PC}} P_{\kappa,t}^{\mathrm{ch}}, \forall v \in V, \forall t \in T, \forall l \in L \tag{3.8}$$

where $P_{v,t,l}^{CH}$ denotes the aggregated charging demand under an active distribution network node v in scenario l at time t, summarized by all the EV charging demand in different charging strategies. $N_{v,l}^{IC}$ and $N_{v,l}^{PC}$ represent the set of EV immediate charging demand and price-responsive charging demand respectively. When the sample size L is large enough, the uncertainty of charging demand can be properly described. The average value of EV charging demand can be obtained by

$$\hat{P}_{v,t}^{CH} = \frac{1}{\left|N_{v,t}^{'}\right|} \sum_{l \in N_{v,t}^{'}} P_{v,t,l}^{CH}, \forall v \in V, \forall t \in T \tag{3.9}$$

where $\hat{P}_{v,t}^{CH}$ denotes the average value in the scenarios and |·| denotes the cardinality of the set. The corresponding confidence level can also be obtained,

$$\underline{P}_{v,t}^{CH} = \inf\{\gamma_{v,t} \mid \text{Prob}(P_{v,t,l}^{CH} \le \gamma_{v,t}) \ge \alpha\}, \forall t \in T, \forall v \in V \tag{3.10}$$

$$\overline{P}_{v,t}^{CH} = \sup\{\gamma_{v,t} \mid \text{Prob}(P_{v,t,l}^{CH} \ge \gamma_{v,t}) \ge \alpha\}, \forall t \in T, \forall v \in V \tag{3.11}$$

$$\underline{\Lambda}_{t}^{CH,C} = \inf\{\gamma_{t} \mid \text{Prob}(\sum_{v \in V} P_{v,t,l}^{CH} \le \gamma_{t}) \ge \alpha\}, \forall t \in T \tag{3.12}$$

$$\overline{\Lambda}_{t}^{CH,C} = \sup\{\gamma_{t} \mid \text{Prob}(\sum_{v \in V} P_{v,t,l}^{CH} \ge \gamma_{t}) \ge \alpha\}, \forall t \in T \tag{3.13}$$

$$\underline{\Lambda}_{v}^{CH,T} = \inf\{\gamma_{t} \mid \text{Prob}(\sum_{t \in T} P_{v,t,l}^{CH} \le \gamma_{t}) \ge \alpha\}, \forall v \in V \tag{3.14}$$

$$\overline{\Lambda}_{v}^{CH,T} = \sup\{\gamma_{t} \mid \text{Prob}(\sum_{t \in T} P_{v,t,l}^{CH} \ge \gamma_{t}) \ge \alpha\}, \forall v \in V \tag{3.15}$$

where $\underline{P}_{v,t}^{CH}$ and $\overline{P}_{v,t}^{CH}$ denote the lower and upper bound of EV charging demand under active distribution network node *v* at time *t*, $\underline{\Lambda}_{t}^{CH,C}$ and $\overline{\Lambda}_{t}^{CH,C}$ denote the lower and upper bound of the location-aggregated EV charging demand at time t with confidence interval *α*. $\underline{\Lambda}_{v}^{CH,T}$ and $\overline{\Lambda}_{v}^{CH,T}$ denote lower and upper bound of the time-aggregated EV charging demand under active distribution network node *v* with confidence interval *α*. All these parameters are obtained as inputs of uncertainty set in the proposed planning model.

3.3. Mathematical Formulation

3.3.1 Deterministic Model

In this section, a deterministic active distribution network planning (Det-P) model with EV charging demand integration is developed. Generally, the framework is to obtain the optimal NDG and DDG sitting and sizing by minimizing the summation of investment cost and operation cost assuming the prospective EV charging demand and the output of NDG are assigned with their expected value. The Det-P model is given as,

$$\min f = f^{INV} + f^{OP} \tag{3.16}$$

$$f^{INV} = \beta^{WP} \sum_{w \in W} c_w^{WP} \delta^{WP} u_w^{WP} I_w^{WP}$$

$$+\beta^{PV} \sum_{c \in C} c_c^{PV} \delta^{PV} u_c^{PV} I_c^{PV} + \beta^{DD} \sum_{g \in G} c_g^{DD} \delta^{DD} u_g^{DD} I_g^{DD} \quad (3.17)$$

$$f^{OP} = \Phi^D \sum_{t \in T} \lambda_t^{EM} \sum_{ij \in L} r_{ij} \frac{\hat{P}_{j,t}^{QU} + \hat{Q}_{j,t}^{QU}}{V_0^2} + \Phi^D \sum_{t \in T} \sum_{w \in W} (-\lambda_t^{EM}) \hat{P}_{w,t}^{WP}$$

$$+\Phi^D \sum_{t \in T} \sum_{c \in C} (-\lambda_t^{EM}) \hat{P}_{c,t}^{PV} + \Phi^D \sum_{t \in T} \sum_{g \in G} (\lambda^{DD} - \lambda_t^{EM}) \hat{P}_{g,t}^{DD} \quad (3.18)$$

where,

$$\beta^{WP} = \frac{\zeta(1+\zeta)^{n^{WP}}}{(1+\zeta)^{n^{WP}} - 1}, \beta^{PV} = \frac{\zeta(1+\zeta)^{n^{PV}}}{(1+\zeta)^{n^{PV}} - 1}, \beta^{DD} = \frac{\zeta(1+\zeta)^{n^{DD}}}{(1+\zeta)^{n^{DD}} - 1} \quad (3.19)$$

subject to,

$$\hat{P}_{j,t} = \sum_{i \in \delta(j)} \hat{P}_{i,t} + \sum_{i \in \delta(j)} r_{ij} \frac{\hat{P}_{i,t}^{QU} + \hat{Q}_{i,t}^{QU}}{\hat{V}_0^2} + \hat{P}_{j,t}^{LD} + \sum_{v \in \Psi_{EV}(j)} \hat{P}_{v,t}^{CH}$$

$$- \sum_{w \in \Psi_{WP}(j)} \hat{P}_{w,t}^{WP} - \sum_{c \in \Psi_{PV}(j)} \hat{P}_{c,t}^{PV} - \sum_{g \in \Psi_{DD}(j)} \hat{P}_{g,t}^{DD}, \forall j \in J, \forall t \in T \quad (3.20)$$

$$\hat{Q}_{j,t} = \sum_{i \in \delta(j)} \hat{Q}_{i,t} + \sum_{i \in \delta(j)} x_{ij} \frac{\hat{P}_{i,t}^{QU} + \hat{Q}_{i,t}^{QU}}{V_0^2}$$

$$+\hat{Q}_{j,t}^{LD} + \sum_{r \in \Psi_{RP}(j)} \hat{Q}_{r,t}^{SVC}, \forall j \in J, \forall t \in T \quad (3.21)$$

$$\hat{V}_{j,t} = \hat{V}_{i,t} + \frac{(r_{ij} \hat{P}_{i,t} + x_{ij} \hat{Q}_{i,t})}{V_0}, \forall j \in J, \forall i \in \delta(j), \forall t \in T \quad (3.22)$$

$$\hat{P}_{j,t}^{QU} \geq K_{\gamma,j,t}^{AP} \hat{P}_{j,t} + B_{\gamma,j,t}^{AP}, \forall j \in J, \forall \gamma \in \Gamma^{AP}, \forall t \in T \quad (3.23)$$

$$\hat{Q}_{j,t}^{QU} \geq K_{\gamma,j,t}^{RP} \hat{Q}_{j,t} + B_{\gamma,j,t}^{RP}, \forall j \in J, \forall \gamma \in \Gamma^{RP}, \forall t \in T \quad (3.24)$$

$$\hat{P}_{w,t}^{WP} = \xi_t^{WP} \delta^{WP} u_w^{WP} I_w^{WP}, \forall w \in W, \forall t \in T \quad (3.25)$$

$$\hat{P}_{c,t}^{PV} = \xi_t^{PV} \delta^{PV} u_c^{PV} I_c^{PV}, \forall c \in C, \forall t \in T \quad (3.26)$$

$$\hat{P}_{g,t}^{DD} \leq \delta^{DD} u_g^{DD} I_g^{DD}, \forall g \in G, \forall t \in T \quad (3.27)$$

$$\sum_{w\in W} u_w^{WP} \le U^{WP},\ \sum_{c\in C} u_c^{PV} \le U^{PV},\ \sum_{g\in G} u_g^{DD} \le U^{DD} \tag{3.28}$$

$$\hat{V}_{j,t} = V^{SB},\ j = 1, \forall t \in T \tag{3.29}$$

$$\underline{Q}_r^{SVC} \le \hat{Q}_{r,t}^{SVC} \le \bar{Q}_r^{SVC}, \forall r \in R, \forall t \in T \tag{3.30}$$

$$\hat{P}_{j,t}^{QU} + \hat{Q}_{j,t}^{QU} \le LC_{ij}^2, \forall j \in J, \forall i \in \delta(j), \forall t \in T \tag{3.31}$$

$$1-\varepsilon \le \hat{V}_{j,t} \le 1+\varepsilon, \forall j \in J, \forall t \in T \tag{3.32}$$

where, the objective function (3.16) is to minimize the overall annual costs including investment and operation. The annual investment cost f^{INV} in (3.17) consists of the installation cost of wind power generators, PV generators and DGs. The capital recovery factors $\beta^{WP}/\beta^{PV}/\beta^{DD}$, defined in (3.19), are used for conversion from total investment cost to annual cost, where ζ denotes yearly interest rate and $n^{WP}/\ n^{PV}/\ n^{DD}$ are lifetime of each DG. The annual active distribution network operation cost saving f^{OP} is given in (3.18), where the first term denotes the cost of active distribution network operation loss, the second and third terms denote the cost saving by wind power and PV generator investment, and the forth term denotes operation revenue/cost due to DG investment. Constraints (3.20)–(3.22) describe the active power flow, reactive power flow and voltage along the branch, considering the integration of the DG output and EV charging demand. The *piecewise linearized Distflow* model is proposed by linearizing the quadratic terms of active power and reactive power based on the DistFlow equations in [29, 30]. The axillary constraints (3.23)–(3.24) are used to estimate the quadratic terms of active and reactive power $P_{j,t}^{QU}\ Q_{j,t}^{QU}$, with piecewise linearization approximation (PLA) method, where $K_{\gamma,c,t}^{AP}\ K_{\gamma,c,t}^{RP}$ and $B_{\gamma,c,t}^{AP}\ B_{\gamma,c,t}^{RP}$ are the constant coefficients. In (3.25) –(3.26), the output of distributed wind power generator and PV generator are described by its average statistical value. In (3.27), the output of DDG is limited by its investment capacity. The total installation number of DGs is limited by(3.28). The voltage of the substation is given in (3.29). The upper and lower limitation of static voltage compensator is given in (3.30). The active distribution network branch capacity limitation is described by (3.31). The nodal voltage constraint is given by (3.32).

3.3.2 Robust Optimization Based Feasibility Checking Constraints

The proposed Det-P model determines an optimal planning solution from economic aspect, where the reliability of the distribution network operation is not considered. The basic idea of adding the feasibility checking constraints into the Det-P model is to make sure the distribution network always remains secure and reliable operation in any conditions of revealed uncertainties. The mathematical method of robust optimization is adopted aiming at defining and finding out a worst-case scenario, which is a set of parameters such that the distribution network operation security for any other scenarios can be guaranteed. Hence, the robust distribution network planning model becomes two-stage, where the first stage problem minimizes the total cost given the expected output of the uncertainties as defined in (3.16)-(3.32), and the second stage problem checks the feasibility of the first stage decision variables, discussed in details in this subsection.

To guarantee the distribution network security and reliability, mathematically the distribution network constraint should not be violated. In this regard, we use non-negative slack variables to relax the constraints, with the robust optimization based feasibility checking model formulated as,

$$\max_{M_I \in \Omega_{US}} \min_{M_{II} \in \Omega_{WS}} \sum_{t \in T} \sum_{j \in J} (S_{j,t}^{V,LB} + S_{j,t}^{V,UB} + S_{j,t}^{LC}) = 0 \tag{3.33}$$

where $S_{j,t}^{V,LB}$ and $S_{j,t}^{V,UB}$ denote the slack variables of voltage drop and voltage rise constraints and $S_{j,t}^{LC}$ denotes the slack variables of distribution network line capacity limitation.

The uncertainty set Ω_{US} is to quantify the uncertainties of four kinds of variables, i.e., EV charging demand, conventional load and wind power generator and PV generator. The uncertainty set Ω_{US} and the variables describing the uncertainty M_I are defined as,

$$\Omega_{US} = \{ \quad M_I : M_I = [P_{v,t}^{CH}, P_{j,t}^{LD}, P_{w,t}^{WP}, P_{c,t}^{PV}]$$

$$\mathrm{X}^{EV} \underline{P}_{v,t}^{CH} \le P_{v,t}^{CH} \le \mathrm{X}^{EV} \overline{P}_{v,t}^{CH}, \forall v \in V, \forall t \in T \tag{3.34}$$

$$\mathrm{X}^{EV} \underline{\Lambda}_{t}^{CH,C} \le \sum_{v \in V} P_{v,t}^{CH} \le \mathrm{X}^{EV} \overline{\Lambda}_{t}^{CH,C}, \forall t \in T \tag{3.35}$$

$$\mathrm{X}^{EV} \underline{\Lambda}_{v}^{CH,T} \le \sum_{t \in T} P_{v,t}^{CH} \le \mathrm{X}^{EV} \overline{\Lambda}_{v}^{CH,T}, \forall v \in V \tag{3.36}$$

$$P_{j,t}^{LD} = \mathrm{X}^{LD} \hat{P}_{j,t}^{LD}, \forall j \in J, \forall t \in T \tag{3.37}$$

$$(3.1)–(3.2) \tag{3.38}$$

where constraints (3.34)–(3.38) describe the uncertainty budget of EV charging demand. Constraints (3.35) and (3.36) are uncertainty budget quantifying node and time-aggregated EV charging demand uncertainty. Constraint (3.37) describes the variation of conventional load. Constraints (3.38) represents the upper-level planning uncertainty and the boundary of NDG.

The set Ω_{WS} defines the distribution network power flow in worst-case scenario. The formulation of the worst-case distribution network power flow is similar to the deterministic power flow in the first-stage optimization. The major difference is from twofold. Firstly, the uncertainties in the second stage, i.e., the EV charging demand, the distribution network load, the output of wind generator and PV generator, become variables quantified by the uncertainty setΩ_{US}, while they are parameters describing the expected values in the first stage. Secondly, the constraints of voltage lower bound, voltage upper bound and line capacity are relaxed with slack variables. Hence, the worst-case power flow set Ω_{WS} and the second-stage variables M_{II} are given as,

$$\Omega_{WS} = \{ M_{\mathrm{I}}, M_{\mathrm{II}} : \qquad M_{II} = [P_{j,t}, Q_{j,t}, P_{j,t}^{QU}, Q_{j,t}^{QU}, V_{j,t}, Q_{r,t}^{SVC}, S_{j,t}^{V,LB}, S_{j,t}^{V,UB}, S_{j,t}^{LC}]$$

$$P_{j,t} = \sum_{i \in \delta(j)} P_{i,t} + \sum_{i \in \delta(j)} r_{ij} \frac{P_{i,t}^{QU} + Q_{i,t}^{QU}}{V_0^2} + P_{j,t}^{LD} + \sum_{v \in \Psi_{EV}(j)} P_{v,t}^{CH} - \sum_{w \in \Psi_W(j)} P_w^{WP} - \sum_{c \in \Psi_{PV}(j)} P_c^{PV} - \sum_{g \in \Psi_{MT}(j)} P_{g,t}^{DD}, \forall j \in J, \forall t \in T \tag{3.39}$$

$$Q_{j,t} = \sum_{i \in \delta(j)} Q_{i,t} + \sum_{i \in \delta(j)} x_{ij} \frac{P_{i,t}^{QU} + Q_{i,t}^{QU}}{V_0^2} + Q_{j,t}^{LD} + \sum_{r \in \Psi_{RP}(j)} Q_{r,t}^{AVR}, \forall j \in J, \forall t \in T \tag{3.40}$$

$$V_{j,t} = V_{j,t} + \frac{(r_{ij} P_{i,t} + x_{ij} Q_{i,t})}{V_0}, \forall j \in J, \forall i \in \delta(j), \forall t \in T \tag{3.41}$$

$$V_{j,t} = V^{SB}, j = 1, \forall t \in T \tag{3.41}$$

$$P_{j,t}^{QU} \geq K_{\gamma,j,t}^{AP} P_{j,t} + B_{\gamma,j,t}^{AP}, \forall j \in J, \forall \gamma \in \Gamma^{AP}, \forall t \in T \tag{3.42}$$

$$Q_{j,t}^{QU} \geq K_{\gamma,j,t}^{RP} Q_{j,t} + B_{\gamma,j,t}^{RP}, \forall j \in J, \forall \gamma \in \Gamma^{RP}, \forall t \in T \tag{3.43}$$

$$\underline{Q}_r^{SVC} \le Q_{r,t}^{SVC} \le \bar{Q}_r^{SVC}, \forall r \in R, \forall t \in T \tag{3.44}$$

$$P_{j,t}^{QU}, Q_{j,t}^{QU} \in R^+, \forall j \in J, \forall t \in T \tag{3.45}$$

$$V_{j,t} + S_{j,t}^{V,LB} \ge 1 - \varepsilon, \forall j \in J, \forall t \in T \tag{3.37}$$

$$V_{j,t} - S_{j,t}^{V,UB} \le 1 + \varepsilon, \forall j \in J, \forall t \in T \tag{3.46}$$

$$P_{j,t}^{QU} + Q_{j,t}^{QU} - S_{j,t}^{LC} \le LC_{ij}^2, \forall j \in J, \forall i \in \delta(j), \forall t \in T \tag{3.47}$$

$$S_{j,t}^{V,LB} \in R^+, S_{j,t}^{V,UB} \in R^+, S_{j,t}^{LC} \in R^+, \forall j \in J, \forall t \in T \tag{3.48}$$

where constraints (3.39)–(3.41) describe the worst-case power flow, constraint (3.42) limits the substation voltage, constraints (3.43)–(3.44) (3.46) describe linearization of quadratic terms of active and reactive power in the worst-case scenario and constraint (3.45) describes the limitation of static voltage compensator output. The voltage upper and lower boundary limitations are given in (3.47) and (3.48). The line capacity limitation is given in (3.49). The slack variables are non-negative, described in (3.50).

It should be noted that the upper bound and lower bound of M_I are variables representing the upper-level planning uncertainty, which will make the problem intractable. Considering the fact that the distribution network constraints of voltage and line capacity will either reach the upper bound or the lower bound in worst-case scenario, the robust optimization based feasibility checking model can be decomposed into the following categories. With each power flow, the input of EV penetration level and conventional load are given as,

$$\mathrm{X}^{EV} = \underline{\mathrm{X}}^{EV}, \mathrm{X}^{LD} = \underline{\mathrm{X}}^{LD}, \text{ if } s = 1 \tag{3.49}$$

$$\mathrm{X}^{EV} = \bar{\mathrm{X}}^{EV}, \mathrm{X}^{LD} = \bar{\mathrm{X}}^{LD}, \text{ if } s = 2 \tag{3.50}$$

where the index s is used for counting the feasibility checking constraints. In other word, the feasibility checking constraints are written twice and (3.51) and (3.52) are interpreted as the input of the uncertainty set Ω_{US} for each feasibility checking constraint. The worst-case scenario s=1 describes power redundant case when the lower bound of distribution network load and the upper bound of NDG output are selected. In this condition, the power generated in distribution network is larger

than the demand. The worst-case scenario s=2 describes power insufficient case when the upper bound of distribution network load and the lower bound of NDG are selected. In this regard, the power generated in the distribution network is smaller than the demand. Thus, the voltage tends to reach its lower bound and the power flow tends to reach the line capacity. It should be also noted that some parameters in uncertainty set is a function of X^{DS}, given as follows,

$$[\underline{P}_{c,t}^{CH,s}, \overline{P}_{c,t}^{CH,s}, \underline{\Lambda}_{t}^{CH,C}, \overline{\Lambda}_{t}^{CH,C}, \underline{\Lambda}_{c}^{CH,T}, \overline{\Lambda}_{c}^{CH,T}] = g(\mathrm{X}^{DS}) \tag{3.51}$$

3.4. Solution Method

3.4.1 Compact Formulation

For simplicity, the compact formulation of model RP-I is written as follows,

$$\min_{\mathbf{x},\hat{\mathbf{y}}} \mathbf{a}^{\mathbf{T}}\mathbf{x} + \mathbf{b}^{\mathbf{T}}\hat{\mathbf{y}} \tag{3.52}$$

$$\text{s.t.} \qquad \mathbf{A}\mathbf{x} + \mathbf{B}\hat{\mathbf{y}} = \mathbf{c}, \mathbf{C}\mathbf{x} + \mathbf{D}\hat{\mathbf{y}} \le \mathbf{d} \tag{3.53}$$

$$\mathbf{x} \in \left\{ \begin{array}{l} \mathbf{x} \mid (\max\limits_{\mathbf{v}^s} \min\limits_{\mathbf{y}^s,\mathbf{z}^s} \mathbf{f}^{\mathbf{T}}\mathbf{z}^s) = 0, \forall s \\ s.t.\ \mathbf{E}\mathbf{x} + \mathbf{F}^s\mathbf{y}^s + \mathbf{G}^s\mathbf{v}^s + \mathbf{H}^s\mathbf{z}^s = \mathbf{g}, \forall s \\ \quad \mathbf{I}^s\mathbf{y}^s \le \mathbf{h}, \forall s \\ \quad \mathbf{J}^s\mathbf{v}^s \le \mathbf{i}^s, \mathbf{z}^s \in R^+, \forall s \end{array} \right\} (3.54)(3.55)(3.56)(3.57)$$

where $\mathbf{x}$ represents integer vector of DG investment capacity, $\hat{\mathbf{y}}$ represents continuous vector of active distribution network operation variables in base case, s is the index of feasibility check, $\mathbf{y}^s$ represents continuous vector of active distribution network operation status in worst-case scenario s, $\mathbf{z}^s$ represents the slack variables of active distribution network operation constraints, $\mathbf{v}^s$ represents binary vector to indicate whether the upper or the lower bound of uncertainty is selected. The variables X^{EV}, X^{LD} in the uncertainty set can be assigned with their either lower or upper bound manually in different scenario s so that the value of $\mathbf{i}^s$ can be determined.

The compact formulation (3.52)–(3.57) is formulated as a two-stage problem and thus can be rewritten separately as,

Main problem (MP): (3.52)–(3.53)

Subproblem (SP):

$$\max_{\mathbf{v}} \min_{\mathbf{y}^s,\mathbf{z}^s} \mathbf{f}^{\mathrm{T}}\mathbf{z}^s \tag{3.58}$$

$$\text{s.t. (3.55)–(3.57)} \tag{3.59}$$

Then the methodology for the main problem and the subproblem can be developed accordingly.

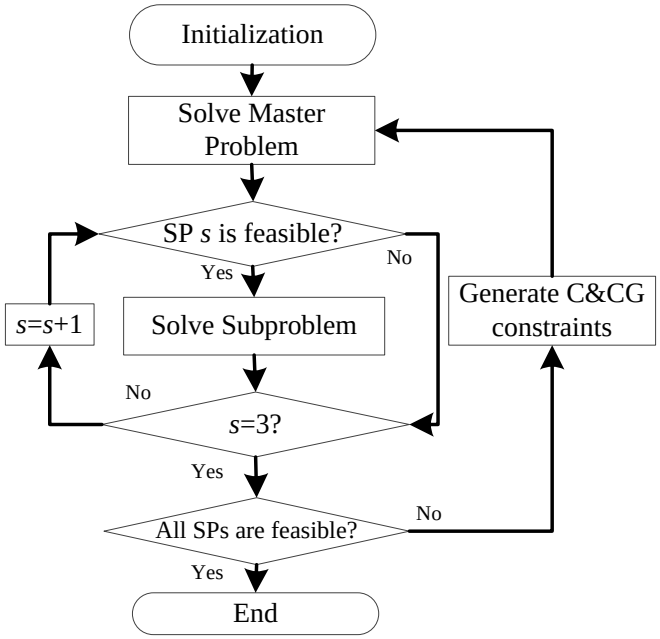

Figure 3.2. The framework of the active distribution network investment algorithm.

3.4.2 Solution Methodology for Subproblem.

Mathematically the SP problem is a bi-level mixed integer linear program (MILP) and can be solved by many methods such as the duality theory. In this study, the inner-level problem is replaced by its dual and the SP is formulated as a single-level bilinear program, which can be solved by either outer approximation method [34] or big-M method [35]. As OA may fail to find the global optimal solution, big-M method is adopted to solve subproblem. The compact formulation of the dual problem of subproblem is given as follows,

$$\max_{\mathbf{v}^s,\boldsymbol{\psi}^s} O^s = (\mathbf{c} - \mathbf{E}\mathbf{x} - \mathbf{G}^s .* \mathbf{v}^s)^T \boldsymbol{\psi}^s - \mathbf{h}^T \boldsymbol{\lambda}^s \tag{3.60}$$

$$\text{s.t.} \quad -\mathbf{F}^{sT}\boldsymbol{\psi}^s + \mathbf{I}^{sT}\boldsymbol{\lambda}^s = \mathbf{0}^T \tag{3.61}$$

$$\mathbf{H}^{sT}\boldsymbol{\psi}^s \le \mathbf{f}^T \tag{3.62}$$

$$\mathbf{J}^s\mathbf{v}^s \le \mathbf{i} \tag{3.63}$$

$$\boldsymbol{\lambda}^s \in \mathbf{R}^+ \tag{3.64}$$

where $\boldsymbol{\psi}^{s\mathbf{T}}$ and $\boldsymbol{\lambda}^{\mathbf{T}}$ are the dual vectors of (3.63) and (3.64) respectively and '.*' in (3.60) is a Hadamard product. Then to linearize the bilinear term in the objective function, auxiliary variables and constraints are introduced to convert the problem into a MILP problem, as follows,

$$\max_{\mathbf{v}^s,\boldsymbol{\psi}^s} O^s = (\mathbf{c} - \mathbf{E}\mathbf{x})^T \boldsymbol{\psi}^s - \mathbf{h}^T \boldsymbol{\lambda}^s - e^T \mathbf{w}^s \tag{3.65}$$

$$\text{s.t.} \quad -M_{Big}\mathbf{v}^s \le \mathbf{w}^s \le M_{Big}\mathbf{v}^s \tag{3.66}$$

$$\mathbf{G}^{s\mathbf{T}}\boldsymbol{\psi}^s - (\mathbf{1} - \mathbf{v}^s)M_{Big} \le \mathbf{w}^s \le \mathbf{G}^{s\mathbf{T}}\boldsymbol{\psi}^s + (\mathbf{1} - \mathbf{v}^s)M_{Big} \tag{3.67}$$

$$(3.61)\text{–}(3.64) \tag{3.68}$$

where M_{Big} is the positive parameter that is sufficient large compared to the bilinear term. Thus the problem is formulated as a MILP, which can be solved by commercial solvers such as Cplex and Gurobi.

3.4.3 Solution Methodology for Main Problem

Note that both the master problem, described with (12a)–(12b), and the subproblem, described with (3.65)–(3.68), are formulated as MILPs. Then the C&CG algorithm is adopted to solve the RP-I problem and named as Al, with details given as follows,

---

Al: C&CG Algorithm

Step 1: Set $k = 1$.

Step 2: Solve (12a)-(12b) with axillary constraints as follows,

$$\mathbf{E}\mathbf{x} + \mathbf{F}^s\mathbf{y}_k^s + \mathbf{G}^s\tilde{\mathbf{v}}_k^s = \mathbf{g}, \mathbf{I}^s\mathbf{y}^s \le \mathbf{h}, \forall s \tag{3.69}$$

Step 3: If $|O^s-0|<\varepsilon^{A1}$ for all the scenario *s*, terminate. Otherwise, solve (15a)-(15d) for scenario *s*. Otherwise, obtain the optimal solution $\tilde{\mathbf{v}}_{k+1}^s$, create axillary variable vector $\mathbf{y}_{k+1}^s$ and add the following constraints,

$$\mathbf{E}\mathbf{x}+\mathbf{F}^s\mathbf{y}_k^s+\mathbf{G}^s\tilde{\mathbf{v}}_k^s=\mathbf{g},\mathbf{I}^s\mathbf{y}^s\le\mathbf{h},\forall s \tag{3.70}$$

Update $k=k+1$ and go to step 2.

In Al, ε^{A1} represents the convergence gap and $\tilde{\mathbf{v}}_k^s$ is the parameter representing the identified uncertainty in worst-case scenario. In the C&CG algorithm, a number of additional constraints (3.70) are directly added into MP. Fig. 3.2 illustrates the worst-case feasibility checking algorithm for the proposed model. If the SP in any scenario *s* is not feasible, the corresponding C&CG constraints will be generated and added to the main problem. The algorithm stops only when all the SPs in worst-case scenario are feasible.

3.5. Case Study

In this section, case studies are conducted to illustrate the proposed model using the modified IEEE 123-node distribution network. All the algorithms are implemented on MATLAB programmed with the toolbox YALMIP [52]. Cplex is used as the MILP solver, with the optimality gap set as 10^{-3}.

Table 3.1. Parameter Settings

Parameter	Value	Parameter	Value
ε	0.05	λ_t^{EM}	0.07$/MWh
V^{SB}	1.0	λ^{DD}	0.15$/MWh
$U^{WP}/U^{PV}/U^{DD}$	6/3/1	α	0.9
$\delta^{WP}/\delta^{PV}/\delta^{DD}$	0.1/0.05/0.1MWh	$\underline{X}^{EV}$ / $\bar{X}^{EV}$	1.0/1.5
η_{ch}	0.9	$\underline{X}^{LD}$ / $\bar{X}^{LD}$	1.0/1.2
P_v^{ch}	6 kW	$\underline{X}^{DS}$ / $\bar{X}^{DS}$	0.1/0.9
Θ	50$/MWh	M_{Big}	1000

3.5.1 Test System

In the modified 123-node active distribution network system, 6 nodes are connected with EV charging facilities and 6 nodes are equipped with static voltage compensators, as shown in Fig. 3.1. 50 EVs are assumed to arrive in a day at each active distribution network node with EV charging facility. The average active distribution network peak load without consideration of the EV charging demand is set as 2.84 MW/1.53 MVAR and the 24 one-hour load value at each of the 24 one-hour time intervals, compared with the peak load, is given as 0.64 0.645 0.635 0.64 0.705 0.81 0.86 0.83 0.85 0.87 0.905 0.83 0.81 0.85 0.89 0.96 1 0.99 0.94 0.91 0.87 0.8 0.72 0.66. The DG investment costs are referred to [36] and other important parameters are given in Table 3.1.

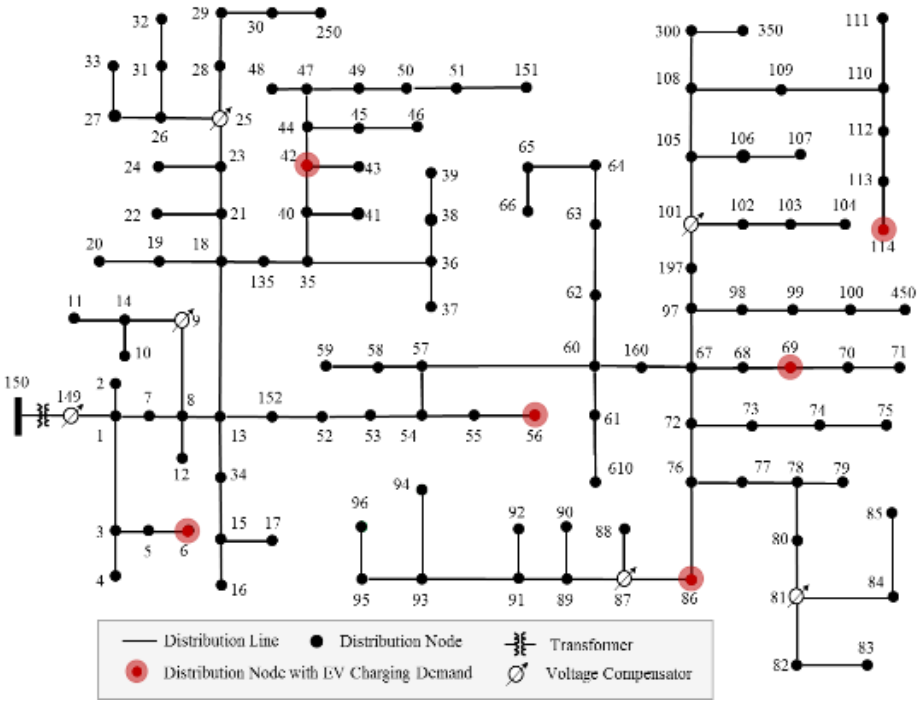

Figure 3.3. Modified IEEE 123-node distribution network for DN planning.

3.5.2 Planning Schemes

The proposed robust optimization based distribution network planning model determines the optimal sizing and siting of all kinds of DGs, hedging against any output uncertainties of EV charging demand and NDGs, with its final planning

scheme given in Table 3.2. It can be observed that the total investment capacity of NDGs is larger than DDGs, which is mainly due to the general economic advantages of nearly zero operation costs. The wind power generator investment is preferably selected compared with the PV generators, as the wind power generators can provide energies during the whole day. It can also be found that the NDGs are located separately in the distribution network so that the energy can be locally supplied. In this way, the energy loss of distribution network is maximumly reduced and the voltage deviation can be reduced to the largest extent.

The voltage profiles at node 75 in both power redundant worst-case scenario and power insufficient worst-case scenario are given in Fig. 3.3 and Fig. 3.4 respectively. The power redundant scenario occurs when the NDG output is high and total distribution network load is low. In this condition, the distribution network voltage shows a significant rise from below 1.0 p.u. to above 1.0 p.u. The NDG investment capacity is well optimized to make sure the voltage deviation is within its upper boundary. The DDG is not committed on in this scenario. The power insufficient scenario occurs when the NDG output is low and total distribution network load is high. In this condition, the distribution network voltage tends to drop below 0.95 p.u., leading to the urgent demand of DDG investment. Fig. 3.5 shows that the DDG output help to maintain the voltage at 0.95 p.u. Hence, it can be concluded that the investment capacity of NDGs is limited by the upper boundary of voltage and the investment capacity of DDGs is determined by the level of voltage drop in power insufficient worst-case scenario.

Table 3.2 Planning Scheme of RP-I Model

Location	Type	Size(MVA)	Location	Type	Size(MVA)
19	WP	0.7	51	PV	0.35
42	WP	1.1	93	PV	0.15
53	WP	1.9	114	DDG	0.5
68	WP	1.5	Total	WP	5.8
87	WP	0.4	Total	PV	0.5
110	WP	0.2	Total	DDG	0.5

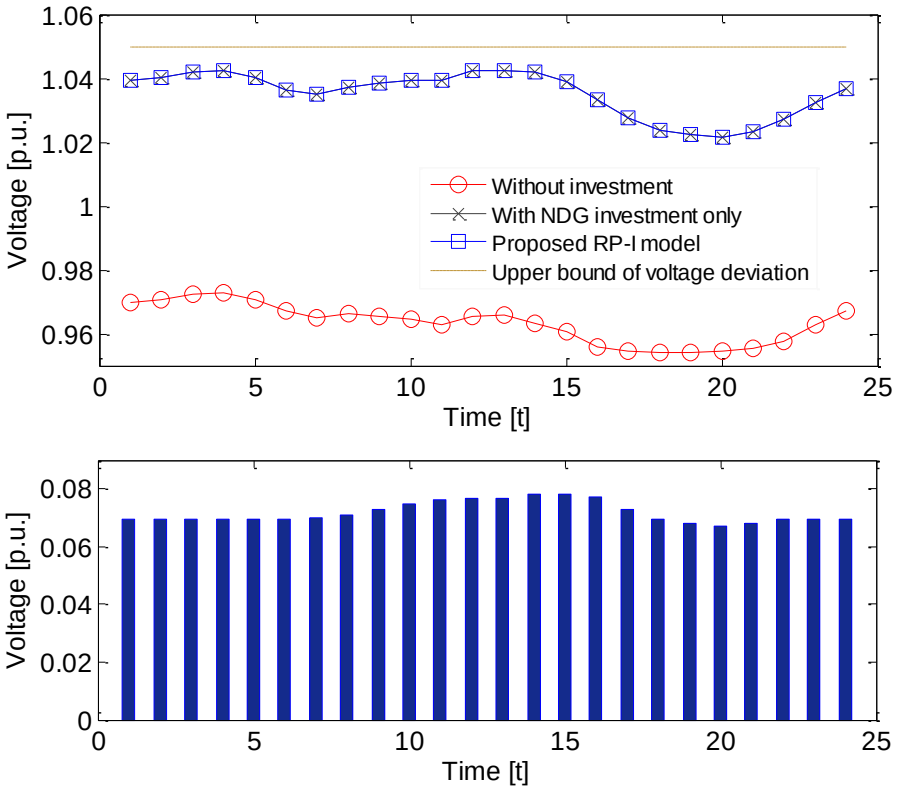

Figure 3.4. Voltage profile at node. 75 in power redundant worst-case scenario

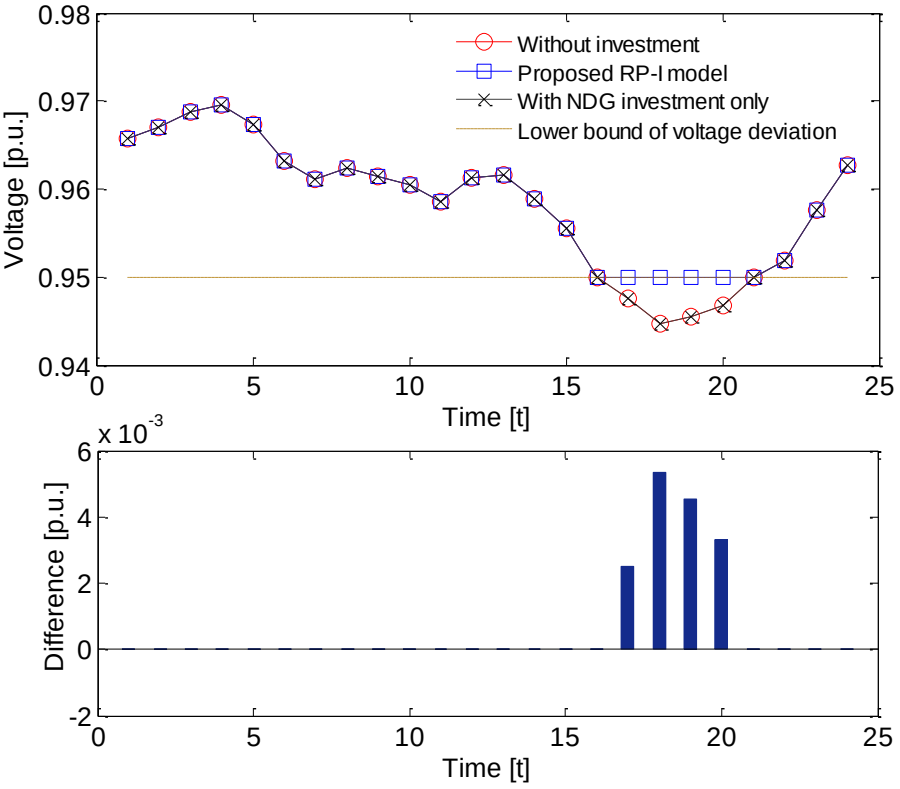

Figure 3.5. Voltage profile at node 75 in power insufficient worst-case scenario

3.5.3 Impact of NDG curtailment

The aforementioned model guarantees the distribution network operation security given any NDG output within its installed capacity. However, it is possible to curtail the excessive NDG output when the constraints violation happens, which may be practically implemented by command-driven electronic devices for NDG. To enable curtailment, [53] proposes the concept of admissible boundary of the wind power generators and PV generators, where the operation security is guaranteed as long as the NDG output is within the admissible boundary and the power out of boundary is curtailed. Hence the curtailment allowed distribution network planning model can be formulated by adding the following objective function and constraints into the original model, simplified as RP-II,

RP-II:

$$\min f = f^{INV} + f^{OP} + f^{CT} \tag{3.73}$$

$$f^{CT}(I_w^{WP}, I_c^{PV}) = \theta \sum_{t\in T}\sum_{w\in W}(\delta^{WP} I_w^{WP} - R_{w,t}^{WP}) + \sum_{t\in T}\sum_{c\in T}(\xi_t^{PV,CA}\delta^{PV} I_c^{PV} - R_{c,t}^{PV}) \tag{3.74}$$

subject to

$$0 \le R_{w,t}^{WP} \le \delta^{WP} I_w^{WP}, \forall w \in W, \forall t \in T \tag{3.75}$$

$$0 \le R_{c,t}^{PV} \le \xi_t^{PV,CA}\delta^{PV} I_c^{PV}, \forall c \in C, \forall t \in T \tag{3.76}$$

(3.17)-(3.53)

where $R_{w,t}^{WP}$ and $R_{c,t}^{PV}$ denote the axillary variables, denoting admissible boundary of the wind power and PV generators and θ denotes the curtailment cost. Notice that the upper bound of NDG output should be replaced by $R_{w,t}^{WP}$ and $R_{c,t}^{PV}$, while the upper bounds of $R_{w,t}^{WP}$ and $R_{c,t}^{PV}$ are limited by the investment capacity.

Fig. 3.6 compares the planning scheme of the NDG curtailment allowed model and the one without curtailment. It can be observed that the total investment capacities of wind power generators and PV generators increase while the capacity

of DDG remain the same when curtailment can be carried out. Consequently, the total revenue shows a slight increase, which is largely due to the profit brought by the wind power plant investment. The DG locations are not given due to space limitation, which are generally similar to the non-curtailment model. It is because the topology of the distribution network remains unchanged. For practical implementation, the curtailment cost θ can be regarded as a weighting factor and adjusted according to planners' preference.

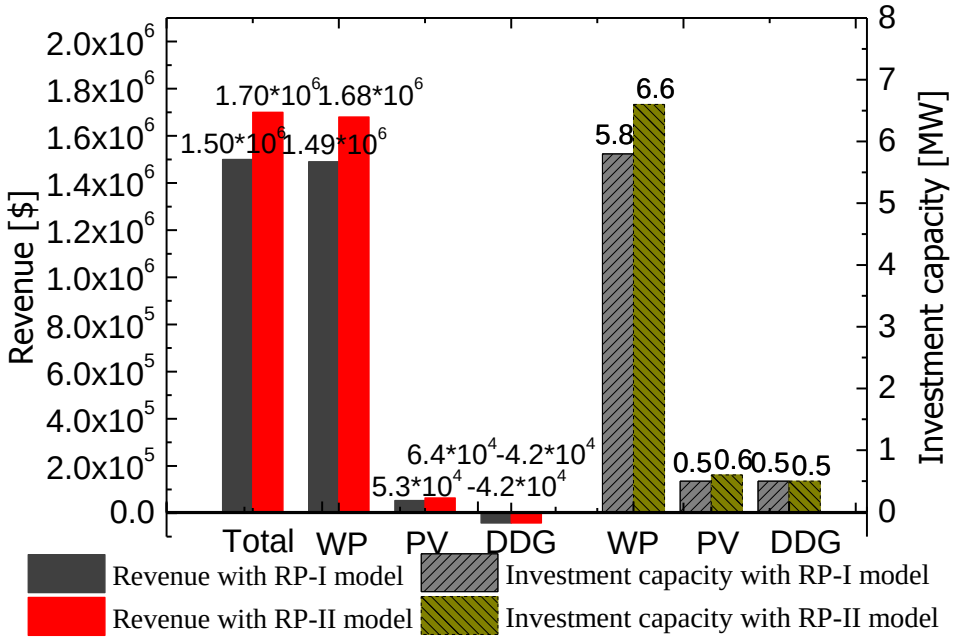

Figure 3.6. Planning schemes of NDG curtailment allowed model.

3.5.4 Impact of Carbon Emission Cost

To hedge against greenhouse effect, carbon emission is usually posed an additional cost, known as carbon emission cost. Especially in a planning problem for power system, the carbon emission cost should be considered in calculating the distribution operation cost. Hence, the following terms should be added to the original objective.

$$f^{CE} = \Phi^{D} \sum_{t \in T} \lambda^{CE} \left(\sum_{w \in W} \hat{P}_{w,t}^{WP} + \sum_{c \in C} \hat{P}_{c,t}^{PV} \right) \tag{3.77}$$

where f^{CE} denotes yearly cost saving due to exempting carbon emission punishment and λ^{CE} denotes the per MW carbon emission cost, set as 10% of the electricity price.

The impact of carbon emission cost on the DG investment schemes is compared in Fig. 3.7. It can be observed that the planning schemes in RP-I model remain the unchanged when the carbon emission cost is considered. It is because the renewable DG investment capacity is limited by the distribution system security, i.e., the voltage rise constraint, rather than the economic return of investment. When it comes to the RP-II model, the investment of renewable DGs is more preferable if carbon emission cost is considered, as seen from the slight increase of wind power generator and PV generator investment in Fig. 3.7. In this case, even though more renewable DG investment will cause energy waste, it helps to reduce the traditional energy consumption and thus exempt more costs due to carbon emission punishment. Besides, the DDG investment capacity is to improve distribution system reliability and thus not affected by the carbon emission cost.

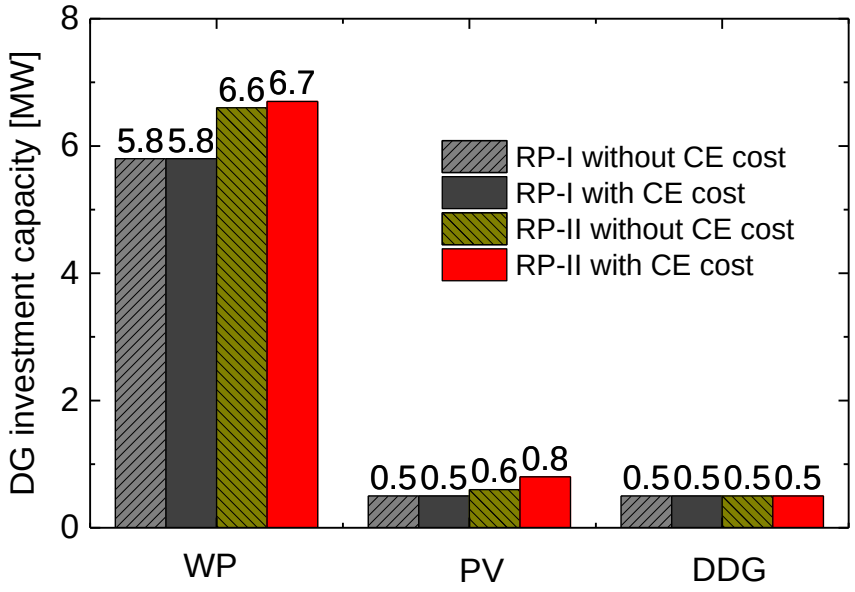

Figure 3.7. Planning schemes considering carbon emission cost

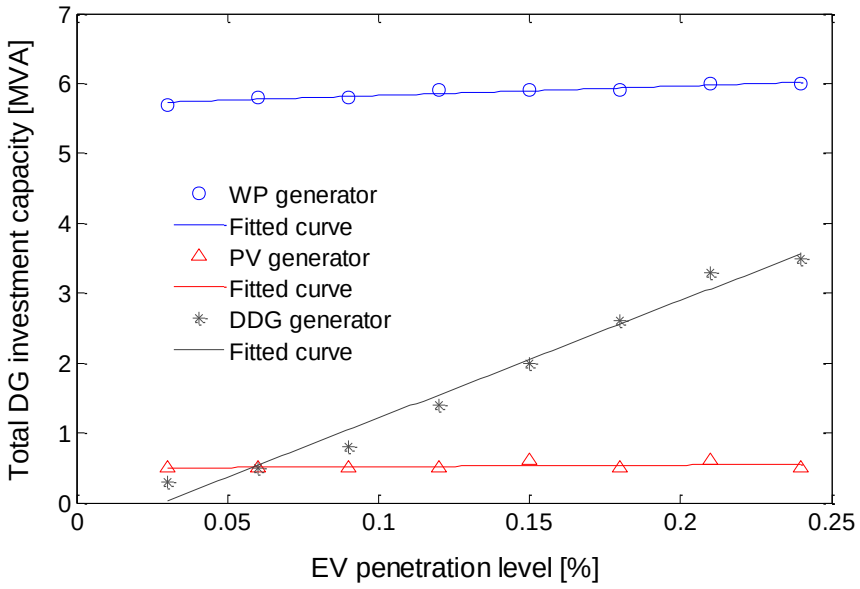

Figure 3.8. Impact of EV penetration level on DG investment

3.5.5 Impact of EV penetration level on DG investment

The impact of EV penetration level on the DG planning scheme is evaluated in this subsection. The EV penetration level is defined as the ratio of total EV charging demand to total distribution network demand during the day, given as,

$$PT_{EV} = \frac{\sum_{t\in T}\sum_{v\in V}\hat{P}_{v,t}^{CH}}{\sum_{t\in T}\sum_{j\in J}\hat{P}_{j,t}^{LD} + \sum_{t\in T}\sum_{v\in V}\hat{P}_{v,t}^{CH}} \tag{3.78}$$

where PT_{EV} denotes the EV penetration level. The total investment capacities of DGs of RP-I model are depicted in Fig. 3.8. It can be found that the DDG installation capacity has a constant increase with the increase of EV penetration level and the installation of wind power generators and PV generators demonstrate a slight increase. As the proposed model tried to find a planning scheme that is robust for any possible uncertainties, the worst-case operation scenario is always found that the large-scale EVs happen to be charged when the NDGs output at the lower bound. Thus, NDGs cannot contribute as much as DDGs to providing energy and guarantee secure distribution network operation against uncertain output of NDGs and large-scale EV charging demand, which illustrates the fact that the installed DDG capacity is more sensitive to the EV penetration level.

3.6. Conclusions

This paper proposes a robust distribution network planning framework accommodating the uncertainty of renewables and large-scale EVs. Advanced modelling of EV charging demand is proposed using polyhedral uncertainty set and data mining method is adopted to obtain the statistical parameter for the output of uncertainty set. Case studies demonstrate the effectiveness of the proposed model and verify the proposed algorithm by determining the optimal DG sizing and siting with both models. Results demonstrate that the NDG investment capacity is limited by the distribution system voltage rise constraint violations. When the NDG curtailment is allowed, the investment capacity can be further increased, especially when the carbon emission tax is considered. The DDG investment demonstrates a considerable growth when the EV penetration level becomes even higher in distribution system.

4. Power System Spinning Reserve Requirement Optimization considering Electric Vehicles' participation

4.1. Introduction

Spinning reserve in power systems is known as the reserve capacity that is spinning, synchronized and ready to dynamically balance system load [54]. In order to withstand sudden outages of some generators and unforeseen fluctuations of the power system demnad and renewable energies [55, 56], the daily operation cost increases as additional generators are committed on and other cheaper generators operate smaller than the optimal output to provide the spinning reserve. Considering the widely application, EVs' potential ability of interrupting charging demand and providing V2G service when the power system contingency happen will benefit the secure and economic operation of power systems. However, the effluences of EVs on the quantification of spinning reserve requirement is still to be further discussed.

To quantify the spinning reserve requirement, both deterministic and probabilistic criteria are developed to keep the power system operating within a given risk level. The reserve set by deterministic criteria is dependent on the capacity of the largest online generator or the certain proportion of the daily peak load, which is quite easy to implement [57]. However, lots of system uncertainties and the stochastic nature of the component failures are not taken into account using the deterministic criteria. To overcome this problem, the probabilistic criteria have drawn lots of attentions due to its advantages on demonstrating the uncertainties of the availability of generators, the outages of transmission networks, generator response rate, and so on [58]. The loss of load probability, the expected energy not

supplied and the unit commitment risk are commonly presented as probabilistic criteria to estimate the power system SRR [54]. A market clearing process with bounded loss of load probability and EENS is proposed as additional linearized constraints of unit commitment formulation [59]. Market clearing models are presented in [60] to optimize the spinning reserve via adding the cost of energy deficit calculated by the value of lost load and EENS into the typical unit commitment problem. However, these spinning reserve optimization methods are based on the adjustification of unit commitment formulation, which needs complicated iterative processes and approximate calculation of the risk levels related to the reserve provision. To address this issue, a cost and benefit analysis model is proposed to optimize the SRR in an auxiliary optimization method before solving the unit commitment problem [61]. The advantage of this model is not only on the computation efficiency improvement by avoiding suboptimal solutions but also on the excellent compatibility with existing unit commitment problems.

In modern power systems, the influences of various factors are considered in the quantification of the SRR. The uncertainty of high penetration of wind power [62] poses a great challenge to the optimization of the spinning reserve [63, 64]. Besides, other emerging impact factors such as carbon capture plants [65], customers' choice on the reliability [66] and bidding uncertainties in the electricity market [67] are taken into consideration in optimizing the spinning reserve. To keep the power system adequacy, some other factors are considered to partly replace the spinning reserve including rapid start units, interruptible loads, voltage and frequency reductions, assistance from interconnected system, and so on [68]. These additional factors and spinning reserve act as operating reserve. In practice, hydro generation is regarded the most common fast start-up unit to provide operation reserve [69]. An energy based technique to assess spinning reserve requirements considering the aid of interconnected systems is proposed in [70]. The influences of interruptible load and demand response on spinning reserve quantification are analyzed in [71].

Considering the unique advantages of flexible charging load and V2G service, EVs can be an effective alternative resource to supply operating reserve in the power system under optimal compensation mechanism. With the large number of

application of EVs in the foreseeable future, the ability of EVs in providing ancillary service are attracting large attentions [72-76]. Among these studies, the optimal EV scheduling schemes or the optimal bidding strategies involved in energy and reserve market are acquired through maximizing the profit of EV aggregators. Especially, power system reserve provided by V2G service can help to mitigate the influences of wind power production uncertainty and facilitate the integration of wind power [77, 78]. EVs can also provide supplemental primary reserve and frequency regulations via V2G technology to enhance power system stability [79, 80].

A cost-efficiency based optimization model of day-ahead spinning reserve requirement optimization considering the integration of EVs is proposed. In the study, EVs participate in contingency reserve optimization and provide energy support through charging interruption and V2G service when energy deficit occurs because of generator outage. Similar to EENS, expected energy supplied by EV is formulated to quantify EVs' ability in providing operating reserve. Comprehensive cost/benefit analysis is carried out to compare the reserve provision cost of thermal generators and that from EVs. It explicitly verifies the merits of EVs' reserve provision such as the reduction of operation cost and the improvement of system reliability. The impacts of the EV penetration level and the compensation to EV owners on SRR allocation are systematically evaluated based on sensitivity analysis to provide useful information to future implementation and effectively bring the concept of V2G into practice.

The nomenclature of Symbols used in this chapter is given as follows,

Sets

G	Set of generators.
T	Set of hourly time intervals.
T_{Δ}	Set of intra-hour time intervals.
V	Set of electric vehicles.
V_c	Set of electric vehicle clusters.

Parameters

C_{BI}	Battery investment cost of V2G service.
C_{Comp}	Compensation cost paid to EV owners.

C_{Int}	Cost to interrupte EV charging demand.
C_{V2G}	Cost to provide EV V2G service.
CR_{EV}	EV compensation rate.
d_{DoD}	Depth of discharge.
E_v^{Coms}	Daily energy consumption of EV *v*.
Lb, Ub	Lower and upper boundaries of SRR in grid search-based SRR optimization methodology.
L_C	Battery cycle life at a depth of discharge.
N_{EV}	Number of EVs.
n_c	Number of EVs in cluster *c*.
$ORR_{i,\tau}$	Outage replacement rate of unit *i* at time τ.
P_{aver}	Average power system demand.
P_{t}^{CH}	Total EV charging demand at time *t*.
P_t^{D}	Power system demand without EV charging demand at time *t*.
$P_{\text{ch,max}}$	Maximum charging power of each EV.
$P_{\text{V2G,max}}$	Maximum V2G discharging limitation of each EV.
$P_i^{\min}$,$P_i^{\max}$	Lower and upper limitation of power output of unit *i*.
PL_{EV}	Penetration level of EVs in power system.
R_i^{up}	Short-term up-regulation reserve rate of unit *i*.
RD_i, RU_i	Hourly ramp-up and ramp-down ability of unit *i*.
$S_{\text{EV,max}}$	EVs' battery capacity.
$S_{\text{clus,min}}$, $S_{\text{clus,max}}$	Lower and upper limitations of equivalent state of charge of EV cluster *c*.
$S_c^{\text{clus,exp}}$	Expected state of charge when EV cluster *c* plugs out.
t_v^{arr} , t_v^{dep}	Arrival and departure time of EV *v*.
$u_{v,t,\tau}^{\text{EV}}$	Binary parameter with 1 indicating EV connected to the grid.
$u_{t',t,\tau}^{\text{CI}}$,$u_{t',t,\tau}^{\text{CII}}$,$u_{t',t,\tau}^{\text{CIII}}$	Binary parameters with 1 indicating the state before, during and after contingency
$u_{t',t,\tau}^{\text{EV,del}}$	Binary parameter with 1 denoting EV reacting to contingency
VOLL	Value of lost load.
α,β,γ	Generator cost function coefficients.
Δt, $\Delta\tau$	Period of each time interval, Δt = 1 hour; $\Delta\tau$ = 10 minutes.
η_{ch}	EV charging efficiency.
λ_i	Expected failure rate of unit *i*.
ξ_t	Uncertainty parameter of EV behaviors.
τ_1	Time interval of post-contingency EV reaction.
τ_2	Time interval of power system contingency.
ω	Proportion of power system demand which is required to

provide, known as load following reserve

Variables

$EENS_t$	Expected energy not supplied.
$EESEV_t^{Int}$	Expected energy supplied by EVs' charging interruption.
$EESEV_t^{V2G}$	Expected energy supplied by EVs' V2G service.
$ES_{j,t}$,$ES_{jk,t}$	Energy shift due to random event of single unit j outage and double units j and k outage.
$E_{v,t'}^{Ch}$	Total EV charging energy between the time EV responds to contingency and the time system recovers.
$E_{v,t'}^{Sup}$	Maximum supplementary recharging energy between the recovery of power system and the departure of EVs.
$E_{v,t'}^{Rem}$	Total energy remained in the EV battery when EVs provide V2G service.
$E_{v,t}^{V2G,lim}$	Energy of V2G limitation during contingency period.
$P_{i,t}$	Power output of unit i at time t.
P_t^{Int}	The power capacity of interruptible EV charging.
P_t^{V2G}	The power capacity of EV V2G service.
P_t^{EVR}	Total power capacity of operating reserve that EVs can provide.
$P_{v,t,\tau}^{ch}$	Charging power of EV v at time t, τ.
P_t^{total}	Total power system demand considering EVs charging demand.
P_{aver}	Average power system demand.
$P_{c,t,\tau}^{ch,clus}$	Equivalent charging power of EV cluster c at time t,τ.
$Pr_{j,t,\tau}$,$Pr_{jk,t,\tau}$	Probability of the random event of single unit j outage and double units j and k outage.
r_t^{req}	Spinning reserve requirement at time t.
$r_{i,t}$	Spinning reserve provided by unit i at time t.
$S_{c,t}^{clus}$	Equivalent state of charge of EV cluster c at time t.
$u_{i,t}^{G}$	On and off status of unit i at time t.

4.2. Mathematical Model

4.2.1 Formulation of Spinning Reserve Requirement

As the model developed in [61], the SRR of each optimization period can be obtained using an auxiliary optimization method before conducting the unit commitment problem. Hourly SRR is separately determined for each time interval based on cost/benefit analysis. The inter-temporal constraints are not considered

in the optimization model [61, 63, 65]. After the hourly SRR is obtained, it is regarded as inputs of typical reserve-constrained unit commitment model. The major advantage of the model mainly is the cost and benefit analysis of reserve provision. It is beneficial and practical to evaluate the effects of EVs on spinning reserve requirement from the economic-efficiency aspect. Considering EVs, the SRR model is given not only to balance the cost of operating generation and the cost of EENS, but also to consider the cost of the energy supplied by EVs.

The SRR model with the consideration of EVs can be formulated as,

$$\min_{r_t^{\text{req}}} f_{\text{SRR}}(r_t^{\text{req}}) = f_{\text{OPER}}(r_t^{\text{req}}) + f_{\text{EENS}}(r_t^{\text{req}}) + f_{\text{EESEV}}(r_t^{\text{req}}) \tag{4.1}$$

where,

$$f_{\text{OPER}}(r_t^{\text{req}}) = \min_{u_{i,t}^{G}, P_{i,t}} \sum_{i \in G} \alpha P_{i,t}^2 + \beta P_{i,t} + \gamma u_{i,t}^{\text{G}} \tag{4.2}$$

$$f_{\text{EENS}}(r_t^{\text{req}}) = VOLL \times EENS_t \tag{4.3}$$

$$f_{\text{EESEV}}(r_t^{\text{req}}) = C_{\text{Int}} EESEV_t^{\text{Int}} + C_{\text{V2G}} EESEV_t^{\text{V2G}} \tag{4.4}$$

subject to:

$$\sum_{i \in G} P_{i,t} - (P_t^{\text{D}} + P_t^{\text{CH}}) = 0, \forall t \in T \tag{4.5}$$

$$r_t^{\text{req}} - \sum_{i \in G} r_{i,t} \le 0, \forall t \in T \tag{4.6}$$

$$r_{i,t} = \min\{u_{i,t}^{\text{G}}(P_i^{\max} - P_{i,t}), u_{i,t}^{G} R_i^{\text{up}}\}, \forall t \in T, \forall i \in G \tag{4.7}$$

$$P_{i,t} \ge u_{i,t}^{\text{G}} P_i^{\min}, \forall t \in T, \forall i \in G \tag{4.8}$$

$$P_{i,t} + r_{i,t} \le u_{i,t}^{\text{G}} P_{i,t}^{\max}, \forall t \in T, \forall i \in G \tag{4.9}$$

$$-u_{i,t-1}^{\text{G}} RD_i \le P_{i,t} - P_{i,t-1} \le u_{i,t-1}^{\text{G}} RU_i, \forall t \in T, \forall i \in G \tag{4.10}$$

The objective function (4.1) is to minimize the overall hourly cost with respect to the SRR r_t^{req}, which consists of the cost of operating generation $f_{\text{OPER}}(r_t^{\text{req}})$, the cost of the expected energy not supplied $f_{\text{EENS}}(r_t^{\text{req}})$ as well as the cost of the expected energy supplied by EV $f_{\text{EESEV}}(r_t^{\text{req}})$. The generation operation cost defined

in (4.2) is the operation cost of generators to meet the demand and provide the amount of SRR r_t^{req} . The cost of EENS defined in (4.3) is the expected compensation paid to the EV users due to the load shedding. The cost of EESEV represented in (4.4) consists of the cost of the EV charging demand interruption and the cost of implementing V2G. The interruption and V2G service cost is decomposed of compensation to EV owners for delayed charging and the battery degradation, where the details will be discussed in the next section. The constraint of power system balance at each period is given as (4.5). The limitations of the spinning reserve provided by generators are defined by (4.6) and (4.7). The limitations of power generation are given as (4.8) and (4.9), and the ramp-up and ramp-down limitation rates of each unit is given as (4.10).

4.2.2 Formulation of EENS and EESEV

EENS can be determined according to the installed capacity of generating units, the probability of forced outage of each generator, the amount of spinning reserve that each generator can provide and the load level [54]. It is determined by summing all the energy curtailment related to the probability of each contingency. When the EVs participate in the operating reserve, EENS, as well as EESEV should be formulated with the reduction of the shedding load due to the contribution of EVs. The formulation of EENS and EESEV is complex as EVs need some time to take actions. The power not supplied in contingency period is depicted in Fig. 4.1, where EENS and EESEV are presented by the areas in different colors. EV reaction time τ_1 is defined as the time delay for EV aggregator to act. To fulfill the post-contingency dispatch of EVs, the aggregator should firstly obtain EV reserve dispatching commands from power system operator; at the same time obtain the information of each EV, such as state of charge and departure time; finally make decision on whether EV's interruption and V2G energy should be conducted based on each EV's urgency priority. Power system contingency time τ_2 is defined as the time period before the contingency reserve is restored by the offline generators. The values of τ_1 and τ_2 are set based on the requirement of interruptible import and contingency reserve restoration, given in Reliability Standards for the Bulk Electric Systems of North America [81]. Then $EENS_t$ can be divided into $EENS_t^{\mathrm{I}}$ and $EENS_t^{\mathrm{II}}$, where $EENS_t^{\mathrm{I}}$ is the expected energy not supplied during τ_1 and $EENS_t^{II}$ represents the expected energy not supplied

between τ_1 and τ_2. Only $EENS_t^{II}$ is reduced because of the existence of the expected energy supplied by the interrupted energy of EV $EESEV_t^{Int}$ and the expected energy supplied by V2G energy $EESEV_t^{V2G}$.

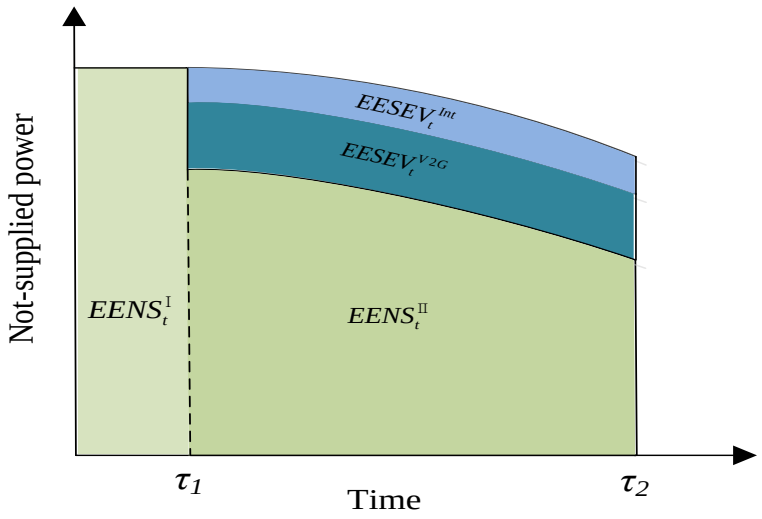

Figure 4.1. Area for evaluating *EENS*, $EESEV_t^{Int}$ and $EESEV_t^{V2G}$

To determine EENS and EESEV, the probability of capacity outage is firstly analyzed. The failed probability of a generator can be estimated as [54],

$$ORR_{i,\tau} = 1 - e^{-\lambda_i \tau} \cong \lambda_i \tau, \forall i \in G, \tau = \tau_1, \tau_2 \tag{4.11}$$

where $ORR_{i,\tau}$ is given as the outage replacement rate and demonstrates the probability that the generator *i* fails and has not yet replaced during time interval τ. Then the time-dependent probability of the random outage event can be determined by (4.12) and (4.13),

$$Pr_{j,t,\tau} = u_{j,t}^{G} ORR_{j,\tau} \prod_{i \in G, i \neq j} (1 - u_{i,t}^{G} ORR_{i,\tau}), \forall j \in G, \forall t \in T, \tau = \tau_1, \tau_2 \tag{4.12}$$

$$Pr_{jk,t,\tau} = u_{j,t}^{G} ORR_{j,\tau} u_{k,t}^{G} ORR_{k,\tau} \prod_{i \in G, i \neq j,k} (1 - u_{i,t}^{G} ORR_{i,\tau}),$$

$$\tau = \tau_1, \tau_2, \forall j,k \in G, \forall t \in T \tag{4.13}$$

where $Pr_{j,t,\tau}$ represents the probability of the random event of single unit *j* outage,

and $Pr_{jk,t,\tau}$ represents the random event of units j and k outage. It should b noticed that the outage events of more than two generators are not taken in account in the study. The energy shift with these contingency scenarios is given as,

$$ES_{j,t} = P_{j,t} - (r_t^{\text{req}} - r_{j,t} - \omega P_t^{\text{D}}), \forall j \in G, t \in T \tag{4.14}$$

$$ES_{jk,t} = P_{j,t} + P_{k,t} - (r_t^{\text{req}} - r_{j,t} - r_{k,t} - \omega P_t^{\text{D}}), \forall j \in G, t \in T \tag{4.15}$$

where ωP_t^{D} represents the proportion of demand which are required to provide, known as load-following reserves [82].

To simplify the expression of EENS and EESEV, a piecewise function $g(x)$ is introduced and given as below:

$$g(x) = \begin{cases} x, & \text{if } x \geq 0 \\ 0, & \text{if } x < 0 \end{cases} \tag{4.16}$$

EENS with the consideration of EVs can be formulated as,

$$EENS_t = EENS_t^{\text{I}} + EENS_t^{\text{II}} \tag{4.17}$$

where

$$EENS_t^{\text{I}} = \sum_{j \in G} Pr_{j,t,\tau_1} g(ES_{j,t}) \tau_1 + \sum_{j \in G} \sum_{k \in G, j<k} Pr_{jk,t,\tau_1} g(ES_{jk,t}) \tau_1, \forall t \in T \tag{4.18}$$

$$\begin{aligned} EENS_t^{\text{II}} = & \sum_{j \in G} Pr_{j,t,\tau_2} g(ES_{j,t} - P_t^{\text{EVR}}) \tau_2 \\ & + \sum_{j \in G} \sum_{k \in G, j<k} Pr_{jk,t,\tau_2} g(ES_{jk,t} - P_t^{\text{EVR}}) \tau_2 \\ & - \sum_{j \in G} Pr_{j,t,\tau_1} g(ES_{j,t} - P_t^{\text{EVR}}) \tau_1 \\ & - \sum_{j \in G} \sum_{k \in G, j<k} Pr_{jk,t,\tau_1} g(ES_{jk,t} - P_t^{\text{EVR}}) \tau_1, \forall t \in T \end{aligned} \tag{4.19}$$

where the $EENS_t^I$, defined in (4.18), can be determined by summarizing the expected energy deficit due to the single generator outage and two generator outage within EV reaction time τ_1 respectively. Considering the fact that *EENS* is a polynomial function of time τ, $EENS_t^{\text{II}}$ cannot be obtained directly. To acquire $EENS_t^{\text{II}}$, the first and second terms of (4.19) represent *EENS* within system contingency time τ_2, and the third and fourth terms of (4.19) represent *EENS* within

time τ_1, both according to the assumption that EVs take action immediately after contingency. The capacity of the EVs' provision of operating reserve P_t^{EVR} is calculated by the sum of the EVs' interruptible charging demand P_t^{Int} and V2G capacity P_t^{V2G}, given as,

$$P_t^{\mathrm{EVR}} = P_t^{\mathrm{Int}} + P_t^{\mathrm{V2G}}, t \in T \tag{4.20}$$

The formulations of the three parameters P_t^{EVR}, P_t^{Int} and P_t^{V2G} are introduced in the next section. Similar to the formulation of $EENS_t^{\mathrm{II}}$, $EESEV_t^{\mathrm{Int}}$ and $EESEV_t^{\mathrm{V2G}}$ can be defined as,

$$\begin{aligned} EESEV_t^{\mathrm{Int}} = & \sum_{j \in G} Pr_{j,t,\tau_2} g[\min(ES_{j,t}, P_t^{\mathrm{Int}})]\tau_2 \\ & + \sum_{j \in G} \sum_{k \in G, j<k} Pr_{jk,t,\tau_2} g[\min(ES_{jk,t}, P_t^{\mathrm{Int}})]\tau_2 \\ & - \sum_{j \in G} Pr_{j,t,\tau_1} g[\min(ES_{j,t}, P_t^{\mathrm{Int}})]\tau_1 \\ & - \sum_{j \in G} \sum_{k \in G, j<k} Pr_{jk,t,\tau_1} g[\min(ES_{jk,t}, P_t^{Int})]\tau_1, \forall t \in T \end{aligned} \tag{4.21}$$

$$\begin{aligned} EESEV_t^{\mathrm{V2G}} = & \sum_{j \in G} Pr_{j,t,\tau_2} g[\min(ES_{j,t} - P_t^{\mathrm{Int}}, P_t^{\mathrm{V2G}})]\tau_2 \\ & + \sum_{j \in G} \sum_{k \in G, j<k} Pr_{jk,t,\tau_2} g[\min(ES_{jk,t} - P_t^{\mathrm{Int}}, P_t^{\mathrm{V2G}})]\tau_2 \\ & - \sum_{j \in G} Pr_{j,t,\tau_1} g(\min(ES_{j,t} - P_t^{\mathrm{Int}}, P_t^{\mathrm{V2G}})]\tau_1 \\ & - \sum_{j \in G} \sum_{k \in G, j<k} Pr_{jk,t,\tau_1} g[\min(ES_{jk,t} - P_t^{\mathrm{Int}}, P_t^{\mathrm{V2G}})]\tau_1, \forall t \in T \end{aligned} \tag{4.22}$$

where $EESEV_t^{\mathrm{Int}}$ and $EESEV_t^{\mathrm{V2G}}$ are derived from the supplied energy during the system contingency time τ_2 which neglects EVs' reaction time, as the first and second terms in (4.21) and (4.22), subtracts the excessive amount of supplied energy during EV reaction time τ_1, as the third and fourth terms in (4.21) and (4.22). As the cost of interrupting the EV charging demand is much smaller than the cost of V2G service provision, the charging interruption will be preferentially carried out in practice. From practical point of view, the possible scenarios can be given as below:

1) If the spinning reserve exceeds the capacity loss of system contingency, no energy deficit occurs and no EVs take action;

2) If the energy deficit is smaller than the EV interruptible capacity P_t^{Int}, only part of charging energy is interrupted;

3) If the energy deficit exceeds the interruptible capacity P_t^{Int} and smaller than the EV capacity P_t^{EVR}, all the EV charging energy is interrupted and part of V2G service is conducted;

4) If the energy deficit exceeds the EV capacity P_t^{EVR}, all the EV charging capacity and all the V2G capacity are scheduled to support power system. Only in this case, energy not supplied occurs.

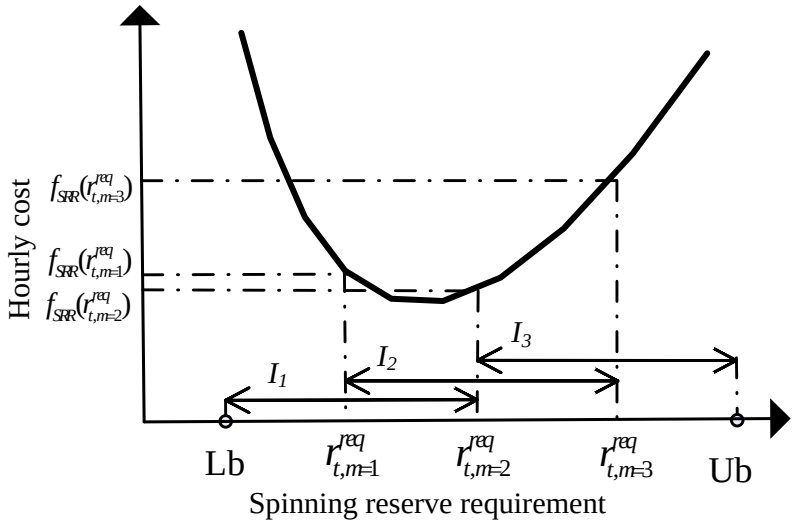

Figure 4.2. Illustration of the iterated grid search algorithm

4.2.3 Optimization Methodology

The proposed SRR optimization model is non-convex but unimodal and the system cost does not change continuously when an additional generator is turned on. The iterated grid search algorithm with three-grid points is used here to solve the problem [83], with the details given as Algorithm 1. In the algorithm, the interval [*Lb Ub*] is the first set that is large enough containing the optimal value of SRR in the first initialization step; then three points of SRR are obtained equably among the given interval in Step 5. According to the searched SRR, generation cost is firstly optimized in Step 6; then EENS and EESEV are obtained in Step 7; the total system cost is determined by summarizing all the costs at last in Step 8.

Comparing the results, a narrower interval [*Lb Ub*] is reset, as shown from Steps 10-16. This process is also visually explained in Fig. 4.2, where I_1 is determined as new optimization interval if $f_{SRR}(r^{req}_{t,m=1})$ is the smallest, I_2 is determined as new optimization interval if $f_{SRR}(r^{req}_{t,m=2})$ is the smallest, and I_3 is determined as new optimization interval if $f_{SRR}(r^{req}_{t,m=3})$ is the smallest. The optimal SRR is finally determined until *Lb* is close enough to *Ub* and used as inputs of reserve-constrained unit commitment.

Algorithm 1 Grid search-based spinning reserve optimization methodology

1: **Initialization**: Set t=1, k=1. Set I_k=[*Lb Ub*] large enough to contain the optimal value of SRR

2: **for** t =1 to 24 **do**

3: **while** *Ub*-*Lb*>ε

4: **for** m=1 to 3 **do**

5: Let $r^{req}_{t,m}$ =*Lb*+*m*/4*(*Ub*-*Lb*)

6: Optimize $f_{OPER}(r^{req}_{t,m})$, as shown in (4.2), with constraints (4.5)-(4.10) to obtain $u^{G}_{i,t}$ $P_{i,t}$ and $r_{i,t}$

7: Calculate $EENS_t$, $EESEV^{Int}_t$ and $EESEV^{V2G}_t$ with (4.11)-(4.22)

8: Calculate $f_{EENS}(r^{req}_{t,m})$ and $f_{EESEV}(r^{req}_{t,m})$ using (4.3)-(4.4) and then calculate $f_{SRR}(r^{req}_{t,m})$ using (4.1)

9: **end for**

10: **If** $f_{SRR}(r^{req}_{t,m=1})< f_{SRR}(r^{req}_{t,m=2})$ & $f_{SRR}(r^{req}_{t,m=1})< f_{SRR}(r^{req}_{t,m=3})$ **Then**

11: Let [*Lb Ub*]=[Lb $f_{SRR}(r^{req}_{t,m=1})$]

12: **Else if** $f_{SRR}(r^{req}_{t,m=2})< f_{SRR}(r^{req}_{t,m=1})$ & $f_{SRR}(r^{req}_{t,m=2})< f_{SRR}(r^{req}_{t,m=3})$ **Then**

13: Let [*Lb Ub*]=[$f_{SRR}(r^{req}_{t,m=1})$ $f_{SRR}(r^{req}_{t,m=3})$]

14: **Else if** $f_{SRR}(r^{req}_{t,m=3})< f_{SRR}(r^{req}_{t,m=1})$ & $f_{SRR}(r^{req}_{t,m=3})< f_{SRR}(r^{req}_{t,m=2})$ **Then**

15: Let [Lb Ub]=[$f_{SRR}(r^{req}_{t,m=2})$ *Ub*]

16: **End if**

17: **End while**

18: Set r^{req}_{t} =1/2*(*Ub*-*Lb*)

19: **End for**

20: Reserve-constrained unit commitment

4.3. Operating Reserve Provided by EVs

In this subsection, the operating reserve that is provided by EVs is mathematically modeled. EV travel behavior is firstly modeled. Then two different charging scheduling schemes are executed based on two typical charging strategies, namely immediate charging and smart charging strategy. The capacities of EV interruptible charging demand and V2G service are determined respectively. The costs to provide these two services consisting of the compensation to EV owners and battery degradation are formulated at last. It should be noticed that modeling the capacity and cost of EVs' service aims at estimating day-ahead EVs' capacity to provide operating reserve, so that the day-ahead SRR can be determined accordingly. The actual post-contingency schedule of EVs is dependent on the real-time EV status determined by the EV aggregator, which is out of the scope of this thesis.

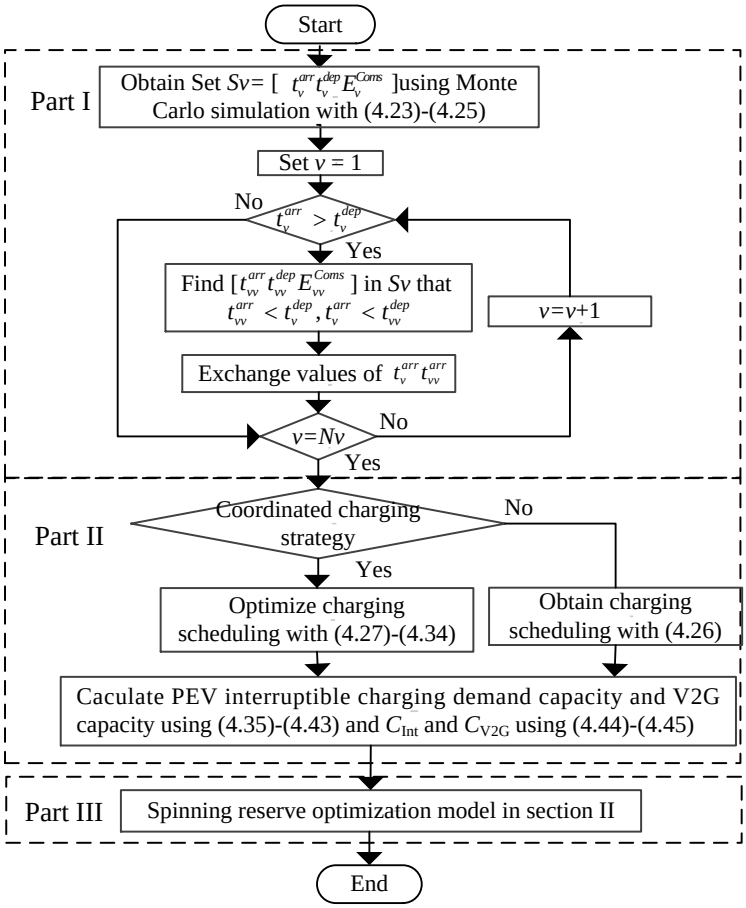

Figure 4.3. Flowchart of modeling operating reserve provided by EVs

4.3.1 EV Travel Behavior

The EV travel data is derived from the national household travel behavior survey, released by the U.S. Department of Transportation Federal Highway Administration [84]. A statistical probability method is carried out to analyze the results of travel behaviors [22]. Segmented normal distribution functions are used to match the time that the EV first plugs out of the grid and the time that EV last plugs into the grid. The probability density functions $f_s(t)$ and $f_e(t)$ are respectively given in (4.23) with μ_s = 8.92 and σ_s = 3.24, (39) with μ_e = 17.47 and σ_e = 3.41.

$$f_{\mathrm{s}}(t)=\begin{cases}\dfrac{1}{\sqrt{2\pi}\sigma_{\mathrm{s}}}\exp[-\dfrac{(t-\mu_{\mathrm{s}})^2}{2\sigma_{\mathrm{s}}^2}], & t\in[0,\mu_{\mathrm{s}}+12]\\ \dfrac{1}{\sqrt{2\pi}\sigma_{\mathrm{s}}}\exp[-\dfrac{(t-24-\mu_{\mathrm{s}})^2}{2\sigma_{\mathrm{s}}^2}], & t\in[\mu_{\mathrm{s}}+12,24]\end{cases} \tag{4.23}$$

$$f_{\mathrm{e}}(t)=\begin{cases}\dfrac{1}{\sqrt{2\pi}\sigma_{\mathrm{e}}}\exp[-\dfrac{(t+24-\mu_{\mathrm{e}})^2}{2\sigma_{\mathrm{e}}^2}], & t\in[0,\mu_{\mathrm{e}}-12]\\ \dfrac{1}{\sqrt{2\pi}\sigma_{\mathrm{e}}}\exp[-\dfrac{(t-\mu_{\mathrm{e}})^2}{2\sigma_{\mathrm{e}}^2}], & t\in[\mu_{\mathrm{e}}-12,24]\end{cases} \tag{4.24}$$

The daily travel mileage is modeled based on a logarithmic normal distribution function as below with μ_m = 2.98 and σ_m =1.14

$$f_{\mathrm{m}}(x)=\frac{1}{\sqrt{2\pi}\sigma_{\mathrm{m}}x}\exp[-\frac{(\ln x-\mu_{\mathrm{m}})^2}{2\sigma_{\mathrm{m}}^2}] \tag{4.25}$$

The Monte Carlo simulation method is adopted to capture the travel behaviors of the vehicles according to the aforementioned probability density functions f_s(t), f_e(t) and f_m(t). The energy consumption before the vehicles are plugged into the grid is estimated according to the travel mileage and per mile energy consumption. The Monte carlo simulation is modified to ensure that the arriving time t_v^{arr} is smaller than the departure time t_v^{dep}, as shown in Part I in Fig. 4.3.

Different EV charging strategies have different influences on the ability of EVs to provide the operating reserve at each time interval. Both typical immediate charging and smart charging strategies are taken into account in the study.

1) Immediate Charging: In this mode, EVs are assumed to be charged once they are plugged into the grid when the last trips end in a day. The charging duration depends on the travel mileage in the day. Based on the assumption that EVs can respond to the contingency in several minutes, the intra-hour index τ is used to formulate a more accurate model and set the interval as 10 minutes in the study. The EV charging load can be given as,

$$P_{v,t,\tau}^{\mathrm{ch}} = \begin{cases} P_{ch,\max},\ if\ u_{v,t,\tau}^{\mathrm{EV}} = 1 \mathrm{and}\, t+\tau <= \dfrac{E_v^{\mathrm{Coms}}}{\eta_{\mathrm{ch}} P_{\mathrm{ch,max}}} + t_v^{\mathrm{arr}} \\ 0, \quad if\ u_{v,t,\tau}^{\mathrm{EV}} = 0 \mathrm{or}\, t+\tau > \dfrac{E_v^{\mathrm{Coms}}}{\eta_{\mathrm{ch}} P_{\mathrm{ch,max}}} + t_v^{\mathrm{arr}} \end{cases} \quad \forall v \in V, \forall t \in T, \forall \tau \in T_{\Delta} \tag{4.26}$$

where $u_{v,t,\tau}^{\mathrm{EV}}$ denotes the state if the EV is connected to the grid; $P_{\mathrm{ch,max}}$ denotes the maximum charging power; E_v^{Coms} represents the daily energy consumption. After EV arrives, it is charged at the maximum rate $P_{\mathrm{ch,max}}$ until the energy is full.

2) Smart Charging: In the smart charging mode, the travel information of each EV, such as the travel time and the daily travel energy consumption, is collected; then the time and the amount of EVs' charging demand are orderly obtained by the system operators or the EV aggregators to benefit the operation of power systems. Here, a smart charging demand optimization model is proposed to optimize the EVs' charging demand at each period via minimizing the daily system load fluctuation. Considering the large quantity of EVs, a clustering method is used in this model to improve the computation efficiency. The EVs with similar pattern of travel time and the daily travel mileage can be classified into the same group, so that is can be scheduled as a whole. EV smart charging strategy has been attracting lots of attentions in smart grid. To conduct smart charging strategy, many studies choose the objective of charging cost minimization in electricity market [74] or generation cost minimization[78]. The objective is set as demand smoothing [27], which can be given as,

$$\min f_{\mathrm{co}} = \sum_{t \in T} (P_t^{\mathrm{total}} - P_{\mathrm{aver}})^2 \tag{4.27}$$

where

$$P_t^{\text{total}} = P_t^{\text{D}} + \frac{1}{1000}\sum_{c\in V_c}\sum_{\tau\in T_\Delta} P_{c,t,\tau}^{\text{ch,clus}} \tag{4.28}$$

$$P_{\text{aver}} = \frac{1}{24}\sum_{t\in T} P_t^{\text{total}} \tag{4.29}$$

subject to:

$$S_{c,t+1}^{\text{clus}} = S_{c,t}^{\text{clus}} + \sum_{\tau\in T_\Delta}\frac{\eta_{ch}P_{c,t,\tau}^{\text{ch,clus}}\Delta\tau}{n_c S_{\text{EV,max}}}, \forall c\in V_c, \forall t\in[t_c^{arr}, t_c^{dep}] \tag{4.30}$$

$$S_{\text{clus,min}} \le S_{c,t}^{\text{clus}} \le S_{\text{clus,max}}, \forall c\in V_c, \forall t\in[t_c^{\text{arr}}, t_c^{\text{dep}}] \tag{4.31}$$

$$S_{c,t_c^{\text{dep}}}^{\text{clus}} \ge S_c^{\text{clus,exp}} \quad \forall c\in V_c \tag{4.32}$$

$$0 \le P_{c,t,\tau}^{\text{ch,clus}} \le \frac{1}{6}n_c P_{\text{ch,max}}, \forall c\in V_c, \forall \tau\in T_\Delta, \forall t\in[t_c^{\text{arr}}, t_c^{\text{dep}}] \tag{4.33}$$

$$P_{c,t,\tau}^{\text{ch,clus}} = 0, \forall c\in V_c, \forall \tau\in T_\Delta, \forall t\notin[t_c^{\text{arr}}, t_c^{\text{dep}}] \tag{4.34}$$

The objective defined in (4.27) is devoted to smoothing the daily system demand. The mathematical definitions of P_t^{total} and P_{mean} are given as (4.28) and (4.29) respectively. The equality constraint of EV charging energy of each cluster is shown as (4.30). The upper and lower limits of equivalent battery capacity of EV clusters are defined by (4.31). The basic travel demand requirement should be satisfied as the inequality (4.32). The constraints of charging power limitation and non-schedulable state are listed as (4.33) and (4.34), respectively.

4.3.2 Capacity Estimation

Once the EV charging demand at each period is obtained using either immediate charging strategy or smart charging strategy, the time-varying capacity of interruptible charging demand and V2G service can be determined based on the specific values of the EVs' parameters, which include the charging demand, the arriving and departing time, energy remained in the EV battery, and so on [85].

The capacity of interruptible charging demand depends not only on the charging demand itself, but also on whether the interrupted load can be recharged before EV's departure. In other words, the charging energy during system contingency can be interrupted only if there is still enough time to recharge this amount of

energy between the recovery of system contingency and EV's departure, which can be represented as,

$$P_{t'}^{\mathrm{Int}} = \xi_t \frac{\sum_{v\in V} \min(E_{v,t'}^{\mathrm{Ch}}, E_{v,t'}^{\mathrm{Sup}})}{1000\sum_{t\in T}\sum_{\tau\in T_\Delta}(u_{t',t,\tau}^{\mathrm{CII}} - u_{t',t,\tau}^{\mathrm{EV,del}})\Delta\tau}, \forall t' \in T \tag{4.35}$$

where

$$E_{v,t'}^{\mathrm{Ch}} = \sum_{t\in T}\sum_{\tau\in T_\Delta}(u_{t',t,\tau}^{\mathrm{CII}} - u_{t',t,\tau}^{\mathrm{EV,del}})P_{v,t,\tau}^{\mathrm{ch}}\Delta\tau, \forall v \in V, \forall t' \in T \tag{4.36}$$

$$E_{v,t'}^{\mathrm{Sup}} = \sum_{t\in T}\sum_{\tau\in T_\Delta} u_{t',t,\tau}^{\mathrm{CIII}}(u_{v,t,\tau}^{\mathrm{EV}} P_{\mathrm{ch,max}} - P_{v,t,\tau}^{\mathrm{ch}})\Delta\tau, \forall v \in V, \forall t' \in T \tag{4.37}$$

where $E_{v,t'}^{\mathrm{Ch}}$ is the amount of total charging energy between the time when EVs respond to contingency and the time when system recovers, $E_{v,t'}^{\mathrm{Sup}}$ represents the maximum amount of supplementary recharging energy between the time when power system recovers from contingency and the time when EV departs, the time index *t'* is to show the time when the contingency occurs. The power system contingency is assumed to happen only at the beginning of each hour for simplicity. The definitions of the binary parameters $u_{t',t,\tau}^{\mathrm{CI}}$, $u_{t',t,\tau}^{\mathrm{CII}} u_{t',t,\tau}^{\mathrm{CIII}}$ and $u_{t',t,\tau}^{\mathrm{EV,del}}$ are defined as,

$$\begin{cases} u_{t',t,\tau}^{\mathrm{CI}} = 1, u_{t',t,\tau}^{\mathrm{CII}} = 0, u_{t',t,\tau}^{\mathrm{CIII}} = 0, & \text{if } t' < t+\tau \\ u_{t',t,\tau}^{\mathrm{CI}} = 0, u_{t',t,\tau}^{\mathrm{CII}} = 1, u_{t',t,\tau}^{\mathrm{CIII}} = 0, & \text{if } t' \le t+\tau < t'+\tau_2 \\ u_{t',t,\tau}^{\mathrm{CI}} = 0, u_{t',t,\tau}^{\mathrm{CII}} = 0, u_{t',t,\tau}^{\mathrm{CIII}} = 1, & \text{if } t'+\tau_2 \le t+\tau \end{cases} \tag{4.38}$$

$$\begin{cases} u_{t',t,\tau}^{\mathrm{EV,del}} = 1, & \text{if } t' \le t+\tau < t'+\tau_1 \\ u_{t',t,\tau}^{\mathrm{EV,del}} = 0, & \text{if } t+\tau_1 \le t' \text{ or } t'+\tau_1 \le t+\tau \end{cases} \tag{4.39}$$

$$\begin{cases} u_{v,t,\tau}^{\mathrm{EV}} = 1, & \text{if } t+\tau \in [t_c^{arr}, t_c^{dep}] \\ u_{v,t,\tau}^{\mathrm{EV}} = 0, & \text{if } t+\tau \notin [t_c^{arr}, t_c^{dep}] \end{cases} \tag{4.40}$$

where $u_{t',t,\tau}^{\mathrm{CI}}$, $u_{t',t,\tau}^{\mathrm{CII}}$ and $u_{t',t,\tau}^{\mathrm{CIII}}$ are the binary parameters with 1 denoting before, during and after contingency, respectively, $u_{t',t,\tau}^{\mathrm{EV,del}}$ is the binary parameter with 1 denoting that the EVs are reacting to contingency, $u_{v,t,\tau}^{\mathrm{EV}}$ is the binary parameter with 1 indicating that EV is connected to the grid. The number 1000 is used to make the transition from kW to MW.

The formulation of the V2G capacity is same as (4.35). However, the

discharging limitation and the energy remained in the battery of EVs when V2G occurs should be considered in the formulation of the V2G capacity as well, represented as,

$$P_{t'}^{\mathrm{V2G}} = \xi_{\mathrm{t}} \frac{\sum_{v \in V} \min(E_{v,t'}^{\mathrm{Rem}}, E_{v,t'}^{\mathrm{V2G,lim}}, E_{v,t'}^{\mathrm{Sup}})}{1000 \sum_{t \in T} \sum_{\tau \in T_{\Delta}} (u_{t',t,\tau}^{\mathrm{CII}} - u_{t',t,\tau}^{\mathrm{EV,del}}) \Delta\tau}, \forall t' \in T \tag{4.41}$$

where

$$E_{v,t'}^{\mathrm{Rem}} = S_{EV,\max} - E_{v}^{\mathrm{Coms}} + \sum_{t \in T} \sum_{\tau \in T_{\Delta}} (u_{t',t,\tau}^{\mathrm{CI}} + u_{t',t,\tau}^{\mathrm{EV,del}}) P_{v,t,\tau}^{\mathrm{ch}} \Delta\tau, \forall v \in V, \forall t' \in T \tag{4.42}$$

$$E_{v,t'}^{\mathrm{V2G,lim}} = \sum_{t \in T} \sum_{\tau \in T_{\Delta}} u_{v,t,\tau}^{\mathrm{EV}} (u_{t',t,\tau}^{\mathrm{CII}} - u_{t',t,\tau}^{\mathrm{EV,del}}) P_{\mathrm{V2G,max}} \Delta\tau, \forall v \in V, \forall t' \in T \tag{4.43}$$

where $E_{v,t'}^{\mathrm{Rem}}$ defined in (4.41) represents the total energy remained in the battery in EVs before carrying out V2G service, derived by summing the energy remained in the battery and the charged energy when EVs are connected to the grid before EVs respond to the contingency to provide V2G service, $E_{v,t}^{\mathrm{V2G,lim}}$ defined in (4.42) denotes the V2G energy limitation due to the limit of EVs' V2G recharging power during EVs' reaction period.

4.3.3 Cost of EVs' Service

The EV owners should be compensated for the delay of charging which is caused by both the interruption and V2G. Also, discharging a battery to provide the V2G service will accelerate its degradation. Then the costs of interrupted charging demand C_{Int} and V2G service C_{V2G} can be respectively denoted as,

$$C_{\mathrm{Int}} = C_{\mathrm{Comp}} \tag{4.44}$$

$$C_{\mathrm{V2G}} = C_{\mathrm{Comp}} + \frac{1000 C_{\mathrm{BI}}}{L_{\mathrm{C}} S_{\mathrm{EV,max}} d_{\mathrm{DoD}}} \tag{4.45}$$

where C_{Comp} is the per MWh cost of compensation paid to EV owners, and the second term of (4.44) is the per MWh investment cost of the battery degradation [27, 86], C_{BI} is battery investment cost of V2G service, L_{C} is the battery cycle life at a given depth of discharge; $S_{EV,max}$ is the battery capacity; d_{DoD} is the depth of

discharge used in obtaining L_C. Thus, $L_C S_{EV,max} d_{DoD}$ denotes the overall energy that a battery can provide throughout its lifetime.

4.4. Case Study

The IEEE reliability test system (RTS -96) [87] is utilized to demonstrate the basic characteristics of the proposed EV-integrated SRR model. The test system consists of 26 units and the hydro generating units are not taken into consideration in any of the case studies. The unit cost data is obtained from [88]. The load of the system varies from 59% to 100% of 2700 MW peak load, without consideration of the EV charging demand. Other parameter settings are given in Table 4.1. The values of the parameters τ_1 and τ_2 are set based on the interruptible import requirement and contingency reserve restoration requirement in Reliability Standards for the Bulk Electric Systems of North America [81]. The details of the battery degradation cost can be referred to [27].

Table 4.1. Parameter Settings

Parameter	Value	Parameter	Value
τ_1	1/6 h	V	10000
τ_2	1 h	$VOLL$	7500 $/MWh
Lb	300 MW	C_{Comp}	125 $/MWh
Ub	500 MW	$C_{BI}/ S_{EV,max}$	100 $/kWh
$P_{ch,max}$	4.5 kW	d_{DoD}	0.8
$P_{V2G,max}$	9 kW	L_C	1000
ω	1%	ε	1MW

For the future practical application, two kinds of uncertainties should be taken into consideration: whether V2G service and smart charging strategy can be fulfilled. Thus six scenarios are tested in the study, as shown in Table 4.2. Total power system demand remains the same among Scenarios 1, 3 and 5 where Scenario 5 acts as benchmark for the other two scenarios. Similarly, the total demands of Scenarios 2, 4 and 6 are the same, and Scenario 6 is utilized as the

benchmark.

Table 4.2. Scenarios of Case Study

Scenario	1	2	3	4	5	6
V2G service	Enabled	Enabled	Not enabled	Not enabled	Not enabled	Not enabled
Charging interruption	Enabled	Enabled	Enabled	Enabled	Not enabled	Not enabled
Charging strategy	Immediate charging	Smart charging	Immediate charging	Smart charging	Immediate charging	Smart charging

4.4.1 Interruptible and V2G Capacity

The interruptible and V2G capacity with both immediate and smart charging strategies available for contingency can be demonstrated in Fig. 4.4. Generally, the V2G capacity is much larger than the interruption capacity as most of the EVs connected on the grid have the ability to feed energy back to power system, while only small proportion of EVs which are in charging conditions has the ability to interrupt charging energy. The V2G capacity demonstrates great difference during the day and night as much more vehicles park at night. The interruption capacity varies a lot with different charging strategies. The energy charging is scheduled mostly at night under the smart charging strategy, and scheduled separately during the day under the immediate charging strategy.

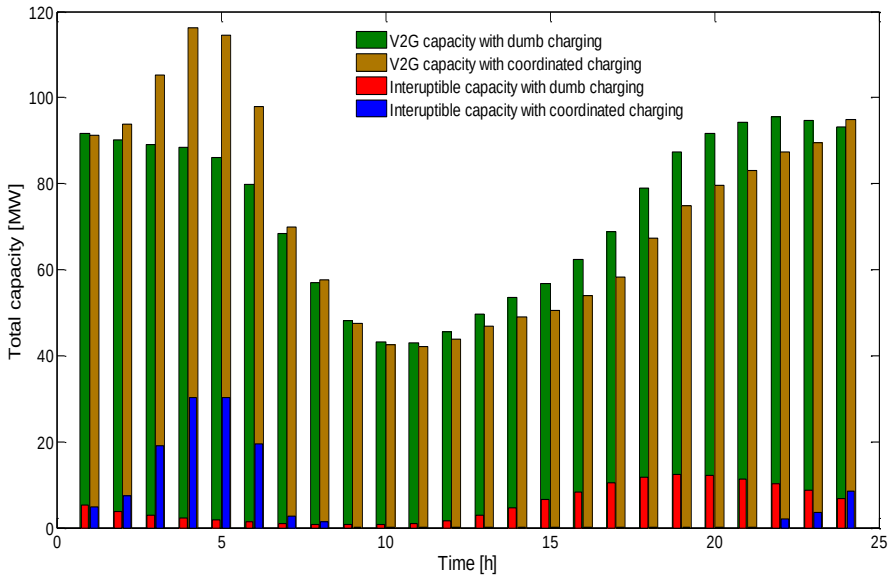

Figure 4.4. Interruptible and V2G capacities with immediate and smart charging strategies.

4.4.2 Economic Efficiency Analysis

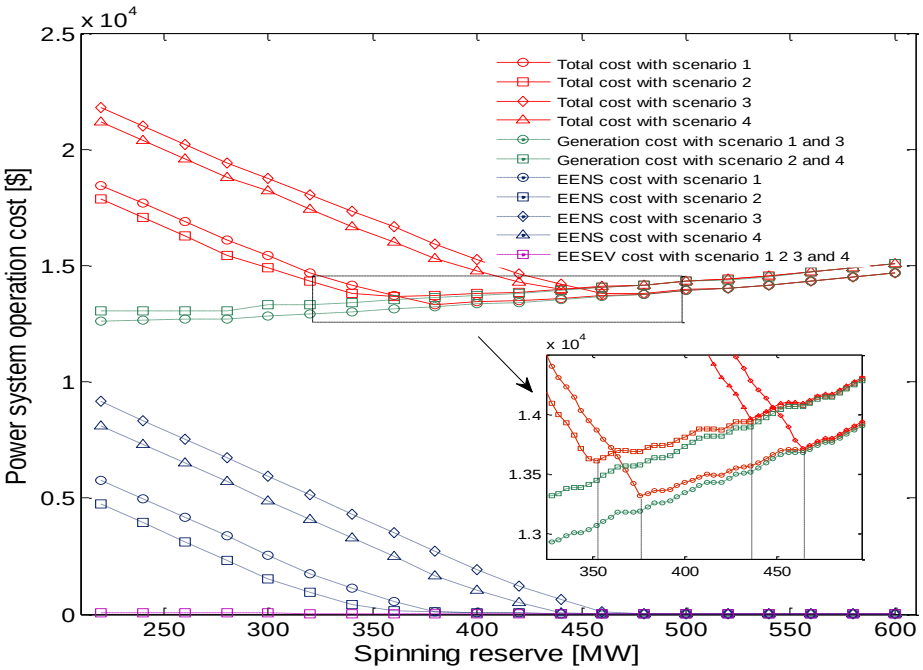

Figure 4.5. Optimization of SRR with regard to the total cost, generation cost, EENS cost and EESEV cost when *t*= 4h

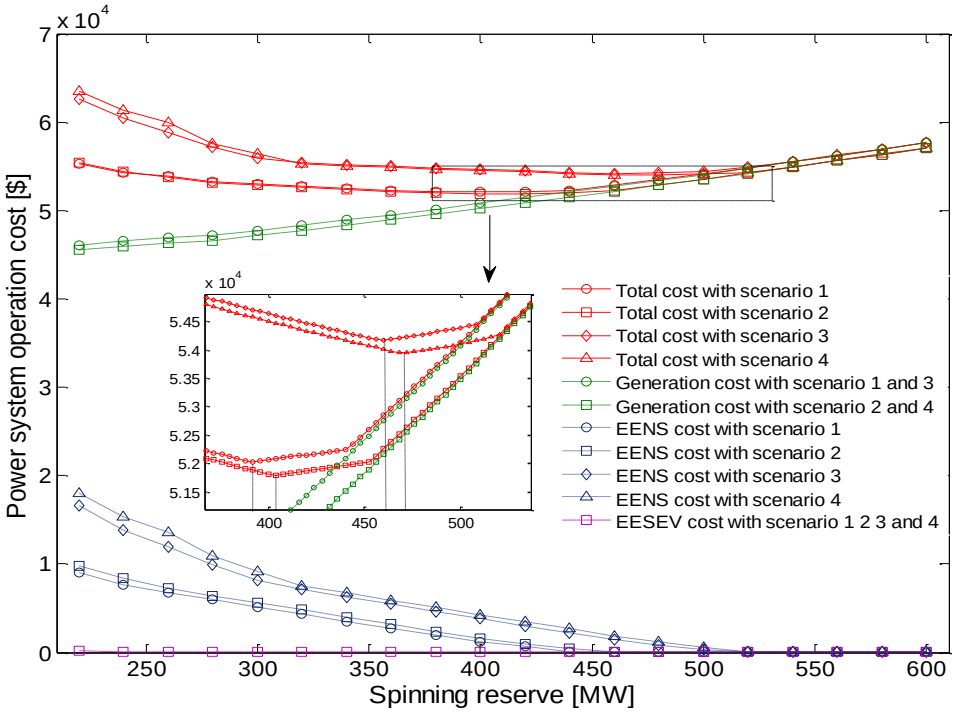

Figure 4.6. Optimization of SRR with regard to the total cost, generation cost, EENS cost and EESEV cost when *t*=18h

In order to demonstrate how the SRR is obtained with the proposed model, various hourly costs, i.e., total system cost, generation cost, EENS cost and EESEV cost with different SRRs are depicted in Figs. 4.5 and 4.6. Only two typical time intervals t = 4 h and t = 18 h are selected respectively indicating the lowest and highest the system demand during the whole day. The optimal SRR is acquired by reaching the minimization of the total cost, as shown in Figs. 4.5 and 4.6. The SRR is optimized through tradeoff among costs of generations, EENS and EESEV. It can be found that larger SRR results in larger generation costs and smaller SRR leads to larger EENS costs. It is proved that the function of total cost is unimodal and the grid search-based SRR optimization methodology can be valid to resolve the proposed cost-oriented optimization model. Generally, the system with larger demand would have larger SRR and larger system cost, through comparing the results depicted in Figs. 4.6 and Fig. 4.5. It can be also found that the SRR is considerably cut down when V2G service is enabled, and the SRR is smaller in the night and larger during the day under smart charging strategy comparing with immediate charging strategy.

Table 4.3. Various Daily Costs of Different Scenarios

Scenario	Total cost ($)	Generation cost ($)	EENS cost ($)	EESEV cost ($)
1	8.2027×10^5	7.9674×10^5	2.2501×10^4	1.0300×10^3
2	8.1988×10^5	7.9651×10^5	2.2303×10^4	1.0594×10^3
3	8.5088×10^5	8.2818×10^5	2.2665×10^4	32.4850
4	8.5041×10^5	8.2774×10^5	2.2643×10^4	28.4796
5	8.5408×10^5	8.3051×10^5	2.3571×10^4	0
6	8.5071×10^5	8.2786×10^5	2.2851×10^4	0

Daily system operation costs can be obtained once the reserve-constrained unit commitment is determined. Various costs of the studied six scenarios are listed in Table 4.3. Comparing Scenarios 1 and 2 with Scenarios 5 and 6 respectively, the large reduction of the total costs solidly indicate the economic effectiveness of EVs' aid in system operating reserve allocation. Particularly, the generation costs are considerably reduced from 8.3051×10^5 $ to 7.9674×10^5 $ under immediate charging strategy and from 8.2786×10^5 $ to 7.9651×10^5 $ under the smart charging strategy due to EVs' contribution, and EENS costs also slightly decrease from 2.3571×10^4 $ to 2.2501×10^4 $ in the immediate charging strategy and from 2.2851×10^4 $ to 2.2303×10^4 $ in the smart charging strategy. On the other hand, the additional compensation costs and the battery costs that system operator should pay for EENS are relatively small, with 1.0300×10^3 $ and 1.0594×10^3 $ in the immediate and smart charging strategies respectively. It is because the frequency of activating EVs to provide energy is quite low. Thus EVs are very economically suitable to partly replace generators to provide contingency reserve. As the interruptible capacity is relatively smaller than the V2G capacity, the EVs' system-supporting effectiveness without V2G is considerably reduced by comparing various costs of Scenarios 3 and 4 with Scenarios 5 and 6 respectively. The results also demonstrate larger benefit brought by the utilization of smart charging strategy. However, the difference value between total costs of Scenarios 1 and 2 is diminished compared with that between Scenarios 5 and 6. It demonstrates that the economic advantage of smart charging strategy is weakened if EVs are required to

provide operating reserve. It is due to that EVs in immediate charging strategy can provide more operating reserves separately during most of the time intervals, as shown in Fig. 4.4 and thus helps to reduce the operating costs. Thus the necessity to shift the charging demand as smart charging is largely weakened.

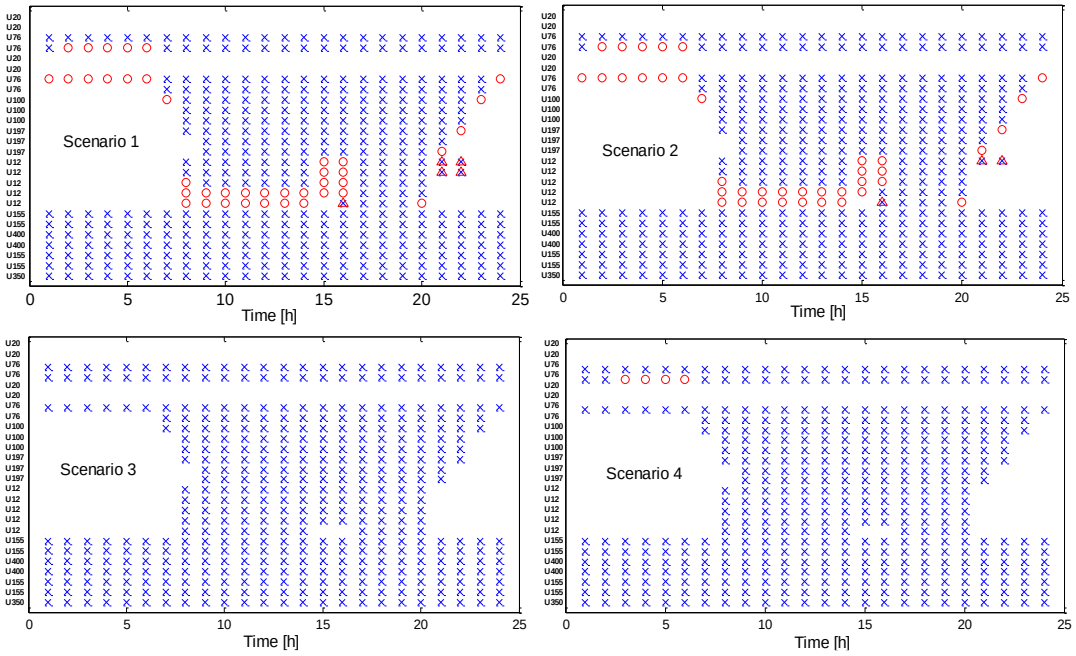

Figure 4.7. Unit commitment under various scenarios

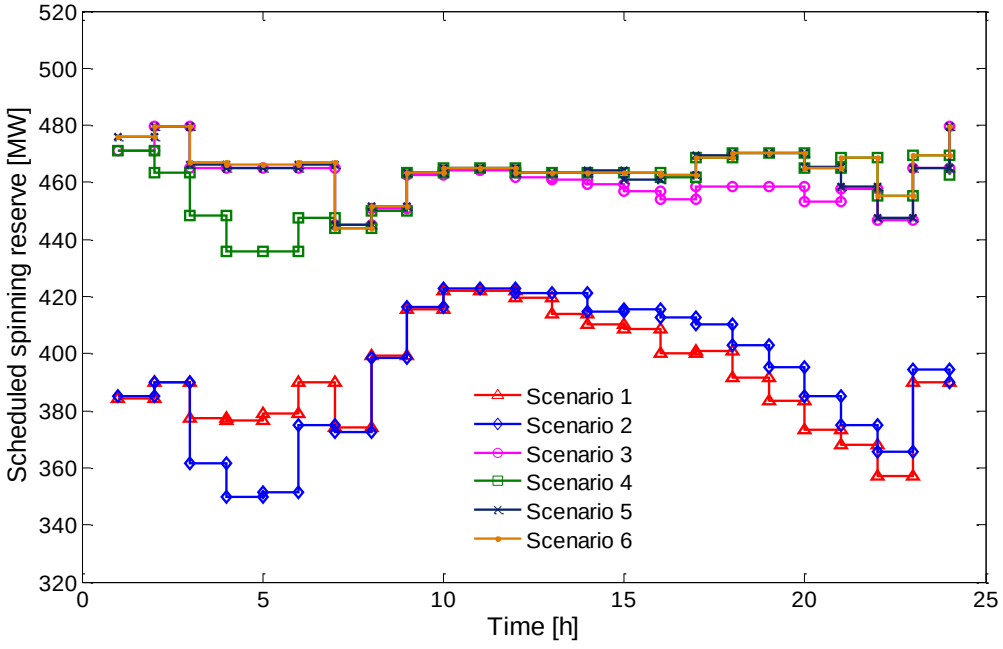

Figure 4.8. Scheduled spinning reserve under various scenarios

4.4.3 Scheduled Spinning Reserve, Unit Commitment and Reliability

Unit commitment under various scenarios is demonstrated in Fig. 4.7, with "×" denoting committed-on unit, "○" denoting turned-off unit opposite the benchmark and "Δ"denoting turned-on unit opposite the benchmark. With regard to different charging strategies, Scenario 5 acts as the benchmark of Scenarios 1 and 3, while Scenario 6 acts as the benchmark of Scenarios 2 and 4. The index per unit represents the generation capacity, for instance, U400 demonstrates the unit with installed capacity of 400 MW. Once the unit commitment is determined, the scheduled hourly spinning reserve under various scenarios can be also obtained, as shown in Fig. 4.8.

When EVs are supposed to provide operating reserve, especially V2G service is enabled in Scenarios 1 and 2, some units with relatively small capacity are turned off compared to the corresponding benchmarks. For example, U76 is turned off in the night and U12 is turned off during the day. Nevertheless, several units, e.g., U12 at t=16 h, 21 h and 22 h, are turned on to partly compensate the vacancy left by the turned-off units with larger capacity, e.g., U197. The amount of scheduled spinning reserve is thus considerably reduced, shown as Scenarios 1 and 2 in Fig. 4.8. When system contingency happens, EVs can interrupt the charging demand and feed energy back to support the power system. Thus system operators do not need to schedule as much spinning reserve as before and some units can be turned off.

When only EV interruption is enabled, the support of EVs to power system is relatively small. In this condition, the unit commitment results are almost the same with benchmark and the amount of scheduled spinning reserve is just slightly smaller than the benchmark as shown in Scenarios 3 and 4 in Figs. 4.7 and 8, respectively. Under the immediate charging strategy in Scenario 3, the unit commitment is exactly the same with benchmark. However, the scheduled spinning reserve is smaller than the benchmark especially during the day. In this case, units with larger capacity, which are supposed to provide spinning reserve, are allowed to increase the outputs as the requirement of spinning reserve is reduced. Under the smart charging strategy, the interruptible EV capacity is very

large as most of EVs are charged together at night. Thus some units, e.g., U78 at *t* = 3 h, 4 h, 5 h and 6 h, are turned off and the scheduled spinning reserve at night is reduced, shown as Scenario 4 in Figs. 4.7 and 4.8 respectively.

The effects of EVs on the power system reliability by interrupting charging demand and feeding energy back to power system when contingency happens are discussed here. Expected energy not supplied is regarded as one of the most important reliability assessment indices. The daily EENS values with different reactions of EVs and different charging strategies are listed in Table 4.4. It is demonstrated that the daily EENS is reduced in Scenarios 1-4 comparing with the benchmarks Scenarios 5 and 6, which proves that the reliability of power system is improved due to the assistance from EVs' post-contingency support. Comparing with the obtained results of other scenarios, Scenarios 1 and 2 have smaller EENS, indicating that V2G service can help to improve system reliability even more. It can be also seen that the smart charging strategy has advantages on enhancing the reliability by comparing Scenarios 1, 3 and 5 with Scenarios 2, 4, and 6 respectively.

Table 4.4. EENS in Different Scenarios

Scenario	1	2	3	4	5	6
EENS(MWh/day)	1.5001	1.4869	1.5110	1.5095	1.5714	1.5234

4.4.4 Discussions of Future Implementations

In the previous sections, the effects of EVs on the spinning reserve allocation in various scenarios are analyzed, given the specific rewards to the EV users and the specific EV penetration level. However, for the practical implementation in the future, these two factors will greatly affect the performance and efficiency of EVs' participation in operating reserve allocation. Sensitivity analysis of EV penetration level and compensation cost is conducted in this section.

In order to address the uncertainty of EV population in the future, various case studies considering different EV penetration levels are fulfilled. The penetration

level of EV charging load can be defined as,

$$PL_{\text{PEV}} = \frac{N_{\text{PEV}} P_{\text{ch,max}}}{P_{\text{aver}}} \times 100\% \tag{4.46}$$

The daily average scheduled spinning reserve is defined as the average value of hourly spinning reserve in one day, to efficiently assess the degree of daily spinning reserve. The average scheduled spinning reserve in different EV penetration levels is depicted in Fig. 4.9. To make the figure clearer, Scenarios 5 and 6 are not drawn here as the average scheduled spinning reserves in these scenarios are not affected by EV penetration level, with 464MW and 465MW respectively. The average scheduled spinning reserve decreases with the increase of EV penetration level, according to the numerical results of Scenarios 1-4 from Fig. 4.9. The V2G service highlights this characteristic, as shown in Scenarios 1 and 2. Although the low penetration level demonstrates that EV charging energy is only a small proportion of the total load of the power system, it has considerable effects on power system spinning reserve allocation. It is because the EV interruptible and V2G capacity cannot be neglected compared with potential energy loss due to generation outage.

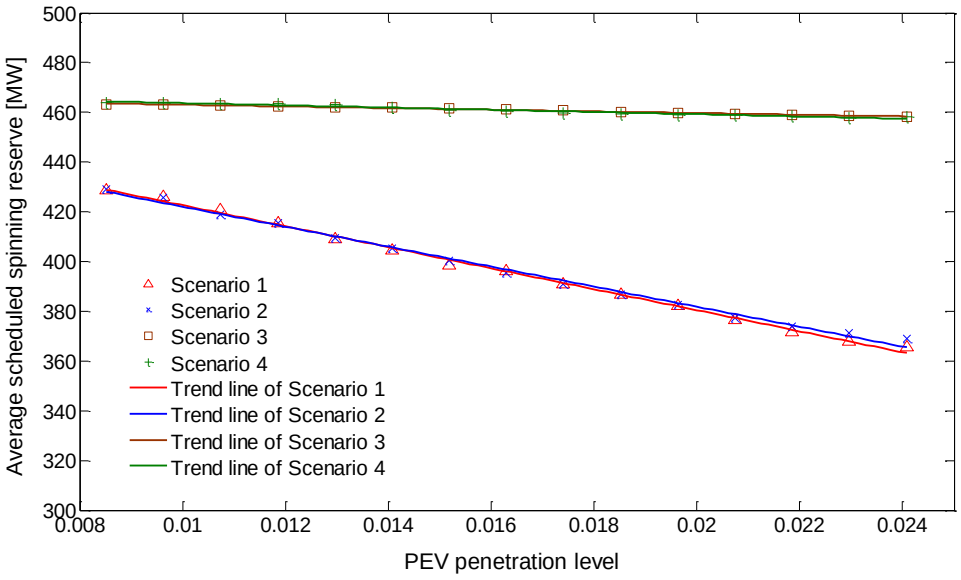

Figure 4.9. Effects of EV penetration level on scheduled spinning reserve

The design of the compensation to the EV owners would affect the motivation

of providing operating reserve in the future. The sensitivity analysis of compensation cost is to find out the potential ability and monetary space for system operators to reward the EV owners for their contributions. The index of compensation rate is defined as the ratio of the compensation cost to the scheduled generation marginal cost, given as,

$$CR_{\mathrm{PEV}} = \frac{C_{\mathrm{Comp}}}{\frac{1}{24}\sum_{t\in T}\frac{\partial f_{\mathrm{SRR}}}{\partial P_{i,t}}} \times 100\%, \tag{4.47}$$

where unit *i* is the marginal generator.

Here the scheduled generation marginal cost is used to estimate the electricity price. The index of compensation cost is to roughly measure the degree of compensation from the view of users. The system total costs under various compensation rates with Scenario 1-4 are demonstrated in Fig. 4.10. The total costs of Scenarios 5 and 6, fixed as 8.5408×10^5 \$ and 8.5071×10^5 \$, are not affected by the compensation rate, which are not depicted in Fig. 4.10. The total cost generally increases with the compensation cost in the studies. However, the increasing speed is reduced with the increase of compensation rate especially for Scenarios 1 and 2. When the compensation rate reaches 350, the system total costs of Scenarios 1 and 3 get close to the cost of Scenario 5, 8.5408×105 \$, and the costs of Scenarios 2 and 4 are close to the cost of Scenario 6, 8.5071×105 \$. At these points, the compensation to EV owners gets close to the value of VOLL, and EV can no longer contribute to reduce the SRR and total operation cost. It can be demonstrated from the figure that the compensation rate is very high, as EV owners will be rewarded with tens or hundreds of times of the normal electricity price. It can be concluded that the system operators have the ability to pay EV owners a large amount of rewards to motivate them to let their vehicles support the power system. Exact determination of the rewards will depend on further investigation in user willingness by e.g. questionnaire survey. The potential ability of power system operators to compensate EV owners considerably enhances the possibility to implement the proposed model in the future.

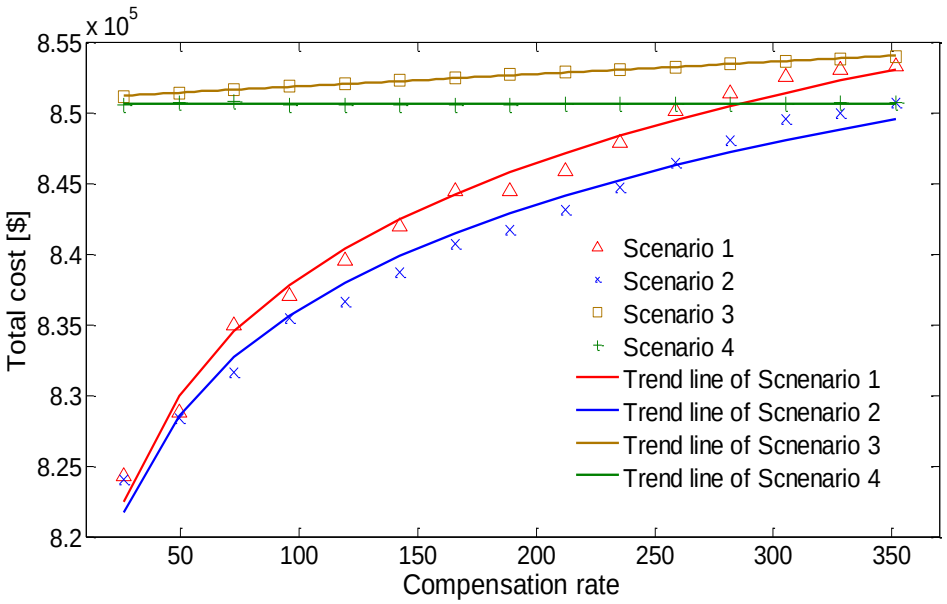

Figure 4.10. Effects of compensation rate on total cost

4.5. Conclusions

This chapter proposes a novel cost-efficiency based SRR optimization model considering EVs' assistance in providing operating reserve. EESEV is innovatively proposed to quantify the expected energy supplied by EVs, with EV raction time taken into consideration. The optimal SRR is quantified based on the minimization of the total costs of generation operation, EENS and EESEV. Different charging strategies are considered in the determination of EV charging demand as well as EV interruptible and V2G capacities for reserve allocation purpose. Numerical case studies demonstrate the reduction of scheduled spinning reserve and the generation operation cost due to the support of EVs. Unit commitment is rescheduled and some generators could be turned off as EVs partly replace spinning reserve. The reliability of power system is also improved with EVs' participation. The economic effectiveness of the proposed model will be significantly improved if V2G can be widely realized in the future. Furthermore, systematical sensitivity analysis implies that the amount of power system spinning reserve has a close relationship with EV penetration level and there exists abundant space to improve the compensation rate to motivate EV owners to provide power

system operating reserve. In general, the proposed model can have significant potential benefits for future practical applications.

5. Risk-Based Day-Ahead Scheduling of Electric Vehicle Aggregator Using Information Gap Decision Theory

5.1. Introduction

In recent years, the penetration of electric vehicles (EVs) in electrical power systems has experienced a dramatic growth accompanying the development of battery technology and smart grids. As an environmentally friendly technology, the wide utilization of EVs would be helpful to reduce air pollutions and greenhouse gas emissions. In addition, the growing concern of energy security is also an important driving factor for the popularity of EVs. However a large number of EVs will produce considerable impacts on the secure and economic operation of existing power systems [89, 90]. With a large-scale application of EVs in the foreseeable future, smart charging of EVs becomes an emerging research focus. Various methodologies have been proposed to coordinate the charging and discharging scheduling strategies of EVs [91, 92].

It has been proven that the participation of EV aggregators in the electricity market has significant advantages in executing smart charging in comparison with individual EVs [93]. In practice, aggregators play a critical role as an intermediary between EV owners and distribution system operators [94], and represent clients to participate in the electricity market. The bidding and scheduling strategies of EV aggregators need to be investigated considering various uncertainties in the electricity market [95-98]. A stochastic optimization approach is employed to formulate the scheduling strategy of EV aggregators in both day-ahead and regulation markets [99]. It is illustrated that the deviations between day-ahead cleared bids and actual real-time energy purchases influence the profit and the

bidding strategy of the aggregator. A bi-level optimization model is proposed in [100] to consider both the aggregator's minimum cost and the market clearing process, which assumes that EV aggregators have potential influences on the electricity market price. Stochastic portfolio management of the EV aggregator is fulfilled to take into account the uncertainty of real-time prices, while involving overall scalability, driving needs and grid constraints as well [101].

Due to various sources of uncertainties in modern power systems, developing appropriate decision models to mitigate the high energy trading risks would be beneficial to different participants in the electricity market [102]. Risk management methods have been widely used as an important tool for the decision makers in electricity markets, such as conventional generators [103], wind-hydro generation companies (GENCOs) [104], large consumers [105], etc. Similarly, an EV aggregator's exposure to the bidding and scheduling risk should be taken into consideration. Risk management based on a risk-aware scheduling approach is introduced into day-ahead scheduling and distributed real-time dispatch of EV charging [106], which could dramatically reduce the charging cost. Conditional value at risk (CVaR), a commonly used risk measurement method, has been incorporated into the formulation of an EV aggregator aiming to deal with the profit volatility of aggregators. It is applied for the management of risk in coordinating vehicle-to-grid (V2G) with energy trading for load-serving entities (LSEs) [107]. The profit of an LSE is maximized while its financial risk is maintained within an acceptable level using CVaR as a risk control measure. In [108], a CVaR based approach is proposed to optimize the EV aggregator's profit in day-ahead and balancing markets with the consideration of risk aversion. Optimal EV charging schedules can be obtained according to different risk-averse attitudes.

An information gap decision theory (IGDT) based approach is proposed to optimize day-ahead scheduling of EV aggregators considering electricity price uncertainty. Theoretically, IGDT is a quantitative risk management and decision making model to take into account severe uncertainties involved in the decision making process [109]. It focuses on the gap between predicted and actual variables. The IGDT-based risk management decision model is formulated

according to the decision makers' attitudes towards risk. Risk-averse decision makers tend to make robust decisions against high costs, while risk-taking decision makers tend to seek more benefits when the cost is low. IGDT has been introduced in various decision activities in power systems, including bidding strategies of GENCOs [110] and demand response retailers [111], restoration decision making for distribution network [112] and multi-year transmission expansion planning [113], and so on.

The application of IGDT is to control financial risk for decision makers, which is similar to other risk management models, such as CVaR [107, 108]. However, the ways to deal with risk by CVaR and IGDT are quite different from each other. For CVaR-based approaches, risk is measured as an extra cost and added to the objective function. Therefore, the weights of the sampled scenarios in stochastic optimization increase with the corresponding severity. The computation burden will exponentially increase when the number of scenarios increases. In contrast, in terms of IGDT-based approaches, risk is controlled by guaranteeing the profit or the cost as the predefined objective set by decision makers, then the maximum confidence interval is approximated. In other words, the IGDT approach can effectively enable decision makers to secure the desired profit irrespective of the potential risks. Notably, the IGDT-based formulation has no assumption on probability density distributions for the uncertain variables, therefore requiring relatively lower computation efforts.

In the study, the initial scheduling of EV aggregators without risk measurement is modeled by a two-step formulation. In the first step, the information of individual driving pattern data is collected and aggregated to simplify the optimization model. In the second step, the profit of EV aggregators in the electricity market is maximized, satisfying the demand of each individual EV. The electricity price in the electricity market will be considerably fluctuating with high uncertainty [114], which is indeed challenging to electricity market participants to arrange proper bidding and scheduling strategies. To take such uncertainty into consideration, an IGBT based day-ahead scheduling framework for EV aggregators to manage potential risks due to electricity price uncertainty while pursuing the desired profit is proposed. Through ensuring a predetermined level of total profit, both robust and opportunistic scheduling strategies can be made for

negative and positive decision makers respectively. Case studies are conducted based on realistic market data. The risk management of the proposed model for the EV aggregator is comprehensively analyzed and discussed according to numerical study results. The performances of robust and opportunistic day-ahead scheduling strategies of the EV aggregator are compared with another scheduling strategy that does not consider the risks of electricity price, demonstrating the effectiveness and advantage of IGDT-based risk management. Furthermore, the after-the-fact analysis is conducted to verify the proposed model.

The nomenclature of Symbols used in this chapter is given as follows

Sets

T	Set of time intervals with index t.
M	Set of categories of electric vehicles with index m.
V_m	Set of EV of category m with index v.
$V_{m,t}^{arr}$	Set of EV of category m arriving at time t with index $v_{m,t}^{arr}$.
$V_{m,t}^{dep}$	Set of EV of category m departing at time t with index $v_{m,t}^{dep}$.
$\Gamma(\alpha,\bar{\gamma})$	Uncertainty sets of electricity price in the information gap decision theory.

Parameters

S_m^{max}	Maximum magnitude of SOC for batteries of EV category m.
$P_{ch,m}^{max}$, $P_{dch,m}^{max}$	Maximum charging/discharging power of EV category m.
E_t^{max}	Maximum energy of EV aggregator at time t.
$P_{CH,t}^{max}$, $P_{DCH,t}^{max}$	Maximum charging/discharging power of EV aggregator at time t.
$Sl_{v_{m,t}^{arr}}$	Battery consumption due to daily travel for EVs belonging to $V_{m,t}^{arr}$.
$u_{v,t}$	Binary variables indicating the grid connection status of EV v at time t, 1 standing for on the grid, 0 off the grid.
$E_{\mathrm{arr},t}$	Energy increase due to EVs arriving at time t.
$E_{\mathrm{dep},t}$	Energy drop due to EVs departing at time t.
λ_{CON}	Price of energy contracted with EV owners.
λ_{BD}	EV battery degradation cost.
C_{BI}	Battery investment cost of V2G service.
E_{B}	Average EV battery capacity.
L_{C}	EV battery cycle life.
d_{DoD}	Depth of discharge
γ_t $\bar{\gamma}$	Predictive electricity price at time t, and the corresponding vector.

η_{CH}, η_{DCH}	Charging/discharging efficiency.
C	Covariance matrix of the price vector γ.
α	IGDT uncertainty index.
f_r	Critical profit target for robustness function.
f_o	Windfall profit target for opportunity function.
E_{cpm}	Energy consumption per mile.

Variables

$E_{t,}$	Energy content of EV aggregator at time t.
$P_{CH,t}$,	Charging power of EV aggregator at time t
$P_{DCH,t}$,	Discharging power of EV aggregator at time t
$P_{EV,t}$,	Trading power of EV aggregator at time t.
γ	Electricity market price vector.

Functions

$\hat{\alpha}(Z, f_r)$	Information gap decision theory robustness function.
$\hat{\beta}\ (Z, f_o)$	Information gap decision theory opportunity function.
$F(Z)$	Profit function of EV aggregator considering no risk
$f_s(t)$	Probability density function of the time when EVs first plug off the grid
$f_e(t)$	Probability density function of the time when EVs last plug into the grid.
$f_m(t)$	Probability density function of daily travel mileage of EVs.

5.2. Deterministic EV Bidding Model

5.2.1 Day-Ahead Bidding in Electricity Market

An EV aggregator acts as a load-serving entity and manages a number of EVs at the local level. The aggregator represents EV owners to participate in the electricity market to purchase and/or sell energy, based on the statistical characteristics of EVs [96]. The framework of an EV aggregator participating in the electricity market is explicitly shown in Fig. 5.1, where charging and discharging schedules of individual EVs are coordinated in order to benefit both EV owners and power grids.

In the study, a two-stage processing mechanism is adopted to keep the balance

between the supply and the demand of energy in the electricity market, as Australian Electricity market (AEM) [81]. The pre-dispatch schedule for each trading interval is determined day-ahead by the ISO. The local marginal price for each trading interval, however, is determined in the on-line dispatch process. The EV aggregator is supposed to arrange its energy schedule in the day-ahead pre-dispatch process while the uncertainty of the electricity market price, which is cleared in the on-line dispatch process, should be also taken into consideration. The aggregator decides on the day-ahead scheduling at each time interval in the following day according to the battery capacity and charging/discharging ability of EVs connected to the grids as well as the electricity price. The electricity price is assumed to be not affected by the EV aggregator because its demand is relatively small compared to the other market participants. The EV aggregator aims to maximize its profit while satisfying the requirements from EV owners. This process can be formulated as a three-step approach in [115]. In the first step, statistical data of individual EVs are collected and aggregated. Then optimal charging and discharging strategies using these aggregated data are scheduled to achieve maximum profit in the second step and the actual dispatch plan is adjusted in the real-time market at last. The emphasis is given to the scheduling strategies for the day-ahead pre-dispatch process, while the real-time dispatch is not taken into consideration.

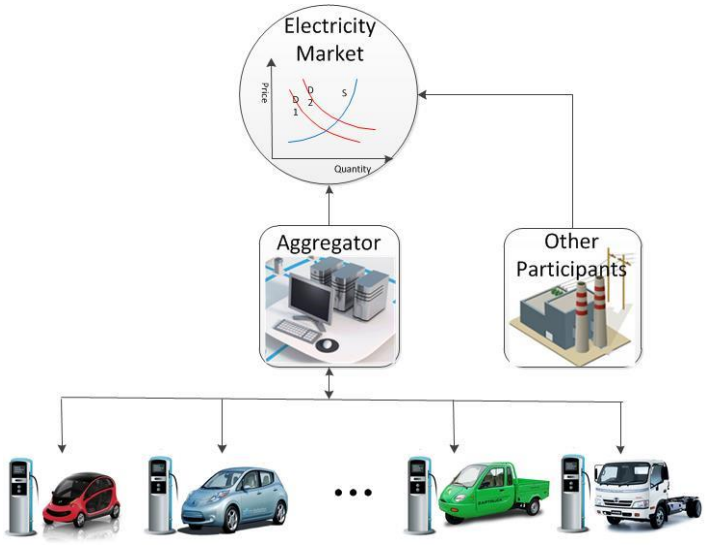

Figure 5.1. The framework of EV aggregator participating in electricity market

5.2.2 Aggregation of Individual Driving Pattern Data

First, the specific information of individual EVs is collected by the aggregators. Then EV aggregators assemble these individual energy demands for the sake of overall management, formulated as follows,

$$E_t^{\max} = \sum_{m=1}^{M} \sum_{v=1}^{V_m} S_m^{\max} u_{v,t} \quad \forall v \tag{5.1}$$

$$P_{\mathrm{CH},t}^{\max} = \sum_{m=1}^{M} \sum_{v=1}^{V_m} p_{\mathrm{ch},m}^{\max} u_{v,t} \quad \forall v \tag{5.2}$$

$$P_{\mathrm{DCH},t}^{\max} = \sum_{m=1}^{M} \sum_{v=1}^{V_m} p_{\mathrm{dch,m}}^{\max} u_{v,t} \quad \forall v \tag{5.3}$$

$$E_{\mathrm{arr},t} = \sum_{m=1}^{M} \sum_{v_{m,t}^{\mathrm{arr}}=1}^{V_{m,t}^{\mathrm{arr}}} (S_m^{\max} - Sl_{v_{m,t}^{\mathrm{arr}}}) \quad \forall v_{m,t}^{\mathrm{arr}} \tag{5.4}$$

$$E_{\mathrm{dep},t} = \sum_{m=1}^{M} \sum_{v_{m,t}^{\mathrm{dep}}=1}^{V_{m,t}^{\mathrm{dep}}} S_m^{\max} \quad \forall v_{m,t}^{\mathrm{dep}} \tag{5.5}$$

where $E_t^{\max}$ denotes the dynamic status of the maximum energy content of the EV aggregator which is also the sum of the maximum magnitude of SOC of individual EV batteries connected to the power system $S_m^{\max}$, $P_{\mathrm{CH},t}^{\max}$ and $P_{\mathrm{DCH},t}^{\max}$ denote the maximum charging and discharging ability of EV aggregators respectively, which depends on the sum of maximum charging power $p_{\mathrm{ch,m}}^{\max}$ and discharging power $p_{\mathrm{dch,m}}^{\max}$ of each EV on the grid. $E_{\mathrm{arr},t}$ represents the increase in energy content due to vehicles arriving at time t. The energy of each electric vehicle plugged into the power grid is the remaining value after the energy consumption in the day, shown in (5.4). $E_{\mathrm{dep},t}$ denotes the energy drop due to vehicle departures. The energy is assumed to be full when the vehicle leaves.

5.2.3 Optimization of EV Aggregators

The computation burden can be very heavy if each individual EV is dispatched directly by the system operators. Therefore an aggregated model is developed in

the study to condense individual driving pattern data into a simplified model, in analogy to a virtual battery with the total capacity, charging and discharging ability changing over time. In practice, the EV aggregator makes a long-term contract with EV owners. The price is fixed as a certain value, rather than catering for the fluctuation of daily electricity price. At the same time, the EV aggregator is granted the privilege to represent the EV owners to bid in the electricity market and thus schedule the EV charging and discharging. For V2G service, the aggregator should compensate the EV owners due to the battery degradation. The total profit of EV aggregators is formulated as follows,

$$\max F(Z) = \sum_{t=1}^{T} (\lambda_{\mathrm{CON}} P_{\mathrm{EV},t} - \gamma_t P_{\mathrm{EV},t} - \lambda_{\mathrm{BD}} P_{\mathrm{DCH},t}) \tag{5.6}$$

s.t.

$$E_t = E_{t-1} + E_{\mathrm{arr},t} - E_{\mathrm{dep},t} + \eta_{\mathrm{CH}} P_{\mathrm{CH},t} - P_{\mathrm{DCH},t} / \eta_{\mathrm{DCH}} \quad \forall t \tag{5.7}$$

$$E_0 = E_T \tag{5.8}$$

$$P_{\mathrm{EV},t} = P_{\mathrm{CH},t} - P_{\mathrm{DCH},t} \quad \forall t \tag{5.9}$$

$$0 \le E_t \le E_t^{\max} \quad \forall t \tag{5.10}$$

$$0 \le P_{\mathrm{CH},t} \le P_{\mathrm{CH},t}^{\max} \quad \forall t \tag{5.11}$$

$$0 \le P_{\mathrm{DCH},t} \le P_{\mathrm{DCH},t}^{\max} \quad \forall t \tag{5.12}$$

where the decision variable set Z is defined by

$$Z = [E \; P_{\mathrm{EV}} \; P_{\mathrm{CH}} \; P_{\mathrm{DCH}}] \tag{5.13}$$

The objective function defined in (5.6) consists of three components in total. The first one is the revenue of energy contracted with EV owners. The second part represents the scheduling cost/revenue in the electricity market. The third component denotes the cost returned to the EV owners for the compensation of the battery degradation due to V2G discharge. The battery degradation cost can be calculated according to [116-118]:

$$\lambda_{\mathrm{BD}} = \frac{1000 C_{\mathrm{BI}}}{L_{\mathrm{C}} E_{\mathrm{B}} d_{\mathrm{DoD}}} \tag{5.14}$$

where C_{BI} denotes the battery investment cost; L_C is the battery cycle life at a certain depth of discharge (DoD); E_B is the average battery capacity; d_{DoD} is the DoD used in determining L_C. Thus, $L_C E_B d_{DoD}$ represents the overall energy throughput that a battery can provide during its lifetime and the number 1000 is used to make the transition from *kWh* to *MWh*.

In the constraints, the energy content E_t depends on the charging power $P_{CH,t}$ and the discharging power $P_{DCH,t}$ as well as the energy of arriving EVs $E_{arr,t}$ and the energy of departing EVs E_{dep}, shown in (5.7). Upper and lower limits of energy content E_t, charging power $P_{CH,t}$ and discharging power $P_{DCH,t}$ are represented in (5.10)-(5.12) respectively.

5.3. IGDT Based Operation Strategy of EV Aggregator

Electricity prices in the electricity market exhibit significant fluctuations due to various reasons. For instance, stochastic and intermittent renewable energy would introduce serious uncertainties [119], [120] and influence the electricity price to some extent [121]. The model described in Section II neglects the risks introduced by the electricity price uncertainty. The proposed model based on IGDT can effectively take risks and uncertainties into consideration. The robustness function and opportunity function, is proposed in this section for either risk-averse or risk-seeking decision makers.

5.3.1 Uncertainty Model

Various models, including Energy-bound models, Minkowski-norm models and Fourier-bound models, are proposed to model the prior information about the uncertainty input in [109]. The ellipsoid-bound IGDT model is adopted, due to its emphasis on the variability and the relationship among different dynamic uncertain parameters compared with the other models [111, 112]. To implement the ellipsoid-bound IGDT model for EV aggregators, the nominal electricity prices and their correlations are forecasted and considered as model inputs. The uncertainty set Γ consists of uncertain prices in the electricity market, and is mathematically formulated as,

$$\Gamma(\alpha, \bar{\gamma}) = \{\gamma : (\gamma - \bar{\gamma})^T C^{-1} (\gamma - \bar{\gamma}) \le \alpha^2\}, \quad \alpha \ge 0 \tag{5.15}$$

where $\bar{\gamma}$ is the vector of nominal price time-series and C denotes covariance matrix between each parameter in the vector. $\Gamma(\alpha, \bar{\gamma})$ can be defined as a quadratic function. It specifies a range of uncertain prices, whose deviations beyond the nominal price $\bar{\gamma}$ can be quantified by the uncertainty index α. The larger the value of α, the greater range of deviation is. The family of the sets can be interpreted as an information gap model of uncertainty [109].

5.3.2 Optimization Framework

Due to uncertainties of electricity price, EV aggregators could adopt either risk-averse or risk-seeking strategies in scheduling their daily operation plan. The information gap decision theory can effectively account for these two attitudes, where different risk attitudes can be reasonably quantified by setting different profit targets. Risk-averse decision makers tend to set lower profit target that they can accept, while risk-seeking decision makers tend to set higher profit target that they want to pursue. Such decision processing can be represented by two functions: the *robustness function* denoting the immunity to fall, and the *opportunity function* denoting the desire to windfall profit. Both functions optimize the uncertainty index as below,

$$\hat{\alpha}(Z, f_{\mathrm{r}}) = \max_{Z,\gamma}\{\alpha : \min_{\gamma \in U(\alpha,\bar{\gamma})} F(Z,\gamma) > f_{\mathrm{r}}\} \tag{5.16}$$

$$\hat{\beta}(\mathrm{Z}, f_{\mathrm{o}}) = \min_{Z,\gamma}\{\alpha : \max_{\gamma \in U(\alpha,\bar{\gamma})} F(Z,\gamma) > f_{\mathrm{o}}\} \tag{5.17}$$

The robustness function $\hat{\alpha}\,\hat{\alpha}(Z, f_{\mathrm{r}})$ defined in (5.16) is the greatest level of uncertainty corresponding to the guaranteed profit larger than the critical profit objective f_{r}. The optimal scheduling strategy is derived via maximizing the immunity against failure while satisfying the critical survival-level performance. The robustness function value $\hat{\alpha}\,(Z, f_{\mathrm{r}})$ can be comprehended as allowable deviations beyond the nominal value. This is consistent with pessimistic decision makers. The opportunity function $\hat{\beta}\,(Z, f_{\mathrm{o}})$ defined in (5.17) denotes the least level of uncertainty which should be acceptable to achieve the windfall profit objective as large as f_{o}. The optimal scheduling strategy is calculated by minimizing the immunity against windfall return while achieving relatively high rewards. The opportunity function acts as the decision tool for optimistic decision makers, who

concern more about the maximum return when the price is desirable. In any case, the windfall reward f_o is usually much greater than the critical reward f_r.

5.3.3 Robustness Function

The robustness function is formulated as a bilevel optimization problem maximizing the uncertainty level in the upper level and minimizing the profit of an EV aggregator in the lower level, shown as follows,

$$\max_{Z,\gamma} \alpha \tag{5.18}$$

s.t.

$$\min_{\gamma \in U(\alpha,\bar{\gamma})} F(Z,\gamma) > f_r \tag{5.19}$$

$$(\gamma-\bar{\gamma})^T \mathrm{C}^{-1}(\gamma-\bar{\gamma}) \le \alpha^2 \tag{5.20}$$

$$\alpha \ge 0 \tag{5.21}$$

$$(5.7) - (5.12) \tag{5.22}$$

The robustness function is difficult to handle using traditional optimization approach. Lagrangian relaxation is used herein to simplify the lower level optimization. The minimum profit of an EV aggregator can be obtained and rewritten as,

$$\min_{\gamma \in U(\alpha,\bar{\gamma})} F(Z,\gamma)=\lambda_{\mathrm{CON}} P_{\mathrm{EV}} - \gamma^T P_{\mathrm{EV}} - \lambda_{\mathrm{BD}} P_{\mathrm{DCH}} \tag{5.23}$$

$$\text{s.t. } (\gamma-\bar{\gamma})^T \mathrm{C}^{-1}(\gamma-\bar{\gamma}) \le \alpha^2 \tag{5.24}$$

Since the optimization is convex, Lagrange relaxation is adopted to simplify the problem, expressed as

$$\nabla_{\mu,\gamma}\{(\lambda_{\mathrm{CON}} P_{\mathrm{EV}} - \gamma^T P_{\mathrm{EV}} - \lambda_{\mathrm{BD}} P_{\mathrm{DCH}}) + \mu(\alpha^2 - (\gamma-\bar{\gamma})^T \mathrm{C}^{-1}(\gamma-\bar{\gamma}))\} = 0 \tag{5.25}$$

where μ is the Lagrangian multiplier. The results can be obtained,

$$\gamma = \bar{\gamma} \pm \frac{\alpha C^T P_{\mathrm{EV}}}{\sqrt{(P_{\mathrm{EV}})^T C P_{\mathrm{EV}}}} \tag{5.26}$$

Substituting (5.26) into (5.23), the following function can be derived,

$$\min_{\gamma \in U(\alpha,\bar{\gamma})} F(\mathrm{Z},\gamma)=\lambda_{\mathrm{CON}}P_{\mathrm{EV}}-\gamma^{T}P_{\mathrm{EV}}-\lambda_{\mathrm{BD}}P_{\mathrm{DCH}}\pm\alpha\sqrt{(P_{\mathrm{EV}})^{T}CP_{\mathrm{EV}}} \quad (5.27)$$

Considering the uncertainty index α is positive, the negative sign is selected for the minimum of $F(Z,\gamma)$. The minimum profit should be at least equal to f_{r}, given as,

$$f_{r}=\lambda_{\mathrm{CON}}P_{\mathrm{EV}}-\gamma^{T}P_{\mathrm{EV}}-\lambda_{\mathrm{BD}}P_{\mathrm{DCH}}-\alpha\sqrt{(P_{\mathrm{EV}})^{T}CP_{\mathrm{EV}}} \quad (5.28)$$

Thus the robustness function in terms of the objective f_r can be rewritten as

$$\hat{\alpha}(\mathrm{Z},\,f_{\mathrm{r}})=\max_{Z}\alpha(\,f_{\mathrm{r}})=\max_{Z}\frac{(\lambda_{\mathrm{CON}}P_{\mathrm{EV}}-\gamma^{T}P_{\mathrm{EV}}-\lambda_{\mathrm{BD}}P_{\mathrm{DCH}})-f_{r}}{\sqrt{(P_{\mathrm{EV}})^{T}CP_{\mathrm{EV}}}} \quad (5.29)$$

Thus the IGDT method is simplified to optimize the objective function defined in (5.29) with the constraints defined in (5.7) - (5.12) being satisfied as well.

5.3.4 Opportunity Function

Similar to the robustness function, the opportunity function is also formulated as a bilevel optimization problem minimizing the uncertainty level in the upper level and maximizing the profit of an EV aggregator in the lower level, shown as follows,

$$\min_{\mathrm{Z},\gamma}\ \alpha \quad (5.30)$$

s.t.

$$\max_{\gamma \in U(\alpha,\bar{\gamma})} F(\mathrm{Z},\gamma) > f_{o} \quad (5.31)$$

$$(\gamma-\bar{\gamma})^{T}\,\mathrm{C}^{-1}(\gamma-\bar{\gamma})\le\alpha^{2} \quad (5.32)$$

$$\alpha\ge 0 \quad (5.33)$$

$$(7)\text{ - }(12) \quad (5.34)$$

Lagrange relaxation method is used again to solve the nested optimization problem, similarly to the way of handling the robustness function. The maximum profit can be formulated as,

$$\max_{\gamma \in U(\alpha,\bar{\gamma})} F(\mathrm{Z},\gamma)=\lambda_{\mathrm{CON}}P_{\mathrm{EV}}-\gamma^{T}P_{\mathrm{EV}}-\lambda_{\mathrm{BD}}P_{\mathrm{DCH}}\pm\alpha\sqrt{(P_{\mathrm{EV}})^{T}CP_{\mathrm{EV}}} \quad (5.35)$$

Considering the uncertainty index α is positive, the positive sign is selected for the maximum of $F(\mathrm{Z},\gamma)$. The maximum profit should be at least equal to f_o, given as,

$$f_o = \lambda_{\mathrm{CON}} P_{\mathrm{EV}} - \gamma^T P_{\mathrm{EV}} - \lambda_{\mathrm{BD}} P_{\mathrm{DCH}} + \alpha\sqrt{(P_{\mathrm{EV}})^T C P_{\mathrm{EV}}} \tag{5.36}$$

It is expected to reach the windfall profit f_o. Let the maximum profit be equal to f_o, the opportunity function can be formulated as,

$$\hat{\beta}(\mathrm{Z}, f_o) = \min_{Z} \alpha(f_o) = \min_{Z} \frac{f_o - (\lambda_{\mathrm{CON}} P_{\mathrm{EV}} - \gamma^T P_{\mathrm{EV}} - \lambda_{\mathrm{BD}} P_{\mathrm{DCH}})}{\sqrt{(P_{\mathrm{EV}})^T C P_{\mathrm{EV}}}} \tag{5.37}$$

The constraints defined in (5.7) - (5.12) need to be satisfied as well.

5.4. Case Study and Discussions

5.4.1 Case Description

The proposed IGDT-based model for day-ahead scheduling of an EV aggregator is validated using practical market data. As EVs are usually parked at night in practice, the scheduling period is set as 12:00 AM to 12:00 AM of the following day and the dispatch interval is defined as one hour [122]. In our case study, the electricity price is forecasted using the method developed in [114]. The charging and discharging efficiency is specified as 0.90 and 0.91 respectively.

A comprehensive survey on EVs and battery technology is represented in [123], where six categories of vehicles, including goods-carrying vehicle (N1), large goods-carrying vehicle (N2), plug-in EV (PEV), extended-range EV (EREV), quadricycle-four wheels (L7e) and passenger vehicle (M1) and their technical parameters are summarized as in Table I. The proportion of each vehicle type, the maximum magnitude of SOC for batteries $S_m^{\max}$, the maximum magnitude of charging power $p_{\mathrm{ch},m}^{\max}$, discharging power $p_{\mathrm{dch},m}^{\max}$ and the energy consumption per mile E_{cpm} of each category of EVs are also listed in Table I. It is assumed in our case study that 100 000 EVs are managed by an aggregator in total. The EV travel data needed in this case study is based on the national household travel behavior survey, conducted by the U.S. Department of Transportation Federal Highway

Administration [84]. For detailed EV charging demand modelling, please refer to the EV travel behavior in section 4.3.1.

Table 5.1. Parameters of Electric Vehicles

Parameters	N1	N2	PEV	EREV	L7e	M1
Proportion	0.05	0.05	0.1	0.1	0.2	0.5
$S_m^{\max}$ (kWh)	23	85	8.2	17	8.7	29
$p_{\mathrm{ch},m}^{\max}$ (kW)	3	10	3	3	3	3
$p_{\mathrm{dch},m}^{\max}$ (kW)	1.5	5	1.5	1.5	1.5	1.5
E_{cpm} (KWh/km)	0.1854	0.5867	0.1562	0.2530	0.1122	0.1608

5.4.2 EV Scheduling Results

In the case studies, the proposed IGDT-based robustness index, i.e., the value of the robustness function defined by (16), and the opportunity index, i.e., the value of opportunity function defined by (17), are calculated based on real data. The profit target defined by the EV aggregator can be regarded as a critical input to measure both negative and positive attitudes towards risk or uncertainty. Therefore, different profit targets are given to explicitly analyze the effects of the risk attitude towards the EV charging/discharging schedule. The corresponding numerical results are displayed in Fig. 5.2.

It can be seen from Fig. 5.2 that the robustness index increases from 0 to 2.128 when the profit target f_{r} decreases from \$5842.7 to \$1500. This is understandable as a lower profit target represents a preference towards risk, and thus permitting a higher uncertainty level. On the contrast, the opportunity index varies from 0 to 1.658 when the windfall high reward is targeted from \$5842.7 to \$10500. A higher profit target represents a more risk-seeking attitude towards the risk, and needs a higher profitable price uncertainty level. It can be observed from Fig. 5.2 that if the robust profit target and the opportunity profit target are specified as \$5842.7, both the robustness index and opportunity index are zero, as shown at point O Such a profit target is the same as the numerical solution to the neutral risk formulation according to (6)-(12).

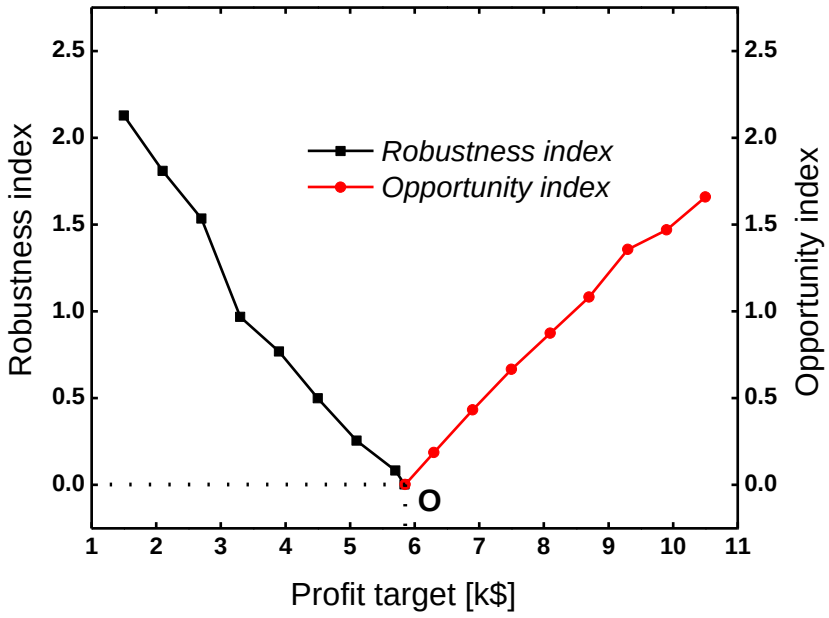

Figure 5.2. Robustness and opportunity index for different profit targets

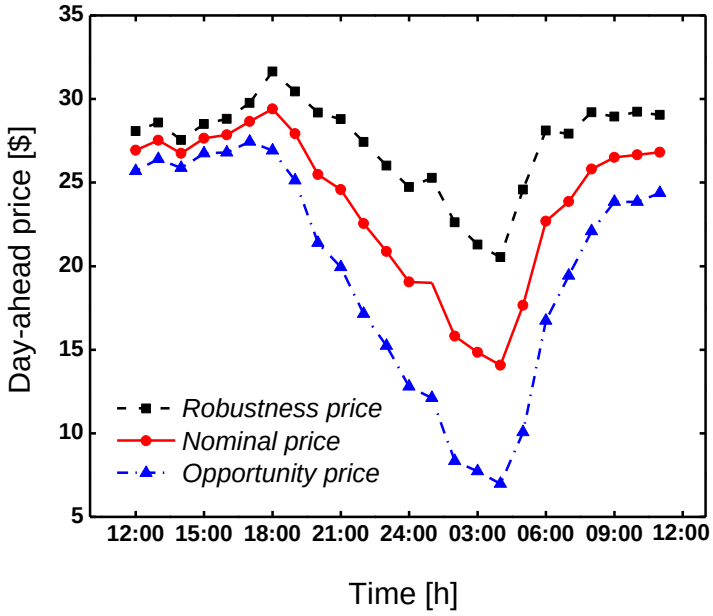

Figure 5.3. Robustness price curve and opportunity price curve

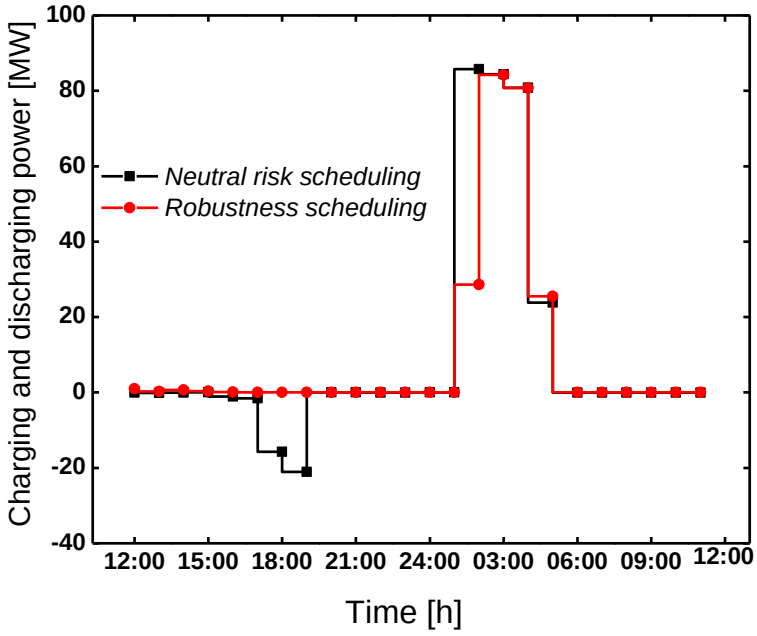

Figure 5.4. Electric vehicle charging and discharging power rate by robust scheduling strategy

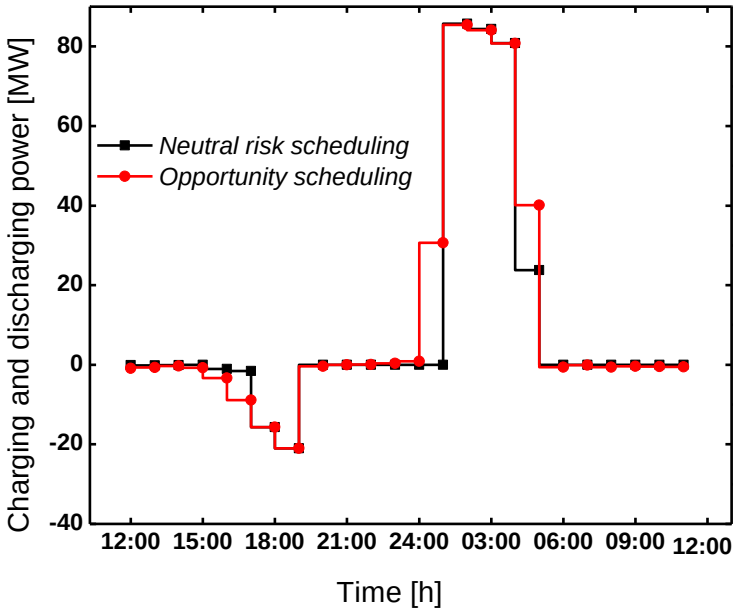

Figure 5.5. Electric vehicle charging and discharging power rate by opportunistic scheduling strategy

For a certain robust profit target, given as f_r = \$3900, the robust price curve is

obtained for such a risk-averse attitude according to (26), and explicitly shown in Fig. 5.3. If the after-the-fact price falls below the robustness price curve, the final profit would not be less than $3900. Similarly, in terms of an opportunistic profit target, given as $8100, the opportunity price curve for such a risk-seeking attitude is achieved and depicted in Fig. 5.3. When the after-the-fact price is below the opportunity price curve shown in Fig. 5.3, the final profit has a chance to achieve $8100 or more.

In the study, various risk-based day-ahead scheduling strategies of an EV aggregator are carried out under different predefined profit targets. A robust scheduling strategy of charging and discharging power with a profit target f_r = $2700 is depicted in Fig. 5.4 while an opportunistic scheduling strategy with a profit target f_o = $9900 is shown in Fig. 5.5. To benchmark the robust and opportunity strategies, the scheduling with no risk consideration is derived and also displayed in Figs. 5.4 and 5.5. As shown in Fig. 5.4, no discharge is arranged during the day for the robust scheduling. It indicates that the extreme risk-averse decision makers choose to abandon the benefit attained by discharging power due to its revenue fluctuation affected by price uncertainty. This is consistent with the behavior of the conservative users. On the other hand, for those who have positive attitudes towards risk, discharging power is dispatched more and contributes relatively more to the aggregator's revenue, as depicted in Fig. 5.5. Such a scheduling method has a chance to acquire high return when the electricity price is beneficial to the aggregator, which is consistent with opportunistic decision makers. By setting allowable deviations beyond the nominal value of the daily revenue, the pessimistic decision makers tend to adopt the conservative strategies to maximize their profits while guaranteeing the survival-level performance. In the contract, the optimistic decision makers choose the opportunity functions as radical strategies by using relatively large predefined windfall reward.

In order to compare the different robust and opportunistic scheduling strategies, the information gap between the estimated and actual prices is assumed to be zero. The expected profits are given in Fig. 5.6. It can be easily found that the maximum expected profit can be obtained using a neutral risk strategy. The expected profits decrease with the degree of the robustness or opportunity. The difference between the expected value of the selected profit target and the maximum profit considering

no risk can be interpreted as robustness cost or opportunity cost. Theoretically, this is an unavoidable trade-off between the scheduling risk and expected profit.

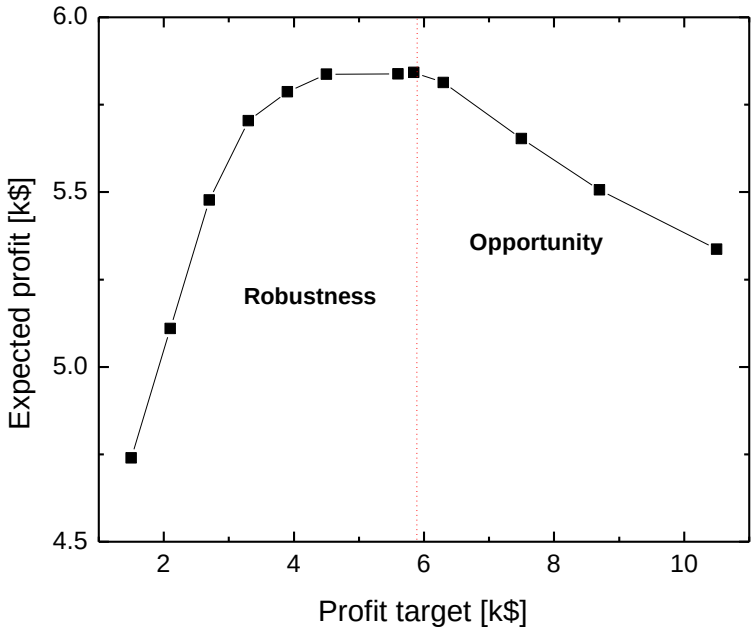

Figure 5.6. Expected profit with no information gap between the estimated and actual prices against different profit targets.

5.4.3 Sensitivity Analysis

To further verify the proposed model, an after-the-fact analysis is conducted herein to evaluate different scheduling methods. Five typical price scenarios are generated to investigate the performance of the proposed model.

Scenarios 1 and 2 are produced according to (26) with a robustness index of 1.5343 and 0.9678 respectively. The price series in Scenario 3 is regarded as the nominal one. Scenarios 4 and 5 are generated with an opportunity index of 0.6662 and 1.4698. Three scheduling strategies are systematically compared and the corresponding profits are shown in Table II. When the electricity price falls in the robust region as in Scenarios 1 and 2, the profit for the robust scheduling is the largest while the profit for opportunistic scheduling is the smallest. When the forecast price is perfectly realized, neutral risk scheduling performs the best. When the price falls in the opportunity region, such as Scenarios 4 and 5, EV aggregator would benefit more from the opportunistic scheduling than the other two

scheduling schemes. It is worth mentioning that the predefined critical target for robust scheduling is set as $2700, which is equal to the result in price Scenario 1. It is demonstrated that the predetermined target is guaranteed with the corresponding scheduling strategy under this price scenario. The predetermined desirable target for opportunity is $9900, equal to the result in Scenario 5. It indicates that the predefined target is achieved under the corresponding price scenario.

Table 5.2 Profit Obtained by Different Immunity Functions Under Different Price Scenarios

Price scenario	Profit for robust scheduling ($)	Profit for neutral risk scheduling ($)	Profit for opportunistic scheduling ($)
1	2700	2085	1224
2	3623	3254	2736
3	5419	5843	5498
4	6670	7323	7416
5	8267	9457	9900

5.5. Conclusions

This chapter develops an information gap decision theory based scheduling methodology for EV aggregators to consider different risk attitudes towards the uncertainty of electricity market prices. The proposed IGDT-based model provides an effective way for EV aggregators to pursue a predefined profit target through effective risk management. The robustness and opportunity functions are proposed in this model to assist EV aggregators to effectively align the desirability of different attitudes towards risk with their immunity to electricity price uncertainty. Based on the two functions, a variety of robust and opportunistic scheduling strategies can be derived to either guarantee a critical reward under unfavorable price scenarios or to capture a windfall profit under desirable price scenarios. The trade-off between the expected profit and potential risk is demonstrated under different scenarios of electricity price fluctuations through case studies. It is

convincing that the framework provides a new decision-support tool for EV aggregators of different preferences to uncertainties to manage their financial risk. Since the model does not require a probability distribution of electricity price uncertainty, the proposed model have an advantage to reduce the computation burden compared with traditional scenario based approaches, indicating a high potential for future practical applications.

6. Conclusions and Discussions

6.1. Conclusions

This thesis focuses on evaluating the challenges and opportunities introduced by large-scale EV charging in power system and developing new method to utilize EV charging flexibility to benefit power system economic and secure operation. All the optimization models are proposed to achieve two goals: to hedge against negative impact as well as to benefit the grid and EV owners. Specifically, this thesis evaluates distribution system electric vehicle hosting capacity, proposes framework for distributed generator investment for EV accommodation, analyzes the potential ability of aggregated EV charging in providing ancillary service and proposes bidding strategy for EV aggregators to participate in electricity market.

The concept of "EV chargeable region" is innovatively proposed to evaluate the maximum DN EV hosting capacity for each node. The EV chargeable region optimization problem is formulated as a two-stage model, where the chargeable region and DN decision variables are optimized in the first stage and the feasibility of the DN worst-case scenario is checked in the second stage. Mathematically, the proposed framework is formulated as a two-stage robust optimization problem with an adjustable uncertainty set. With the aid of this model, not only operating constraint violation of DN is prevented, but also EV owners' charging requests, i.e., immediate charging or price-response charging, are guaranteed to the largest extent. EV owners' daily report of charging demand to the EV aggregator may be waived, as the EV charging profile can be well managed directly by the EV owners themselves. Thus, urgent usage of EVs can be maximally guaranteed. Besides, the communication mechanism of the proposed framework is simple and only needed to convey the information of EV chargeable region from the distribution network operator to EV charging controllers at distribution network nodes. Obviously, the

communication is unidirectional and operates once a day. Overall, the proposed framework demonstrates a high potential for practical applications. To accommodate more EV charging demand in distribution networks and to obtain financial revenue, a robust active distribution network planning framework considering the integration of renewables and large-scale EVs is further proposed. Two decision-dependent robust planning strategies are proposed based on advanced modelling of EV charging demand. The optimal DG sizing and sitting are determined that is robust against any realization of uncertainty of EV charging and distributed generation output as well as the uncertainty of EV owners' willingness in participation in charging coordination.

To evaluate EVs' potential ability in providing ancillary service for power system, a novel cost-efficiency based SRR optimization model is proposed. The concept of EESEV is innovatively proposed to quantify the expected energy supplied by EVs, with EV reaction time taken into consideration. The optimal SRR is quantified based on the minimization of the total costs of generation operation, EENS and EESEV. Numerical case studies demonstrate the reduction of scheduled spinning reserve and the generation operation cost due to the support of EVs. The reliability of power system is also improved with EVs' participation. The economic effectiveness of the proposed model will be significantly improved if V2G can be widely realized in the future. Furthermore, systematical sensitivity analysis implies that the amount of power system spinning reserve has a close relationship with EV penetration level and there exists abundant space to improve the compensation rate to motivate EV owners to provide power system operating reserve. To obtain better welfare for EV owners, an information gap decision theory based scheduling methodology is developed to consider different risk attitudes towards the uncertainty of electricity market prices. The proposed IGDT-based model provides an effective way for EV aggregators to pursue a predefined profit target through effective risk management. The robustness and opportunity functions are proposed in this model to assist EV aggregators to effectively align the desirability of different attitudes towards risk with their immunity to electricity price uncertainty. Based on the two functions, a variety of robust and opportunistic scheduling strategies can be derived to either guarantee a critical reward under unfavorable price scenarios or to capture a windfall profit under desirable price

scenarios. The trade-off between the expected profit and potential risk is demonstrated under different scenarios of electricity price fluctuations through case studies. It is convincing that the framework provides a new decision-support tool for EV aggregators of different preferences to uncertainties to manage their financial risk. Since the model does not require a probability distribution of electricity price uncertainty, the proposed model have an advantage to reduce the computation burden compared with traditional scenario based approaches, indicating a high potential for future practical applications.

6.2. Discussions

Traditionally, it is the responsibility of power system to serve energy for its customers, with power quality and reliability guaranteed anytime. With the development of smart grid, demand side tends to contribute to power balance by adjusting its actual demand, known as demand response. Flexible electric vehicle charging demand, regarded as a specific type of demand response, is modeled and discussed in this thesis. Due to the lack of real data, some assumptions are made in the modelling of EV charging demand. As the EVs are emerging participant in electricity market, it remains uncertain how many EVs are willing to respond to electricity price, compromise their driving duties and even agree to feed energy back to the grid. In other words, it is not clear how much compensation the EV owners will accept to provide ancillary service and how much compensation the power system operators are willing to pay to lower the power supply costs. Although the sensitivity analysis is conducted with various scenarios in the thesis, the assumptions can be obviated once actual data is available. Another difficulty to implement the proposed models is the methodology to aggregate the geographically separate EV charging demand. Although EV aggregator is assumed to manage these load in the thesis, obstacles still exist to put the algorithm to practice. From the view of the authors, it is relatively easy to implement EV coordination in a distribution network and the similar EV charging management method has been put into practice in fact, while practical value of the aggregated EVs' participation in electricity market and ancillary service still demand further investigation. Nevertheless, the potential possibility should be never neglected due

to its huge economic benefits. Besides, with more and more other demand response programs emerging, it should take into account the interaction between EVs and other demand response resources, especially the interaction with different relevant uncertain elements. Methodologies such as game theory are suggested to be introduced to estimate these influences.

The optimization methodologies used in this thesis, e.g., robust optimization, have their inherent defect. Robust optimization addresses input uncertainty based on the assumption that uncertain parameters belong to a convex bounded uncertainty set and maximizing the minimum value of the objective over the uncertainty set, at the same time ensuring the feasibility for the constraints in the worst-case scenario. Specifically, the uncertainty set consists in confidence intervals and a budget-of-uncertainty constraint. Hence, the uncertain parameters are selected to construct the worst-case scenario, and thus is deemed too conservative for practical implementation. In this thesis, we allow the decision-maker to control the degree of conservatism of the solution through proposing different cases to determine various optimization solutions from different attitudes of decision makers towards the robustness. For practical implementation, how to manage and control the robustness should be seriously estimated. Besides, the algorithms are generally two-stage and make every decision before the realization of the uncertainties. However, there are many optimization problems where only a subset of the decisions should be made before the realization of the uncertainty, but the remaining decisions can be made later after observing the realized uncertainties. Multi-period optimization models are supposed to find out a series of decisions at different points in time occurs. Thus, multi-period robust optimization is suggested to better handle uncertainty problem and control the robustness.

Reference

[1] S. C. Davis, S. W. Diegel, and R. G. Boundy, *Transportation Energy Data Book: Edition 34*. Oak Ridge National Laboratory, Aug. 2015.

[2] J. D. Hamilton, *Oil prices, Exhaustible Resources, and Economic Growth.* National Bureau of Economic Research, 2012.

[3] McCubbin, D. R., and M. A. Delucchi., "The Health Costs of Motor-Vehicle-Related Air Pollution," *Journal of Transport Economics and Policy,* vol. 33, pp. 253–286.

[4] United States Environmental Protection Agency, [online]. Available: https://www.epa.gov/ghgemissions/sources-greenhouse-gas-emissions.

[5] D. A. Kirsch, *The Electric Vehicle and the Burden of History.* Transport Research Laboratory, 2000.

[6] K. B. Naceur and J. F. Gagne, *Global EV Outlook 2016: Beyond One Million Electric Cars*. France: International Energy Agency, 2016.

[7] J. S. Cunningham, *An Analysis of Battery Electric Vehicle Production Projections.* U.S.: Massachusetts Institute of Technology, 2009.

[8] A. M. Foley, I. J. Winning, and B. P. Ó. Gallachóir, "State-of-the-art in electric vehicle charging infrastructure," *IEEE Vehicle Power and Propulsion Conference (VPPC),* 2010.

[9] K. Clement-Nyns, E. Haesen, and J. Driesen, "The Impact of Charging Plug-In Hybrid Electric Vehicles on a Residential Distribution Grid," *IEEE Transactions on Power Systems,* vol. 25, pp. 371-380, Feb 2010.

[10] J. D. Graham, N. M. Messer, and D. Hartmann, *Plug-in Electric Vehicles: A Practical Plan for Progress*. Indiana University, 2011.

[11] L. P. Fernandez, T. G. S. Roman, R. Cossent, C. M. Domingo, and P. Frias, "Assessment of the Impact of Plug-in Electric Vehicles on Distribution Networks," *IEEE Transactions on Power Systems,* vol. 26, pp. 206-213, 2011.

[12] S. Shafiee, M. Fotuhi-Firuzabad, and M. Rastegar, "Investigating the Impacts of Plug-in Hybrid Electric Vehicles on Power Distribution Systems," *IEEE Transactions on Smart Grid,* vol. 4, pp. 1351-1360, 2013.

[13] A. Ashtari, E. Bibeau, S. Shahidinejad, and T. Molinski, "PEV Charging Profile Prediction and Analysis Based on Vehicle Usage Data," *IEEE Transactions on Smart Grid,* vol. 3, pp. 341-350, 2012.

[14] O. Sundstrom and C. Binding, "Flexible Charging Optimization for Electric Vehicles Considering Distribution Grid Constraints," *IEEE Transactions on Smart Grid,* vol. 3, pp. 26-37, 2012.

[15] S. Weckx, D. R, x, Hulst, B. Claessens, and J. Driesensam, "Multiagent Charging of Electric Vehicles Respecting Distribution Transformer Loading and Voltage Limits," *IEEE Transactions on Smart Grid,* vol. 5, pp. 2857-2867, 2014.

[16] S. Deilami, A. S. Masoum, P. S. Moses, and M. A. S. Masoum, "Real-Time Coordination of Plug-In Electric Vehicle Charging in Smart Grids to Minimize Power Losses and Improve Voltage Profile," *IEEE Transactions on Smart Grid,* vol. 2, pp. 456-467, 2011.

[17] J. d. Hoog, T. Alpcan, M. Brazil, D. A. Thomas, and I. Mareels, "A Market Mechanism for Electric Vehicle Charging Under Network Constraints," *IEEE Transactions on Smart Grid,* vol. 7, pp. 827-836, 2016.

[18] P. Richardson, D. Flynn, and A. Keane, "Local Versus Centralized Charging Strategies for Electric Vehicles in Low Voltage Distribution Systems," *IEEE Transactions on Smart Grid,* vol. 3, pp. 1020-1028, 2012.

[19] P. Richardson, D. Flynn, and A. Keane, "Optimal Charging of Electric Vehicles in Low-Voltage Distribution Systems," *IEEE Transactions on Power Systems,* vol. 27, pp. 268-279, 2012.

[20] J. d. Hoog, T. Alpcan, M. Brazil, D. A. Thomas, and I. Mareels, "Optimal Charging of Electric Vehicles Taking Distribution Network Constraints Into Account," *IEEE Transactions on Power Systems,* vol. 30, pp. 365-375, 2015.

[21] A. O. Connell, D. Flynn, and A. Keane, "Rolling Multi-Period Optimization to Control Electric Vehicle Charging in Distribution Networks," *IEEE Transactions on Power Systems,* vol. 29, pp. 340-348, 2014.

[22] W. Yao, J. Zhao, F. Wen, Y. Xue, and G. Ledwich, "A Hierarchical Decomposition Approach for Coordinated Dispatch of Plug-in Electric Vehicles," *IEEE Transactions on Power Systems,* vol. 28, pp. 2768-2778, 2013.

[23] D. Wu, D. C. Aliprantis, and K. Gkritza, "Electric Energy and Power Consumption by Light-Duty Plug-In Electric Vehicles," *IEEE Transactions on Power Systems,* vol. 26, pp. 738-746, 2011.

[24] A. Lojowska, D. Kurowicka, G. Papaefthymiou, and L. Sluis, "Stochastic Modeling of Power Demand Due to EVs Using Copula," *IEEE Transactions on Power Systems,* vol. 27, pp. 1960-1968, 2012.

[25] D. Tang and P. Wang, "Probabilistic Modeling of Nodal Charging Demand Based on Spatial-Temporal Dynamics of Moving Electric Vehicles," *IEEE Transactions on Smart Grid,* vol. 7, pp. 627-636, 2016.

[26] S. Bae and A. Kwasinski, "Spatial and Temporal Model of Electric Vehicle Charging Demand," *IEEE Transactions on Smart Grid,* vol. 3, pp. 394-403, 2012.

[27] G. Wang, J. Zhao, F. Wen, Y. Xue, and G. Ledwich, "Dispatch Strategy of PHEVs to Mitigate Selected Patterns of Seasonally Varying Outputs From Renewable Generation," *IEEE Transactions on Smart Grid,* vol. 6, pp. 627-639, 2015.

[28] Metropolitan Travel Survey Archive [Online]. Available: http://www.surveyarchive.org/.

[29] M. Baran and F. F. Wu, "Optimal sizing of capacitors placed on a radial distribution system," *IEEE Transactions on Power Delivery,* vol. 4, pp. 735-743, 1989.

[30] M. E. Baran and F. F. Wu, "Optimal capacitor placement on radial distribution systems," *IEEE Transactions on Power Delivery,* vol. 4, pp. 725-734, 1989.

[31] K. Turitsyn, P. Sulc, S. Backhaus, and M. Chertkov, "Options for Control of Reactive Power by Distributed Photovoltaic Generators," *Proceedings of the IEEE,* vol. 99, pp. 1063-1073, 2011.

[32] H. G. Yeh, D. F. Gayme, and S. H. Low, "Adaptive VAR Control for Distribution Circuits With Photovoltaic Generators," *IEEE Transactions on Power Systems,* vol. 27, pp. 1656-1663, 2012.

[33] C. Chen, J. Wang, F. Qiu, and D. Zhao, "Resilient Distribution System by Microgrids Formation After Natural Disasters," *IEEE Transactions on Smart Grid,* vol. 7, pp. 958-966, 2016.

[34] M. A. Duran and I. E. Grossmann, "An outer-approximation algorithm for a class of mixed-integer nonlinear programs," *Mathematical programming,* vol. 36, pp. 307-339, 1986.

[35] B. Zeng and L. Zhao, "Solving two-stage robust optimization problems using a column-and-constraint generation method," *Operations Research Letters,* vol. 41, pp. 457-461, 9// 2013.

[36] W. El-Khattam, K. Bhattacharya, Y. Hegazy, and M. M. A. Salama, "Optimal investment planning for distributed generation in a competitive electricity market," *IEEE Transactions on Power Systems,* vol. 19, pp. 1674-1684, 2004.

[37] A. Soroudi, M. Ehsan, R. Caire, and N. Hadjsaid, "Possibilistic Evaluation of Distributed Generations Impacts on Distribution Networks," *IEEE Transactions on Power Systems,* vol. 26, pp. 2293-2301, 2011.

[38] B. Zou, J. Wang, and F. Wen, "Optimal investment strategies for distributed generation in distribution networks with real option analysis," *IET Generation, Transmission & Distribution,* 2016.

[39] Y. M. Atwa, E. F. El-Saadany, M. M. A. Salama, and R. Seethapathy, "Optimal Renewable Resources Mix for Distribution System Energy Loss Minimization," *IEEE Transactions on Power Systems,* vol. 25, pp. 360-370, 2010.

[40] M. F. Shaaban, Y. M. Atwa, and E. F. El-Saadany, "DG allocation for benefit maximization in distribution networks," *IEEE Transactions on Power Systems*, vol. 28, pp. 639-649, 2013.

[41] A. Keane and M. O. Malley, "Optimal Allocation of Embedded Generation on Distribution Networks," *IEEE Transactions on Power Systems*, vol. 20, pp. 1640-1646, 2005.

[42] J. Zhao, F. Wen, Z. Y. Dong, Y. Xue, and K. P. Wong, "Optimal Dispatch of Electric Vehicles and Wind Power Using Enhanced Particle Swarm Optimization," *IEEE Transactions on Industrial Informatics*, vol. 8, pp. 889-899, 2012.

[43] W. Wei, F. Liu, and S. Mei, "Charging Strategies of EV Aggregator Under Renewable Generation and Congestion: A Normalized Nash Equilibrium Approach," *IEEE Transactions on Smart Grid*, vol. 7, pp. 1630-1641, 2016.

[44] I. Ziari, G. Ledwich, A. Ghosh, and G. Platt, "Integrated Distribution Systems Planning to Improve Reliability Under Load Growth," *IEEE Transactions on Power Delivery*, vol. 27, pp. 757-765, 2012.

[45] S. Tan, J. X. Xu, and S. K. Panda, "Optimization of Distribution Network Incorporating Distributed Generators: An Integrated Approach," *IEEE Transactions on Power Systems*, vol. 28, pp. 2421-2432, 2013.

[46] B. G. Gorenstin, N. M. Campodonico, J. P. Costa, and M. V. F. Pereira, "Power system expansion planning under uncertainty," *IEEE Transactions on Power Systems*, vol. 8, pp. 129-136, 1993.

[47] M. Banzo and A. Ramos, "Stochastic Optimization Model for Electric Power System Planning of Offshore Wind Farms," *IEEE Transactions on Power Systems*, vol. 26, pp. 1338-1348, 2011.

[48] R. A. Jabr, "Robust Transmission Network Expansion Planning With Uncertain Renewable Generation and Loads," *IEEE Transactions on Power Systems*, vol. 28, pp. 4558-4567, 2013.

[49] R. A. Jabr, I. Džafić, and B. C. Pal, "Robust Optimization of Storage Investment on Transmission Networks," *IEEE Transactions on Power Systems*, vol. 30, pp. 531-539, 2015.

[50] Z. Wang, B. Chen, J. Wang, J. Kim, and M. M. Begovic, "Robust Optimization Based Optimal DG Placement in Microgrids," *IEEE Transactions on Smart Grid*, vol. 5, pp. 2173-2182, 2014.

[51] M. E. Baran and F. F. Wu, "Network reconfiguration in distribution systems for loss reduction and load balancing," *IEEE Transactions on Power Delivery*, vol. 4, pp. 1401-1407, 1989.

[52] "J. Löfberg [online]. Available: https://yalmip.github.io/," 2016.

[53] C. Wang, F. Liu, J. Wang, W. Wei, and S. Mei, "Risk-Based Admissibility Assessment of Wind Generation Integrated into a Bulk Power System," *IEEE Transactions on Sustainable Energy*, vol. 7, pp. 325-336, 2016.

[54] R. Allan, *Reliability evaluation of power systems*: Springer Science & Business Media, 2013.

[55] C. Wan, Z. Xu, and P. Pinson, "Direct interval forecasting of wind power," *IEEE Transactions on Power Systems*, vol. 28, pp. 4877-4878, 2013.

[56] C. Wan, Z. Xu, P. Pinson, Z. Y. Dong, and K. P. Wong, "Optimal prediction intervals of wind power generation," *Power Systems, IEEE Transactions on*, vol. 29, pp. 1166 - 1174, May 2014.

[57] A. J. Wood and B. F. Wollenberg, *Power generation, operation, and control*: John Wiley & Sons, 2012.

[58] H. B. Gooi, D. P. Mendes, K. R. W. Bell, and D. S. Kirschen, "Optimal scheduling of spinning reserve," *IEEE Transactions on Power Systems*, vol. 14, pp. 1485-1492, 1999.

[59] F. Bouffard and F. D. Galiana, "An electricity market with a probabilistic spinning reserve criterion," *IEEE Transactions on Power Systems*, vol. 19, pp. 300-307, 2004.

[60] F. Bouffard, F. D. Galiana, and A. J. Conejo, "Market-clearing with stochastic security-part I: formulation," *IEEE Transactions on Power Systems*, vol. 20, pp. 1818-1826, 2005.

[61] M. A. Ortega-Vazquez and D. S. Kirschen, "Optimizing the Spinning Reserve Requirements Using a Cost/Benefit Analysis," *IEEE Transactions on Power Systems,* vol. 22, pp. 24-33, 2007.

[62] C. Wan, Z. Xu, P. Pinson, Z. Y. Dong, and K. P. Wong, "Probabilistic Forecasting of wind power generation using extreme learning machine," *IEEE Transactions on Power Systems,* vol. 29, pp. 1033-1044, 2014.

[63] M. A. Ortega-Vazquez and D. S. Kirschen, "Estimating the Spinning Reserve Requirements in Systems With Significant Wind Power Generation Penetration," *IEEE Transactions on Power Systems,* vol. 24, pp. 114-124, 2009.

[64] M. A. Matos and R. J. Bessa, "Setting the operating reserve using probabilistic wind power forecasts," *IEEE Transactions on Power Systems,* vol. 26, pp. 594-603, 2011.

[65] S. Lou, S. Lu, Y. Wu, and D. S. Kirschen, "Optimizing spinning reserve requirement of power system with carbon capture plants," *IEEE Transactions on Power Systems,* vol. 30, pp. 1056-1063, 2015.

[66] M. Jaefari-Nokandi and H. Monsef, "Scheduling of spinning reserve considering customer choice on reliability," *IEEE Transactions on Power Systems,* vol. 24, pp. 1780-1789, 2009.

[67] J. Khorasani and H. R. Mashhadi, "Bidding analysis in joint energy and spinning reserve markets based on pay-as-bid pricing," *Generation, Transmission & Distribution, IET,* vol. 6, pp. 79-87, 2012.

[68] J. Wang, X. Wang, and Y. Wu, "Operating reserve model in the power market," *IEEE Transactions on Power Systems,* vol. 20, pp. 223-229, 2005.

[69] O. Nilsson, L. Soder, and D. Sjelvgren, "Integer modelling of spinning reserve requirements in short term scheduling of hydro systems," *IEEE Transactions on Power Systems,* vol. 13, pp. 959-964, 1998.

[70] N. Chowdhury, "Energy method of spinning reserve assessment in interconnected generation systems," *IEEE Transactions on Power Systems,* vol. 8, pp. 865-872, 1993.

[71] F. Aminifar, M. Fotuhi-Firuzabad, and M. Shahidehpour, "Unit Commitment With Probabilistic Spinning Reserve and Interruptible Load Considerations," *IEEE Transactions on Power Systems,* vol. 24, pp. 388-397, 2009.

[72] D. Dallinger, D. Krampe, and M. Wietschel, "Vehicle-to-grid regulation reserves based on a dynamic simulation of mobility behavior," *IEEE Transactions on Smart Grid,* vol. 2, pp. 302-313, 2011.

[73] E. Sortomme and M. A. El-Sharkawi, "Optimal scheduling of vehicle-to-grid energy and ancillary services," *IEEE Transactions on Smart Grid,* vol. 3, pp. 351-359, 2012.

[74] R. J. Bessa and M. A. Matos, "Optimization Models for EV Aggregator Participation in a Manual Reserve Market," *IEEE Transactions on Power Systems,* vol. 28, pp. 3085-3095, 2013.

[75] P. Sanchez-Martin, S. Lumbreras, and A. Alberdi-Alen, "Stochastic Programming Applied to EV Charging Points for Energy and Reserve Service Markets," *IEEE Transactions on Power Systems,* vol. 31, pp. 198-205, 2016.

[76] M. R. Sarker, Y. Dvorkin, and M. A. Ortega-Vazquez, "Optimal Participation of an Electric Vehicle Aggregator in Day-Ahead Energy and Reserve Markets," *IEEE Transactions on Power Systems,* vol. PP, pp. 1-10, 2015.

[77] C. Liu, J. Wang, A. Botterud, Y. Zhou, and A. Vyas, "Assessment of Impacts of PHEV Charging Patterns on Wind-Thermal Scheduling by Stochastic Unit Commitment," *IEEE Transactions on Smart Grid,* vol. 3, pp. 675-683, 2012.

[78] M. Ghofrani, A. Arabali, M. Etezadi-Amoli, and M. S. Fadali, "Smart Scheduling and Cost-Benefit Analysis of Grid-Enabled Electric Vehicles for Wind Power Integration," *IEEE Transactions on Smart Grid,* vol. 5, pp. 2306-2313, 2014.

[79] Y. Ota, H. Taniguchi, T. Nakajima, K. M. Liyanage, J. Baba, and A. Yokoyama, "Autonomous Distributed V2G (Vehicle-to-Grid) Satisfying Scheduled Charging," *IEEE Transactions on Smart Grid,* vol. 3, pp. 559-564, 2012.

[80] H. Liu, Z. Hu, Y. Song, J. Wang, and X. Xie, "Vehicle-to-Grid Control for Supplementary Frequency Regulation Considering Charging Demands," *IEEE Transactions on Power Systems,* vol. 30, pp. 3110-3119, 2015.

[81] (Feb. 2016) North American Electric Reliability Corporation, Reliability Standards for the Bulk Electric Systems of North America [Online]. Available: http://www.nerc.com/pa/Stand/Reliability%20Standards%20Complete%20Set/RSCompleteSet.pdf

[82] M Milligan and eta, "Operating Reserves and Wind Power Integration: An International Comparison," *National Renewable Energy Laboratory,* Oct. 2010.

[83] J. Kim, "Iterated grid search algorithm on unimodal criteria," *Ph.D.dissertation, Dept. Statist., Virginia Polytechnic Inst. and State Univ.,Blacksburg, VA.,* 1997.

[84] A. Santos, N. McGuckin, H. Y. Nakamoto, D. Gay, and S. Liss, "Summary of Travel Trends: 2009 National Household Travel," *U.S. Department of Transportation Federal Highway Administration, Washington, DC, USA, Rep. FHWA-PL-11022, Jun. 2011.*

[85] N. Z. Xu and C. Y. Chung, "Uncertainties of EV Charging and Effects on Well-Being Analysis of Generating Systems," *IEEE Transactions on Power Systems,* vol. 30, pp. 2547-2557, 2015.

[86] S.-L. Andersson, A. K. Elofsson, M. D. Galus, L. Goransson, S. Karlsson, F. Johnsson, *et al.*, "Plug-in hybrid electric vehicles as regulating power providers: Case studies of Sweden and Germany," *Energy Policy,* vol. 38, no. 6, pp. 2751–2762, Jun. 2010.

[87] P. Wong, P. Albrecht, R. Allan, R. Billinton, Q. Chen, C. Fong, *et al.*, "The IEEE Reliability Test System-1996. A report prepared by the Reliability Test System Task Force of the Application of Probability Methods Subcommittee," *IEEE Transactions on Power Systems,* vol. 14, pp. 1010-1020, 1999.

[88] C. Wang and S. M. Shahidehpour, "Effects of ramp-rate limits on unit commitment and economic dispatch," *IEEE Transactions on Power Systems,* vol. 8, pp. 1341-1350, 1993.

[89] K. Schneider, C. Gerkensmeyer, M. Kintner-Meyer, and R. Fletcher, "Impact assessment of plug-in hybrid vehicles on pacific northwest distribution systems," in *Power and Energy Society General Meeting - Conversion and Delivery of Electrical Energy in the 21st Century, 2008 IEEE*, 2008, pp. 1-6.

[90] M. Kintner-Meyer, K. Schneider, and R. Pratt, "Impacts assessment of plug-in hybrid vehicles on electric utilities and regional US power grids, Part 1: Technical analysis," *Pacific Northwest National Laboratory (a)*, 2007.

[91] E. Sortomme and M. A. El-Sharkawi, "Optimal Scheduling of Vehicle-to-Grid Energy and Ancillary Services," *Smart Grid, IEEE Transactions on*, vol. 3, pp. 351-359, 2012.

[92] Y. He, B. Venkatesh, and L. Guan, "Optimal Scheduling for Charging and Discharging of Electric Vehicles," *Smart Grid, IEEE Transactions on*, vol. 3, pp. 1095-1105, 2012.

[93] R. J. Bessa and M. A. Matos, "Global against divided optimization for the participation of an EV aggregator in the day-ahead electricity market. Part I: Theory," *Electric Power Systems Research*, vol. 95, pp. 309-318, Feb. 2013.

[94] J. A. P. Lopes, F. J. Soares, and P. M. R. Almeida, "Integration of Electric Vehicles in the Electric Power System," *Proceedings of the IEEE*, vol. 99, pp. 168-183, 2011.

[95] N. Rotering and M. Ilic, "Optimal Charge Control of Plug-In Hybrid Electric Vehicles in Deregulated Electricity Markets," *Power Systems, IEEE Transactions on*, vol. 26, pp. 1021-1029, 2011.

[96] M. Pantos, "Exploitation of Electric-Drive Vehicles in Electricity Markets," *Power Systems, IEEE Transactions on*, vol. 27, pp. 682-694, 2012.

[97] D. Papadaskalopoulos, G. Strbac, P. Mancarella, M. Aunedi, and V. Stanojevic, "Decentralized Participation of Flexible Demand in Electricity Markets—Part II: Application With Electric Vehicles and Heat Pump Systems," *Power Systems, IEEE Transactions on*, vol. 28, pp. 3667-3674, 2013.

[98] M. A. Ortega-Vazquez, F. Bouffard, and V. Silva, "Electric Vehicle Aggregator/System Operator Coordination for Charging Scheduling and

Services Procurement," *Power Systems, IEEE Transactions on,* vol. 28, pp. 1806-1815, 2013.

[99] S. I. Vagropoulos and A. G. Bakirtzis, "Optimal Bidding Strategy for Electric Vehicle Aggregators in Electricity Markets," *Power Systems, IEEE Transactions on,* vol. 28, pp. 4031-4041, 2013.

[100] M. Gonzalez Vaya and G. Andersson, "Optimal Bidding Strategy of a Plug-In Electric Vehicle Aggregator in Day-Ahead Electricity Markets Under Uncertainty," *Power Systems, IEEE Transactions on,* vol. PP, pp. 1-11, 2014.

[101] F. Ruelens, S. Weckx, W. Leterme, S. Vandael, B. J. Claessens, and R. Belmans, "Stochastic portfolio management of an electric vehicles aggregator under price uncertainty," in *Innovative Smart Grid Technologies Europe (ISGT EUROPE), 2013 4th IEEE/PES*, 2013, pp. 1-5.

[102] A. J. Conejo, M. Carrión, and J. M. Morales, *Decision Making under Uncertainty in Electricity Markets* vol. 153: Springer, 2010.

[103] S. Martin, Y. Smeers, and J. A. Aguado, "A Stochastic Two Settlement Equilibrium Model for Electricity Markets With Wind Generation," *Power Systems, IEEE Transactions on,* vol. 30, pp. 233-245, 2015.

[104] A. A. Sanchez de la Nieta, J. Contreras, and J. I. Munoz, "Optimal coordinated wind-hydro bidding strategies in day-ahead markets," *Power Systems, IEEE Transactions on,* vol. 28, pp. 798-809, 2013.

[105] M. Carrión, A. B. Philpott, A. J. Conejo, and J. M. Arroyo, "A Stochastic Programming Approach to Electric Energy Procurement for Large Consumers," *Power Systems, IEEE Transactions on,* vol. 22, pp. 744-754, 2007.

[106] L. Yang, J. Zhang, and H. V. Poor, "Risk-Aware Day-Ahead Scheduling and Real-time Dispatch for Electric Vehicle Charging," *Smart Grid, IEEE Transactions on,* vol. 5, pp. 693-702, 2014.

[107] A. T. Al-Awami and E. Sortomme, "Coordinating Vehicle-to-Grid Services With Energy Trading," *Smart Grid, IEEE Transactions on,* vol. 3, pp. 453-462, 2012.

[108] I. Momber, A. Siddiqui, T. G. S. Roman, and L. Soder, "Risk Averse Scheduling by a PEV Aggregator Under Uncertainty," *Power Systems, IEEE Transactions on,* vol. PP, pp. 1-10, 2014.

[109] Y. Ben-Haim, *Info-gap Decision Theory: Decisions under Severe Uncertainty*: Academic Press, 2006.

[110] M. P. Cheong, D. Berleant, and G. B. Sheble, "Information gap decision theory as a tool for strategic bidding in competitive electricity markets," in *Probabilistic Methods Applied to Power Systems, 2004 International Conference on*, 2004, pp. 421-426.

[111] M. Kazemi, B. Mohammadi-Ivatloo, and M. Ehsan, "Risk-Constrained Strategic Bidding of GenCos Considering Demand Response," *Power Systems, IEEE Transactions on,* vol. 30, pp. 376-384, 2015.

[112] K. Chen, W. Wu, B. Zhang, and H. Sun, "Robust Restoration Decision-Making Model for Distribution Networks Based on Information Gap Decision Theory," *Smart Grid, IEEE Transactions on,* vol. PP, pp. 1-1, 2014.

[113] S. Dehghan, A. Kazemi, and N. Amjady, "Multi-objective robust transmission expansion planning using information-gap decision theory and augmented ε-constraint method," *Generation, Transmission & Distribution, IET,* vol. 8, pp. 828-840, 2014.

[114] C. Wan, Z. Xu, Y. Wang, Z. Y. Dong, and K. P. Wong, "A Hybrid Approach for Probabilistic Forecasting of Electricity Price," *Smart Grid, IEEE Transactions on,* vol. 5, pp. 463-470, 2014.

[115] S. Vandael, B. Claessens, M. Hommelberg, T. Holvoet, and G. Deconinck, "A Scalable Three-Step Approach for Demand Side Management of Plug-in Hybrid Vehicles," *Smart Grid, IEEE Transactions on,* vol. 4, pp. 720-728, 2013.

[116] S. L. Andersson, A. K. Elofsson, M. D. Galus, L. Göransson, S. Karlsson, F. Johnsson, *et al.*, "Plug-in hybrid electric vehicles as regulating power providers: Case studies of Sweden and Germany," *Energy Policy,* vol. 38, pp. 2751-2762, 6. 2010.

[117] J. Tomić and W. Kempton, "Using fleets of electric-drive vehicles for grid support," *Journal of Power Sources*, vol. 168, pp. 459-468, 6/1/ 2007.

[118] G. Wang, J. Zhao, F. Wen, Y. Xue, and G. Ledwich, "Dispatch Strategy of PHEVs to Mitigate Selected Patterns of Seasonally Varying Outputs From Renewable Generation," *Smart Grid, IEEE Transactions on*, vol. 6, pp. 627-639, 2015.

[119] C. Wan, Z. Xu, P. Pinson, Z. Y. Dong, and K. P. Wong, "Probabilistic Forecasting of Wind Power Generation Using Extreme Learning Machine," *Power Systems, IEEE Transactions on*, vol. 29, pp. 1033-1044, 2014.

[120] C. Wan, Z. Xu, P. Pinson, Z. Y. Dong, and K. P. Wong, "Optimal Prediction Intervals of Wind Power Generation," *Power Systems, IEEE Transactions on*, vol. 29, pp. 1166-1174, May 2014.

[121] T. Jonsson, P. Pinson, H. A. Nielsen, H. Madsen, and T. S. Nielsen, "Forecasting Electricity Spot Prices Accounting for Wind Power Predictions," *Sustainable Energy, IEEE Transactions on*, vol. 4, pp. 210-218, 2013.

[122] W. Yao, J. Zhao, F. Wen, Y. Xue, and G. Ledwich, "A Hierarchical Decomposition Approach for Coordinated Dispatch of Plug-in Electric Vehicles," *Power Systems, IEEE Transactions on*, vol. 28, pp. 2768-2778, 2013.

[123] R. Ball, N. Keers, M. Alexander, and E. Bower, "Modelling Electric Storage Devices for Electric Vehicles," MERGE Project Deliverable 2.1Jan. 2011.